Assessing the use of $\delta^{18}O\text{-}PO_4$ analysis for tracing source inputs and the cycling of phosphorus: Applications to the Grand River

by

Amy Morgan Morrison

A thesis

presented to the University of Waterloo

in fulfillment of the

thesis requirement for the degree of

Master of Science

in

Biology

Waterloo, Ontario, Canada, 2014

Author's Declaration

I hereby declare that I am the sole author of this thesis. This is a true copy of the thesis, including any required final revisions, as accepted by my examiners.

I understand that my thesis may be made electronically available to the public.

Abstract

Phosphorus (P) is often the limiting or co-limiting nutrient in freshwater bodies, and plays a decisive role in the eutrophication issues plaguing these environments. P demonstrates dynamic movement upon entering rivers, often travelling between phases and biological compartments rapidly. The dynamic cycling of P in rivers can make it challenging to link a source and its effect, with P release and desorption being dependent on a variety of factors. There is significant value in a tool, such as isotopic analysis, that can distinguish between sources. Isotopic analysis could enlighten us on the role of the in-stream, biological processes on mitigating excessive P loading such as that experienced downstream of any major nutrient point source. Radiolabeling of the phosphate pool using artificial ^{32}P or ^{33}P in microcosms has been commonly used for studying P kinetics allowing for quick and reproducible measurements of the rates of uptake and release. Difficulties exist in relaying these "within-beaker" rates to the whole-river. Assumptions based on the cross-sectional geometry of a river site as well as the roughness of the substratum are required. The tracing of the oxygen isotopes of dissolved phosphate ($\delta^{18}O$- PO_4) could be a valuable tool for P research in order to better our understanding of source phosphate (PO_4^{3-}) inputs and P cycling without perturbations to the biological communities. This technique has been used a few times in freshwater systems, with the most commonly employed methods unsuitable for river water with high dissolved organic matter (DOM). The use of this technique, as well as radiolabelling of the PO_4^{3-} pool, has been used in this thesis to elucidate information on the effect of two of the largest WWTPs in the Grand River watershed on P cycling and demand. This will also allow for an evaluation of the conditions that permit $\delta^{18}O$ -PO_4 analysis to provide valuable insight on P cycling in lotic environments.

The use of $\delta^{18}O$- PO_4 analysis was assessed for the Grand River, a highly impacted river in Southern Ontario that receives inputs from 30 WWTPs. Significant nutrient inputs within the watershed have led to prolific aquatic plant growth, particularly within the central Grand River

where this study is focused. Two of the largest WWTPs in the watershed fall within this region and these plants are in close proximity to each other (approximately 20 km apart). These nutrient sources contribute to the eutrophic conditions within the river, and lead to low dissolved O_2 levels below the plants. Upstream of these plants is the confluence of the Conestogo River, a tributary of the Grand River, which drains upstream land used primarily for agriculture.

Various laboratory tests were carried out to assess the suitability of several DOM removal methods on Grand River water and WWTP effluent prior to mass spectrometric analysis with varying results. Sample analysis showed all river sites to possess $\delta^{18}O$- PO_4 values that were elevated relative to equilibrium. These sites are not equilibrium-controlled and, instead, possess $\delta^{18}O$- PO_4 signatures controlled by either source inputs, or isotopic fractionation. Both the Conestogo River and the second WWTP were shown to deliver PO_4^{3-} that was elevated relative to equilibrium. WWTP effluent in this study displayed a large $\delta^{18}O$ -PO_4 range, ranging from 10.4 to 22.9‰. Most of the variation in isotopic composition was found at the second plant, which had high soluble reactive phosphorus (SRP) and a range of 12.5 to 22.8‰ (n = 3). The first plant showed little variation with much lower SRP and a mean value of 11.4 (SD ± 1.0‰, n = 2). The elevated $\delta^{18}O$- PO_4 signatures collected from the second WWTP suggest that this plant is supplying the Grand River with isotopically distinct PO_4^{3-}. This could be used as a way to establish the effect of the second WWTP on the downstream PO_4^{3-} pool.

Phosphate uptake and release by the epilithon and seston were measured using ^{32}P-PO_4 additions in recirculating beaker experiments. Two sites, one downstream of the first WWTP and one below the second WWTP, were assessed for gross and net PO_4^{3-} uptake rates. The gross uptake rates at both sites were low (0.04 to 0.10 µg P cm^{-2} h^{-1}), with long turnover times for the dissolved phosphate pool (12 to 40 h). Long uptake lengths (30 to 144 km) were measured, indicating low nutrient retention capabilities downstream of the two WWTPs. These significant P contributions appear to have large-scale effects on the river's P-kinetics, limiting its ability to act as a net nutrient

sink even in the more productive summer months. The biomass response below the WWTPs is insufficient to compensate for the elevated PO_4^{3-} concentrations and low rates of PO_4^{3-} uptake.

Due to the limited use of $\delta^{18}O$ -PO_4 analysis in river systems, no model exists for predicting the response of $\delta^{18}O$ -PO_4 with distance downstream of a point source. Coupling rates of PO_4^{3-} uptake and release with the effluent $\delta^{18}O$ -PO_4 values provides such a model and generates guidance for future use of this method in lotic environments. WWTP "plume chases" were previously carried out in the Grand River, and involved measuring SRP at several sites downstream of the WWTP discharge points. SRP was used as a proxy for PO_4^{3-} concentration in this study, and is operationally defined by what passes through a 0.20-µm membrane filter and is molybdate reactive. Best-fit estimates of PO_4^{3-} uptake and release were determined using these plume chase events. The rates calculated using the ^{32}P-PO_4 uptake and release beaker experiments were up to 50 times lower than the best-fit parameters. This exercise illustrates the unsuitability of relaying estimates of P kinetics collected through beaker experiments to an ecosystem level.

Model predictions for the river reach below the second WWTP show that effluent $\delta^{18}O$ -PO_4 signatures should be observable many kilometers from the plant. Because of the unique mean isotopic composition observed for the second WWTP, sampling could occur at a variety of locations downstream to observe the effect of this plant on the river. The river reach below the first WWTP reduces the incoming P loads much quicker than the second reach, which is in part due to the much lower effluent SRP released by the first plant. It is still possible to isolate effluent derived $\delta^{18}O$-PO_4 values downstream of this plant. The return to equilibrium is projected to occur several kilometers from the first plant's confluence, suggesting the applicability of this method in both stream reaches. It would appear $\delta^{18}O$ -PO_4 could be a valuable tool for eliciting information on P cycling in effluent-impacted river ecosystems, with the Grand River possessing elevated but seemingly typical uptake lengths amongst eutrophic streams.

Acknowledgments

Foremost, I would like to express my sincere thanks to Bill Taylor for his continual support of my work, and for his patience, encouragement and knowledge that guided me during the research and writing of this thesis. I would also like to thank Sherry Schiff for providing me with the opportunity to work on this project, as well as all of the guidance, knowledge and encouragement she provided me over the past few years. I would like to offer my sincere gratitude to Richard Elgood who has helped me in countless ways with offering technical knowledge and constant assistance with field and lab work. I would like to thank Dr. Adina Paytan, Steven Silva, Sara Peek, and everyone in the Paytan lab who offered me guidance, and ran my samples at the Menlo Park lab.

I would like to thank the other members of my thesis committee Dr. Ralph Smith, and Dr. Veronique Hiriart-Baer for their encouragement and insightful comments that helped to shape and improve this thesis. I would like to offer a big thanks to Jennifer Hood who provided significant guidance, knowledge, and assistance, as well as Margaret Vogel who introduced me to P research and taught me the in-and-outs of P analysis. I would also like to thank Eduardo Cejudo for providing me with his plume chase data, as well as all of the help he provided me. I would further like to thank Madeline Rosamond for the travel time data she so graciously allowed me to use. I would like to thank the GRCA for providing the river discharge data and travel times used in this thesis, and the Region of Waterloo for allowing me wastewater treatment plant access.

I'd also like to thank Jason Venkiteswaran, Gao Chen, Bonnie DeBaets and everyone from the Taylor and Schiff labs, who provided me with scientific advice and counsel. I offer a big thanks to Amanda Dumas who aided me throughout two sampling summers, as well as Amanda Bichel, Daniel Worndl, Stephanie Bromwell, Mike Lyon, Fraser Cummings, Janessa Zheng, and Sarah Sine who all helped me personally with field and lab work.

Finally, I would like to thank my family and friends for their constant support and love during this time, and at all times. Most of all, I would like to thank Adam for his understanding and love. In the end, his encouragement was what made this thesis possible.

Table of Contents

List of Figures

List of Tables

Chapter 1: Introduction and the use of stable and radioisotopes to study phosphorus cycling

1.1 Introduction

1.1.1 P enrichment in streams

The term cultural eutrophication describes the accelerated rates of plant and algal production brought on by human activities in freshwater environments. Caused by an influx of biologically limiting nutrients, eutrophication can increase plant and algal biomass towards nuisance levels (Dodds, 2006). Major concerns associated with eutrophication include loss of biodiversity, oxygen-depletion, and human health impacts caused by toxic algae (Withers et al, 2009). Among the impaired rivers in the United States, 60% are experiencing problems associated with eutrophication (Carpenter et al., 1998). Cities are often located along large rivers, causing these rivers to be particularly susceptible to human impacts (Dodds, 2006). Phosphorus (P) inputs are among the main causes of eutrophication, with P often acting as the limiting or co-limiting nutrient for the growth of aquatic biota in freshwater bodies.

Anthropogenic P sources can be broken down into two classes: diffuse and point source. Non-point source, or diffuse loading, causes P to be transported to surface water based on rain events as surface runoff or sub-surface flow (Withers & Jarvie, 2008). The impact of diffuse sources on rivers is highly dependent on the flow conditions. Since much of the P is tightly bound to soil particles, in conditions of high flow the P can be flushed downstream almost entirely, if allowed to settle it can become a significant P source to the river (Mainstone & Parr, 2002). Thus, P concentrations measured during high flow are often assumed to represent diffuse source inputs delivered by runoff or erosion. P concentrations measured during periods of low flow are thought to represent point-source inputs (Jarvie et al., 2012).

Point sources deliver continuous P from discrete locations, with the supplied P often present in highly bioavailable forms (Mainstone & Parr, 2002). Increases in point source P concentrations have been attributed to use of phosphates in detergents, toothpastes, plasticizers, and baking powder (Knud-Hansen, 1994, Gruau et al, 2005, Withers & Jarvie, 2008, Paytan & McLaughlin, 2011). Natural river waters possess phosphate (PO_4^{3-}) concentrations between 1 and 24 μg P L^{-1} with the worldwide median for unpolluted rivers at 10 μg P L^{-1} (Meybeck, 1982). Where point sources enter these levels can be brought above 1000 μg P L^{-1}, with the downstream river reaches exhibiting high PO_4^{3-} concentrations prior to recovery (Wetzel, 2001). The rate of recovery will be dependent on how quickly the available PO_4^{3-} is assimilated by the in-channel processes (Haggard & Sharpley, 2007).

Studies focusing on the cycling and transport of P through rivers are not only important for river ecosystems, but also for the lakes and oceans they drain into with rivers being the largest P transporters to these larger water bodies (Ruttenberg, 2003). It is of critical importance to understand the in-stream processes that control the cycling of P in river ecosystems, due to the concerns associated with eutrophication. These processes alter both the timing and amount of P delivered downstream.

1.1.2 P cycling in streams

Phosphorus is present in both particulate and dissolved forms in natural waters, the latter being operationally defined by what passes through a 0.20-μm membrane filter. The dissolved fraction is composed of organic and inorganic fractions, with the inorganic often defined by the portion that is molybdate reactive (Murphy & Riley, 1962). This operationally defined P class is called soluble reactive phosphorus (SRP), or sometimes dissolved reactive phosphorus (DRP). SRP is thought to be largely PO_4^3, the most bioavailable P form, and is rapidly taken up by the biota.

Sources of P to pristine, freshwater rivers include: the weathering of minerals, particularly apatite; atmospheric deposition; stream bank erosion; and riparian vegetation (Withers & Jarvie,

2008). These natural P sources generally provide low amounts of P, with anthropogenic inputs being the major P contributors to many rivers systems. P will bind readily to iron or aluminum and can become trapped in the sediments in mineral or organic forms. Translocation of PO_4 from the river water to the benthos occurs via biological uptake by macrophytes or periphytic communities, direct adsorption to particulates or benthic substrata, and sinking processes (Fig. 1.01). P demonstrates dynamic movement upon entering rivers, often travelling between phases and biological compartments rapidly (Mainstone & Parr, 2002). P entering a river or stream is rapidly assimilated and retained by the "within-river" processes (Jarvie et al., 2012). These processes can cause P enriched streams to act as P sinks, providing short-term storage prior to re-release (Haggard & Sharpley, 2007). The amount of P retention that occurs in a river is highly dependent on the form of P entering, and the residence time of the water (Withers & Jarvie, 2008).

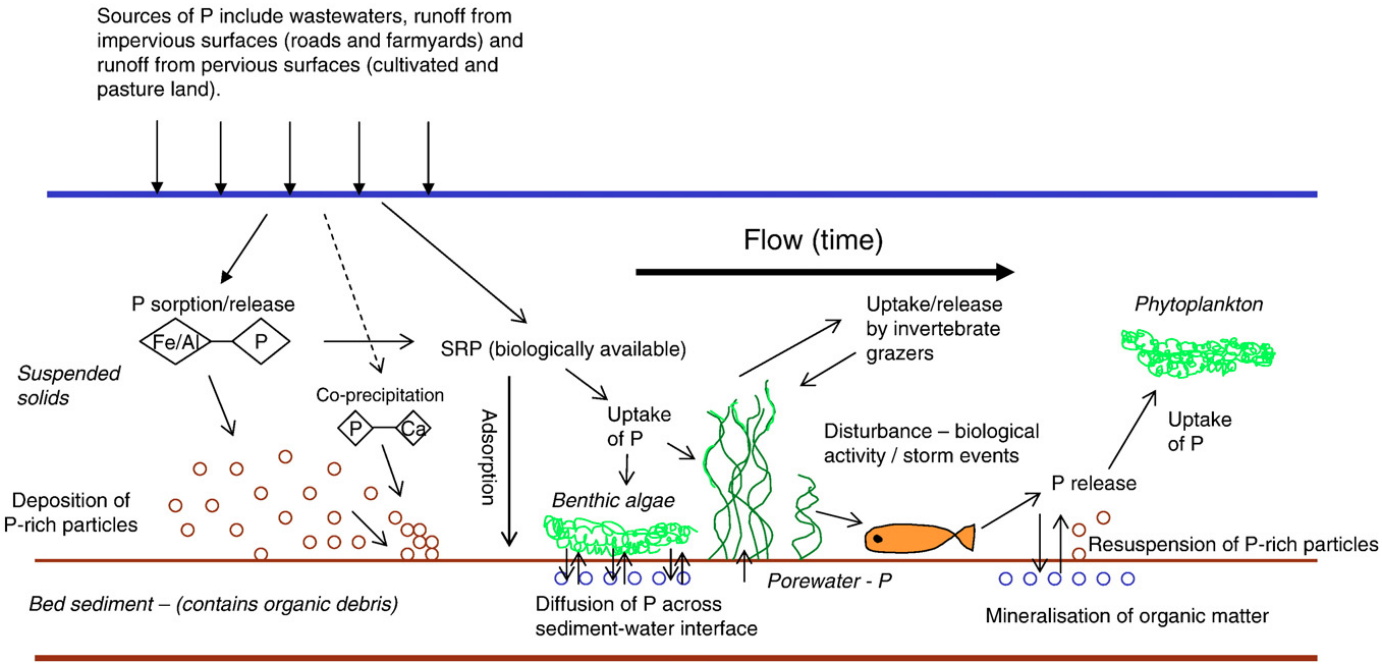

Figure 1.01: Schematic diagram of P uptake, release, adsorption and remineralization processes that effect the concentration and forms of P in stream environments, taken from Withers & Jarvie (2008).

The dynamic movement of P in rivers can make it difficult to link anthropogenic P sources with their effect on downstream water quality. The processes affecting P retention have significant control on the transport of P downstream, making it challenging to use P concentration data alone to assess source impacts, particularly across varying time scales (Jarvie et al., 2012). One such difficulty exists in trying to separate non-point sources from point sources. The usual assumptions that low flow sampling divulges information on point source influences will not always hold, depending on these in-stream processes. For example, in-stream storage can cause WWTP derived P to become immobilized until conditions of high flow cause them to be washed out. The assumption that high flow P loading reflects the contribution of agricultural sources could cause an underestimation of the importance of WWTP inputs (Jarvie et al., 2012). There is significant value in a tool, such as isotopic analysis, that can distinguish between sources, and enlighten us on the role and rates in which the biological compartments mitigate excessive P loading.

1.1.3 Isotopic analysis and notation

Isotopic signatures allow for tracing of the sources and fate of components moving through an aquatic environment. Oxygen (O) possesses three naturally occurring stable isotopes, ^{16}O, ^{17}O, and ^{18}O. The differences in atomic mass [between the isotopes] cause a quantitative difference in reaction rate, leading to isotopic fractionation effects between the sources and products involved in a chemical transformation. Fractionation refers to the separation of one isotope relative to another, leading to differences in the isotopic ratios of reactant and product. Isotopic composition is often expressed in standard delta notation, being used to compare a sample to a standard. For example, the expression for ^{18}O and ^{16}O isotopes would be written as:

$$\delta^{18}O = \left[\frac{Rsample}{RVSMOW} - 1\right] * 1000 \quad (1.1)$$

where R_{sample} is the $^{18}O/^{16}O$ in the sample, and R_{VSMOW} is the ratio for Vienna Standard Mean Ocean Water. The $\delta^{18}O$ signatures are measured using mass spectrometry, which determines the isotopic composition based on the element's mass-to-charge ratio.

Radioisotopes are also used for tracing the movement of nutrients through an aquatic environment, however their detection is due to emissions of gamma rays or subatomic particles as they undergo radioactive decay. The radiation emitted during their decay can be quantified. Samples spiked with a given radioisotope can be analyzed in terms of the presence and movement of the radiolabelled nutrient pool between biological compartments. Radioactivity is measured in counts per minute (CPM) which can be related to the activity of the added isotope by correcting this data for a blank, resulting in units of disintegrations per minute (DPM).

1.1.4 Use of isotopic analysis to study P cycling

Stable and radioisotopes have been used as tracers for the geochemical cycling of nutrients in both marine and freshwater environments. The naturally occurring radioisotopes of P (^{32}P, ^{33}P) have been successfully utilized to assess P cycling (Lal et al., 1988, Lal & Lee, 1988, Benitez-Nelson & Buesseler, 1998). This tool has been used predominantly to measure uptake rates and turnover times in the various dissolved and particulate P pools in the upper ocean. These natural, cosmogenic radioisotopes are largely delivered to the water column via wet precipitation, and allow for direct measurements of P uptake. Analysis, however, requires the collection of thousands of liters of water due to the low concentration of the isotope (Benitez-Nelson & Buesseler, 1998). Radiolabeling of the PO_4^{3-} pool using additions of ^{32}P or ^{33}P has also been commonly used for studying P kinetics in rivers (Newbold et al., 1983, Mullholland et al., 1990, Hwang et al. 1998). P kinetic studies usually involve the isolation of biological communities into chambers or beakers, allowing for uptake, regeneration and turnover time to be assessed within the beakers. This analysis allows for quick, and reproducible measurements of P kinetics, however radical perturbations occur to the enclosed biological communities.

The difficulties associated with tracing P using stable isotope analysis lies in the fact that P possesses only one stable isotope, ^{31}P. In natural environments, P is primarily found in a form strongly bound to O, for example orthophosphate (PO_4^{3-}; Li, 2009). The P-O bond is resistant to

inorganic hydrolysis at surface-water temperatures and pressures which allows for the stable isotope tracing of O in PO_4^{3-} to examine P cycling (Elsbury et al, 2009).

Up to this point, $\delta^{18}O\text{-}PO_4$ analysis has largely been applied to marine samples including oceans, coastal bays, and estuaries (Longinelli & Nuti, 1973, Longinelli et al., 1976, Colman et al, 2005, McLaughlin et al., 2006a, McLaughlin et al., 2006b, McLaughlin et al., 2006c, Puceat et al., 2010, McLaughlin et al., 2013). It has been used only a handful of times on PO_4^{3-} stripped from whole water samples taken from lakes and rivers (Markel et al., 1994, Breaker, 2009, Elsbury et al., 2009). More recent applications to sediments, soils and bacteria have been carried out to observe the cycling of P through the different biological compartments (Markel et al., 1994, Tamburini et al., 2010, Jaisi et al., 2011, Huo et al., 2011, Goldhammer et al., 2011, Weiner et al., 2011, Angert et al., 2012). The use of this tool could provide insight on P cycling in natural river systems, without the use of PO_4^{3-} enrichment, chambers, or enclosed experiments.

While both radio- and stable isotope analysis provide insight into nutrient cycling, the use of natural stable isotopes can allow for an examination of a nutrients transformations between phases and space without any perturbations to the system, and over long time scales (Paytan & McLaughlin, 2011). The use of both stable and radioisotopes to assess P cycling in a stream environment could provide a fuller picture on P- uptake, release, and any dominant P sources causing nutrient enrichment in the downstream river reaches.

Structure of the thesis

One objective of this thesis was to assess the use of $\delta^{18}O\text{-}PO_4$ analysis in the Grand River. A second objective was to model PO_4^{3-} dynamics and $\delta^{18}O\text{-}PO_4$ signatures downstream of a point source input, using the rates of PO_4^{3-} uptake and release determined through radiolabelling of the PO_4^{3-} pool. These two isotopic methods will be used to investigate the effect of two of the largest WWTPs in the Grand River watershed on P cycling and demand in the downstream river reaches.

This first chapter provides an introduction to P cycling in lotic environments and covers the role of P in the eutrophication issues plaguing many freshwater systems. This chapter also includes a discussion of the different methods used to examine P movement, with special attention to the isotopic methods involving ^{32}P additions, and an introduction to the stable isotope approach.

The second chapter includes a detailed discussion on the use of $\delta^{18}O\text{-}PO_4$ for studying P cycling, as well as a background on the current methods used for analyzing DIP samples. Here, the difficulties experienced in analyzing samples possessing high DOM will be examined. A discussion of the sample types that allowed for the best results will also be included as determined by O yields, nitrogen (N) contamination, and sample reproducibility.

The third chapter uses $^{32}P\text{-}PO_4^{3-}$ analysis to find rates of PO_4^{3-} uptake, release, steady-state PO_4^{3-} concentration, turnover time, and uptake length. This chapter includes a discussion of the effect of two WWTPs on downstream P kinetics, with a comparison of the rates obtained in this study to those obtained in other studies where both pristine and effluent-impacted systems have been examined, including a comparison to a previous study in the Upper Grand River (Barlow-Busch et al., 2006).

Finally, the fourth chapter will use the rates from chapter 3 with the effluent $\delta^{18}O\text{-}PO_4$ values from chapter 2, to create a model predicting the response of PO_4^{3-} concentration and $\delta^{18}O\text{-}PO_4$ with distance downstream of a WWTP input, using the Waterloo and Kitchener WWTPs as case studies. This model will generate expected results for future $\delta^{18}O\text{-}PO_4$ analysis in riverine environments, and determine under what conditions this type of analysis will be useful for elucidating important information on P cycling in lotic systems.

Chapter 2: Promises and limitations of $\delta^{18}O$-PO_4 analysis for assessing PO_4^{3-} in the Grand River

2.1 Introduction

2.1.1 Interpreting the oxygen isotopes of phosphate

Phosphorus (P) present in the environment is largely found in a form that is tightly bound to oxygen (O), i.e. orthophosphate (PO_4^{3-}), presenting the opportunity to use the O isotopic composition as a tracer. The P-O bond is resistant to inorganic hydrolysis at environmental water temperatures and pressures (Blake et al., 1997). This bond can however be broken during enzyme-mediated biological reactions involving PO_4^{3-}. Such reactions cause O exchange with the surrounding water and can include: transfers during ATP utilization; phosphorylation/ de-phosphorylation reactions taking place during signal transduction; and enzyme activation/deactivation (Blake et al., 1997).

As biological cycling and recycling of P occurs within a system, the resulting O isotopic signatures of the PO_4^{3-} will reach equilibrium with the water and overprint source PO_4^{3-} signatures. The activity of pyrophosphatase is believed to be the main driver of these intracellular reactions towards equilibrium values (Blake et al., 2005). The empirical equation first developed by Longinelli & Nuti (1973) is widely used to calculate this equilibrium $\delta^{18}O_P$:

$$T\ (^{o}C) = 111.4 - 4.3\ (\delta^{18}O_P - \delta^{18}O_w) \quad (2.1)$$

where T is the environmental temperature, $\delta^{18}O_P$ is the isotopic signature of the PO_4^{3-}, and $\delta^{18}O_w$ is the isotopic signature of the environmental water. Revisions were recently made to this equation during a comparison study of past methods used for PO_4^{3-} isolation to more recent forms of analysis. The new equation displayed an offset of approximately 2‰ from the original (Puceat et al., 2010). Research on paleoclimate using the original equation would have underestimated

temperature by 4-8 ^{o}C (Puceat et al., 2010). The revised equilibrium equation is:

$$T\ (^{o}C) = 118.7 - 4.22\ (\delta^{18}O_P - \delta^{18}O_W) \quad (2.2)$$

Agreement with this equilibrium is believed to indicate rapid PO_4^{3-} cycling, where inputs are less than the biological PO_4^{3-} requirements of the biomass in the system (Colman et al., 2005). Deviations from this equilibrium are usually indicative of aquatic systems that possess greater P inputs than biological P requirements, or severe P limitations causing fractionation effects due to extracellular phosphatases (McLaughlin et al., 2013). The former allows for lower rates of recycling and P turnover, and source DIP O isotopic composition to be observed. When this occurs, these values can be used as tracers for PO_4^{3-} sources entering the system, allowing for unidentified sources to be exposed and the relative contribution of these sources to be estimated (Elsbury et al., 2009). Many P sources can be identified based on their distinct isotopic compositions, and research has gone into documenting some of the common anthropogenic sources and their $\delta^{18}O$-PO_4 values (Gruau et al., 2005, Young et al., 2009).

Extremely PO_4^{3-} limited systems have also been found to deviate from this theoretical equilibrium if dissolved organic phosphorus (DOP) becomes an important P source. DOP is accessed via extracellular and cell-surface enzyme activity that releases PO_4^{3-} from DOP for uptake by bacteria, algae or plants. This initial dephosphorylation results in O exchange that can be related to the number of phosphoester bonds possessed by the phosphatic compound. When bacteria were grown on RNA, a phosphodiester, the resulting PO_4^{3-} was found to retain two, and exchange two O molecules with the environmental water, indicating hydrolysis at the two P-O-C bonds (Blake et al., 1998). Hydrolysis of these compounds takes place in two steps: the first step being the hydrolysis of the phosphodiester to a phosphomonoester, followed by a second cleavage that releases PO_4^{3-}. This will result in a fractionation factor from both processes that usually shifts the $\delta^{18}O$-PO_4 below the theoretical equilibrium (Liang & Blake, 2009, Angert et al., 2012).

The equation that describes this relationship for a phosphodiester is:

$$\delta^{18}O_P = 0.5 \times \delta^{18}O_{P\text{-organic}} + 0.5 \times (\delta^{18}O_W + F), \quad F = (F_1 + F_2)/2 \qquad (2.3)$$

F represents the combined fractionation factor from the two-step hydrolysis of a phosphodiester (Angert et al., 2012). These enzyme-related fractionation effects may explain the disequilibrium values observed in extremely P-limited environments, e.g., the Sargasso Sea (McLaughlin et al., 2013).

The observed variations in the O isotopic composition of PO_4^{3-} either represent P cycling through the biological compartments causing equilibrium or kinetic fractionation effects, or the mixing of isotopically distinct sources (McLaughlin et al., 2006a).

2.1.2 Methods for $\delta^{18}O$-PO_4 analysis

The use of the O isotopes of PO_4^{3-} to study the geochemical cycling of P has been limited in freshwater environments due to the notably laborious and time consuming nature of collecting sufficient PO_4^{3-}, and for the elimination of interferences in the analytical procedure. Older methods were developed largely for the analysis of paleoclimate, and were carried out on oceanic, biogenic apatite samples (Longinelli & Nuti, 1973, Longinelli et al., 1976). The use of these techniques for DIP was infrequent, as it required the isolation of large amounts of PO_4^{3-} from whole water samples, with PO_4^{3-} being present in biologically limiting amounts. The use of ferric hydroxide coated acrylic fibres (Krishnaswami et al., 1972), and later polypropylene sheets (Benitez-Nelson & Buesseler, 1998) was developed for the concentration of trace elements. This method was applied to the task of concentrating DIP from seawater and rainwater (Lal et al., 1988, Benitez-Nelson & Buesseler, 1998). Although the use of polypropylene sheets was found to significantly increase the effectiveness of DIP scavenging, hundreds to thousands of liters of water were still required for the isolation of small amounts of PO_4^{3-}. Karl & Tien (1992) developed a method for the quantitative removal of P from water using the co-precipitation of brucite ($MgOH_2$) and PO_4^{3-}, termed MagIC. This simple and effective method allows for DIP scavenging in seawater through the addition of

sodium hydroxide (NaOH) to whole seawater samples, with low-speed centrifugation to collect the resulting brucite precipitate.

The technique by Karl & Tien has been applied to current methods for $\delta^{18}O$-PO_4 analysis (McLaughlin et al., 2004). The PO_4^{3-} is then carried through steps with the goal to isolate and purify it, precipitate it as silver phosphate (Ag_3PO_4), and finally analyze it for O isotopic analysis on a mass spectrometer coupled to a thermal combustion elemental analyzer or TCEA (Paytan and McLaughlin, 2011). Older methods involved isolating PO_4^{3-} as bismuth phosphate ($BiPO_4$) (Longinelli & Nuti, 1976), however, due to the hygroscopic nature of $BiPO_4$ and the need for larger sample sizes, Ag_3PO_4 has become the compound of choice. These newer methods allow for small sample sizes, only requiring 200 to 500 μg of Ag_3PO_4, and the convenient analysis of several samples at a time (Li, 2009).

Allowance for small sample sizes could open the door for this method to be used on freshwater samples where DIP concentrations are low. $\delta^{18}O$-PO_4 analysis has the potential to yield information on P cycling and the partitioning of P sources in rivers, which is important for assessing the delivery of P to downstream receiving waters.

2.1.3 Research objectives

This chapter will assess the applications and potential value of using the stable isotopic composition of O ($\delta^{18}O$) in PO_4^{3-}, in order to discern if this is a useful tool for studying PO_4^{3-} in the highly impacted Grand River. The following questions will be addressed:

1) Can a current $\delta^{18}O$-PO_4 method be used, or modified, to process WWTP effluent and river samples that typically have higher DOM than marine waters?
2) What sample types produce reliable results, as shown by O yields, P recovery, N content and reproducibility?

3) Do the source inputs possess unique isotopic compositions? That is, does enough variability exist between $\delta^{18}O\text{-}PO_4$ source signatures and the theoretical equilibrium to allow for these P sources to be discerned in the Grand River?

2.2 Materials and Methods

2.2.1 The Grand River

The Grand River lies in the largest watershed in Southern Ontario, spanning 6800 km^2 (GRCA, 2011). It flows from its source near Georgian Bay to its mouth in L. Erie winding 290 km, and is joined by three major tributaries: the Conestogo, the Speed, and the Nith Rivers. Almost one million people live in the Grand River watershed with major cities including Kitchener, Waterloo, Guelph, Cambridge and Brantford (GRCA, 2011). These cities rely on ground water and the river as raw water sources. At the same time, there are 30 wastewater treatment plants, servicing 80% of the population, expelling treated wastewater into the river or its tributaries (Fig. 2.01). The temperate climate and fertile soils of the watershed have resulted in 76% of the land drained by the Grand River being used for agriculture, with only 17% left forested (Cooke, 2006). The river is used for drinking water for approximately 600,000 people (Anderson, 2012), an aquatic habitat for a number of economically and environmentally important species, water for irrigation and livestock, industrial uses, and recreation (Cooke, 2006).

These uses have been impaired by excessive macrophyte and algal growth, particularly downstream of the WWTPs, causing O_2 depletion with some of the lowest dissolved O_2 levels documented at Blair (Cooke, 2006). With the population of people living in the Grand River watershed expected to increase by a third in the next twenty years, coping with increased demand on the river will be an important management objective (GRCA, 2011). Among the wastewater treatment plants are the Kitchener and Waterloo plants, the first and third largest by flow,

respectively, servicing the Kitchener- Waterloo region with a population of approximately 300, 000 (Anderson, 2012).

The Grand River watershed can be separated into three geologically distinct regions (Cooke, 2006). The upper Grand and Conestogo basins are mainly clay till, generating significant amounts of runoff from land that is primarily used for agriculture. Belwood Lake and Conestogo Lake are reservoirs that capture a large amount of this runoff (Cooke, 2006). The central watershed (Waterloo, Kitchener, and Cambridge) is largely composed of sands and gravels, with groundwater aquifers providing drinking water for these cities. The southern portion is mainly clay tills used for agricultural purposes, again generating diffuse P runoff (Cooke, 2006).

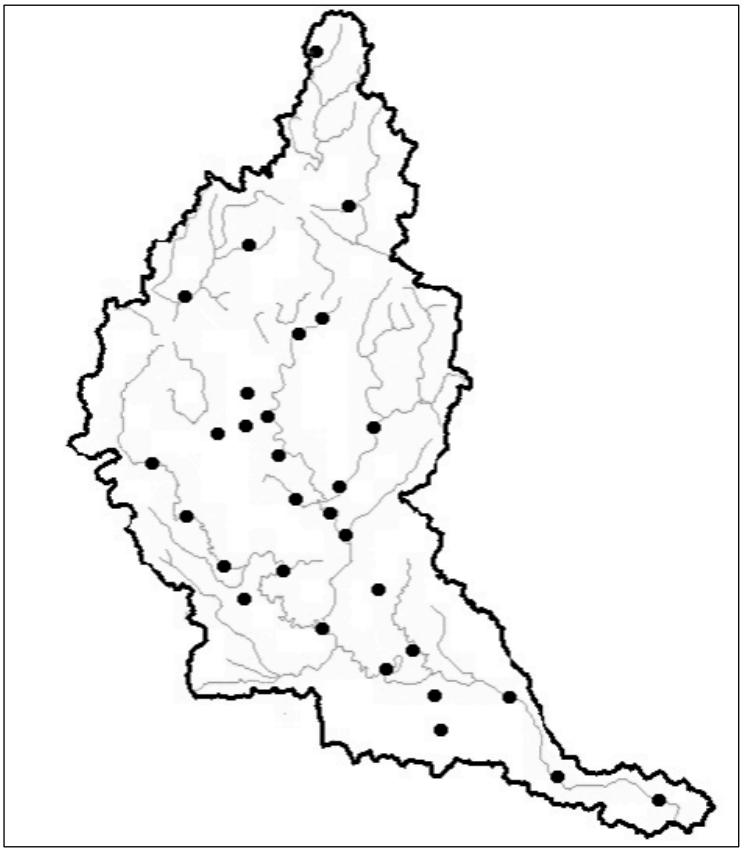

Figure 2.01: Map showing the placement of the municipal WWTPs located in the Grand River watershed (GRCA, 2013)

Long-term (1965 to 2009) longitudinal trend analysis in nutrient concentrations showed total phosphorus (TP) to increase from the river's headwaters to the mouth among all years (Hood, 2012). Both TP and SRP were found to increase in the region of Waterloo, downstream of the two WWTPs (Hood, 2012). Considering the growing population within the watershed, an assessment of the contributions and impacts of these P sources is necessary in order to make accurate predictions for the health of the system.

2.2.2 Research sites

Three reaches of the Grand River in the Region of Waterloo were the focus of sampling for $\delta^{18}O\text{-}PO_4$ determination. Samples were taken from a site within each reach, as well as from what was believed to be the dominant P source contributing to that reach (Fig. 2.02). The first and most upstream sampling site, Bridgeport (BRP), was within the City of Kitchener approximately 87 km from the headwaters. Sampling took place below the bridge at the intersection of Bridge Street and Lancaster Street. This site is located within a 7^{th} order stream reach, downstream of the confluences of Canagagigue Creek, Laurel Creek, and the Conestogo River. The Conestogo River (approximately 10 km upstream of Bridgeport) drains upstream land used primarily for agriculture and is thought to be a significant source of agriculturally derived nutrients to the Grand. During periods of high-flow, particularly in the winter and spring months, TP and SRP in the Grand River can double within this reach compared to upstream values. During periods of low-flow SRP concentrations are usually low, often below 5 $\mu g\ P\ L^{-1}$. (GRCA, 2011).

The second chosen reach is below the Waterloo WWTP, the third largest WWTP in the Grand River watershed by flow (Anderson, 2012). Samples were taken from the Waterloo WWTP final effluent, and regular sampling was carried out at a site approximately 5 km downstream of the plant in Kitchener adjacent to the bridge on Victoria Street (VIC). The last reach was below the Kitchener WWTP, the largest WWTP in the watershed. Samples were taken from the plant's final effluent, and regular sampling occurred at a site located 6 km downstream, in Cambridge near the

village of Blair (BLA). During summer low flow, TP concentrations at Blair usually exceed the provincial water quality objective of 30 μg P L^{-1}, with the median TP concentration twice this value (GRCA, 2011). As mentioned, a significant amount of SRP makes up the TP pool at Blair, which is characteristic of WWTP-impacted water (Withers & Jarvie, 2008).

Biweekly sampling occurred at Bridgeport, Victoria and Blair, between May to September, 2012. Effluent $\delta^{18}O\text{-}PO_4$ sample collection took place three times over the summer of 2012, between July and September.

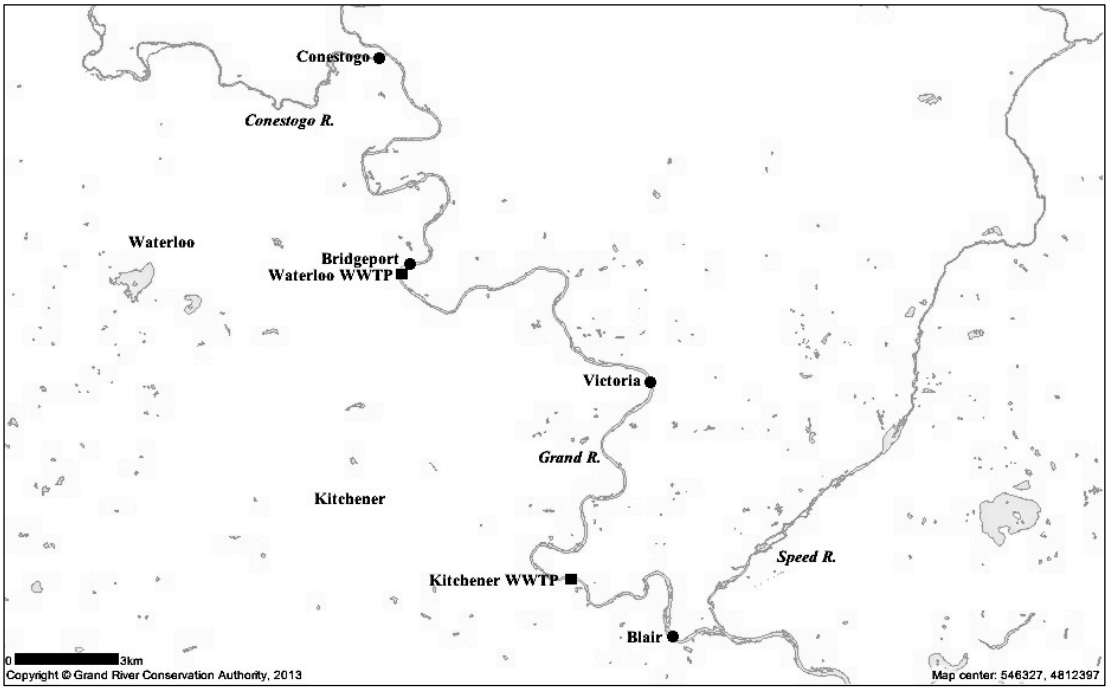

Figure 2.02: The Grand River watershed, showing the locations of the Waterloo and Kitchener WWTPs and the sampling sites. Sampling sites include: Bridgeport, Victoria, Blair, and a site along the Conestogo River in the town of Conestogo (GRCA, 2013).

2.2.3 Sample collection and analysis

Regular sampling at Bridgeport, Victoria, and Blair included the collection and analysis of water samples for SRP, $\delta^{18}O\text{-}H_2O$, and $\delta^{18}O\text{-}PO_4$. This section will describe the collection procedures for these sample types, but a complete description of the analysis protocol used for $\delta^{18}O\text{-}PO_4$ can be found in section 2.2.4. Other parameters collected in the field include temperature, conductivity, pH, and a qualitative account of the river and weather conditions.

The collection of 20 mL of Grand River water for SRP analysis was carried out in triplicate at each site, using field filtration in 60-mL syringes with 0.2-µm filters held in filter holders. The collection vessels, 45-mL centrifuge tubes, were rinsed three times with filtered river water. Likewise the syringes were rinsed three times with unfiltered water and filters were rinsed with approximately 10 mL of river water. All equipment was acid washed in 10% hydrochloric acid (HCl), rinsed with deionized water, and allowed to air dry prior to use. Samples were placed in a cooler with ice in the field and refrigerated upon return to the laboratory. SRP samples were analyzed as soon as possible upon returning from the field, always within 2 d. The ascorbic acid-phosphomolybdate spectrophotometric method (Murphy & Riley, 1962) was used, with a CARY 100 Bio UV-Visible Spectrophotometer.

The collection of 30 mL of water for $\delta^{18}O\text{-}H_2O$ analysis was also carried out at each site. Samples were collected in 30-mL airtight containers that had been acid washed in 10% HCl, rinsed with deionised water and allowed to air dry. Samples were chilled in the field and frozen upon return to the laboratory. Care was taken to reduce headspace and prevent evaporation. $\delta^{18}O\text{-}H_2O$ analysis was carried out at the University of Waterloo Environmental Isotope Laboratory.

River water samples were also collected for $\delta^{18}O\text{-}PO_4$ analysis at each site. These were collected in 20-L plastic, collapsible carboys that were acid washed with HCl, rinsed with deionised water and allowed to air dry, prior to use. The number of carboys collected from each site depended on the previously observed SRP at each site, and the water collected ranged from 20 to

90 L. Effluent samples were also collected in 20-L carboys but only 10 L were collected. Samples were chilled in the field and filtered immediately upon return to the lab.

2.2.4 Method for $\delta^{18}O\text{-}PO_4$ analysis with high DOM concentrations

McLaughlin et al. (2004) developed an effective method for the analysis of seawater samples that has been applied to various marine settings (McLaughlin et al., 2006a; McLaughlin et al., 2006b; McLaughlin et al., 2006c; McLaughlin et al., 2013), but only a few times for lakes and rivers (Elsbury et al., 2009; Breaker, 2009). DIP samples were collected from May to October 2012, on a biweekly basis from the Grand River sites located at Bridgeport, Victoria, and Blair. Water was filtered through 2 and 0.3-µm cartridge filters consecutively, and collected in a new set of acid washed 20-L carboys. Following filtration, the MagIC technique for PO_4^{3-} scavenging was adapted for fresh water samples through the addition of magnesium chloride ($MgCl_2$; Karl & Tien, 1992). I added 150 g of $MgCl_2 \bullet 6H_2O$ and 275 mL of 1-M NaOH to each 20-L carboy. The precipitate was chilled, and left to settle over night.

Gravity filtration was used to remove the supernatant the following morning. Some samples were collected in 2 to 4 carboys per site (based on volume requirements), and were treated as separate samples for the initial steps. Following MagIC and gravity filtration these samples were combined in one carboy and allowed to settle for an additional night. This was followed by gravity filtration, resulting in approximately 3 to 5 L of $MgOH_2$ precipitate. The samples were then slowly transferred to 250-mL, acid washed, HDPE bottles where small amounts of sample were centrifuged at 3500 rpm for 10 min and the supernatant was discarded. The 20-L carboy was rinsed with 10-M nitric acid (HNO_3) and the solution was added to the sample. From this point the analysis followed the method of McLaughlin et al. (2004; Fig. 2.3) with modifications for riverine samples with high concentrations of dissolved organic matter.

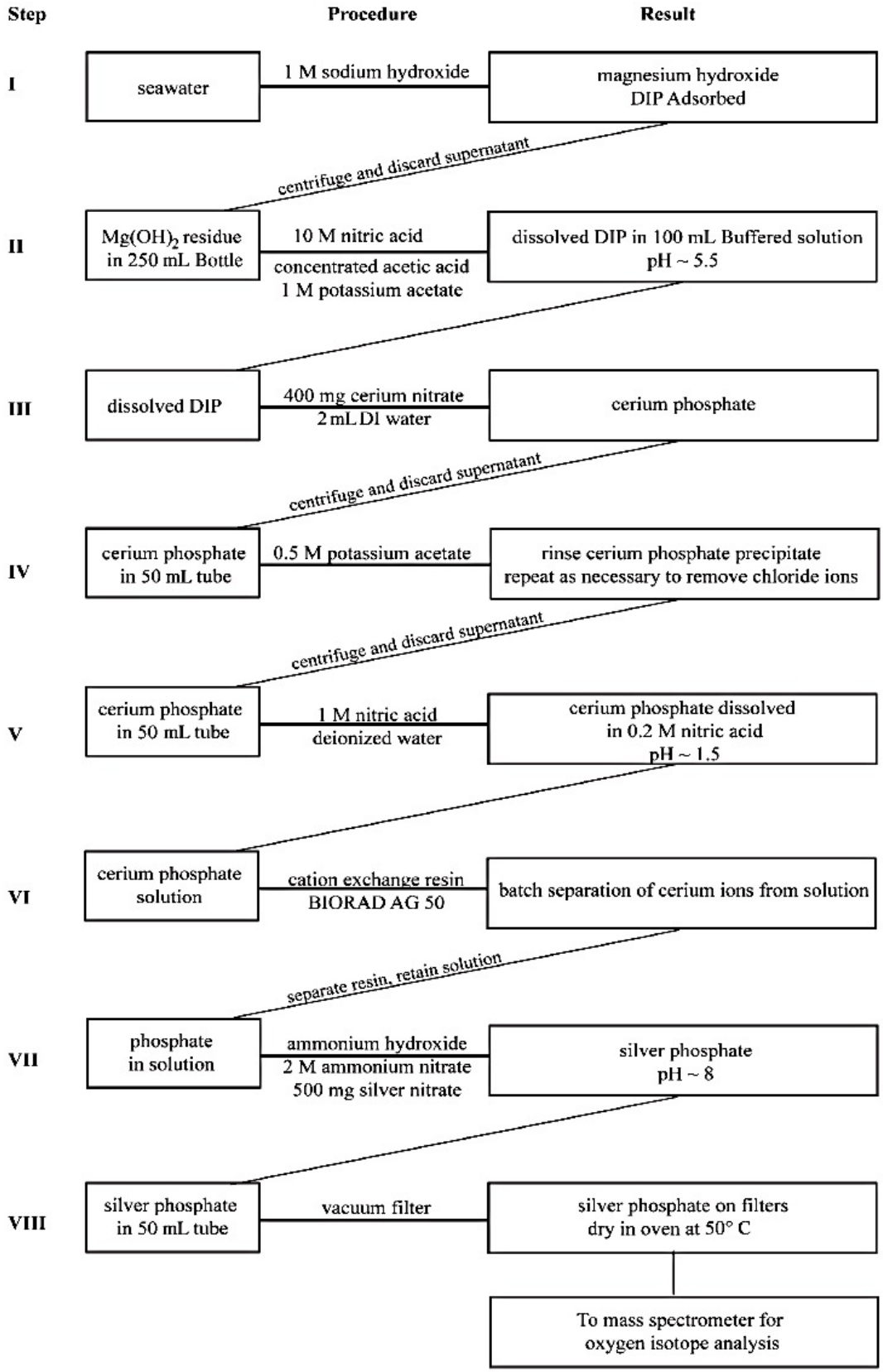

Figure 2.03: Steps involved in concentrating, purifying and isolating Ag_3PO_4 for isotopic analysis (McLaughlin et al., 2004).

Incorporation of dissolved organic matter (DOM) into the precipitate was one of the largest difficulties associated with applying this method to Grand River samples. Dissolved organic carbon (DOC) is often used as a proxy for DOM, and was used as such in this thesis. Grand River water possesses between 6 to 8 mg C L^{-1}. Since DOC has a significant amount of O, this represents a substantial source of interfering O that could cause erroneous isotopic values (Gruau et al., 2005). DOC content of the samples was tracked between steps by collecting 30 mL of the supernatant following the precipitation reactions.

Published procedures for DOM removal have been successfully applied to natural samples, including the use of DAX-8 resin and hydrogen peroxide (H_2O_2; Tamburini et al., 2010, Zohar et al., 2010), humic and fulvic acid precipitation (Zohar et al., 2010), activated-C (Gruau et al., 2005), additional rinses and filtering (Li, 2009), and repeat MagIC (Goldhammer et al., 2010). Due to the heterogeneous nature of organic matter, different environments can possess extremely different mixtures of compounds making up the DOM pool (Aukes, 2012). Certain methods will yield superior DOM removal results compared to others depending on the environment and types of DOM present. Several of these methods were tested in order to determine the most effective method for Grand River samples based on successful DOM removal, ease of use, and preservation of PO_4^{3-}. These include running filtered Bridgeport water collected on May 9th through a column packed with activated C and testing the DOC before and after charcoal treatment. Ultrafiltration was also attempted using a Minimate Tangential Flow Filtration Capsule with an initial molecular weight cut-off of 3000 Daltons.

The use of DAX-8 Supelite resin was tested by packing a glass column with conditioned DAX-8. The resin was conditioned in accordance with Tamburini et al. (2010) through the use of methanol (CH_3OH) and Millipore water. 500 mL of filtered Bridgeport water was acidified using 10-M HNO_3 to a pH of approximately 1. Following this, the water was run through the column with samples collected every 100 mL for SRP and DOC determination. The resin and H_2O_2 pre-treatment

was included in future samples; however the resin was added directly to the samples and filtered out, following Tamburini et al. (2010). $MgOH_2$ samples were dissolved using concentrated acetic acid ($C_2H_4O_2$), 30 mL of conditioned DAX-8 resin was added, and they were left on a shaking table for a minimum of 3 h.

The acidified samples were adjusted to a pH of approximately 6 using 8-M potassium hydroxide (KOH) for cerium phosphate ($CePO_4$) precipitation. Following precipitation, the $CePO_4$ was centrifuged at 3500 rpm for 10 minutes repeatedly in 50-mL polypropylene centrifuge tubes for volume reduction. Small aliquots (~20 mL) of supernatant were collected throughout this procedure for SRP analysis. When all of the $CePO_4$ was in the new set of tubes the samples were rinsed 7 to 10 times with 0.5-M potassium acetate (KCH_3CO_2). McLaughlin et al. (2004) describe the use of 3 rinses for full chloride ion (Cl^-) removal, however Li (2009) found increasing the number of rinses to between 5 and 10 could maximize DOM removal and minimize the PO_4^{3-} loss that can accompany more than 10 rinses. The number of rinses used on the Grand River samples was dependent on the stability of the $CePO_4$ floc, with 8 being the average number of rinses before the floc would become unstable, causing PO_4^{3-} loss. Complete Cl^- removal was tested for through the addition of small amounts of $AgNO_3$ to the discarded rinse water. If AgCl precipitation was observed, further rinses were carried out (McLaughlin et al., 2004).

Samples free of Cl^- were dissolved with 1-M HNO_3 and Millipore water. BioRad AG-50X8 was conditioned using 7-M HNO_3, followed by repeated rinses with Millipore water until the resin water had a neutral pH. The resin was added to the dissolved $CePO_4$ samples, and left on a shaking table for a minimum of 12 h in order to remove Ce^{3+}. The resin was separated from the samples through the use of Kimball glass columns, and the Ce-free PO_4^{3-} was collected in a new set of 50-mL centrifuge tubes. These samples were brought to a neutral pH using 8-M KOH, and the $CePO_4$ precipitation step was repeated in accordance with Li (2009; Fig. 2.04). This was found to improve O yields by further reducing the amount of contaminating OM.

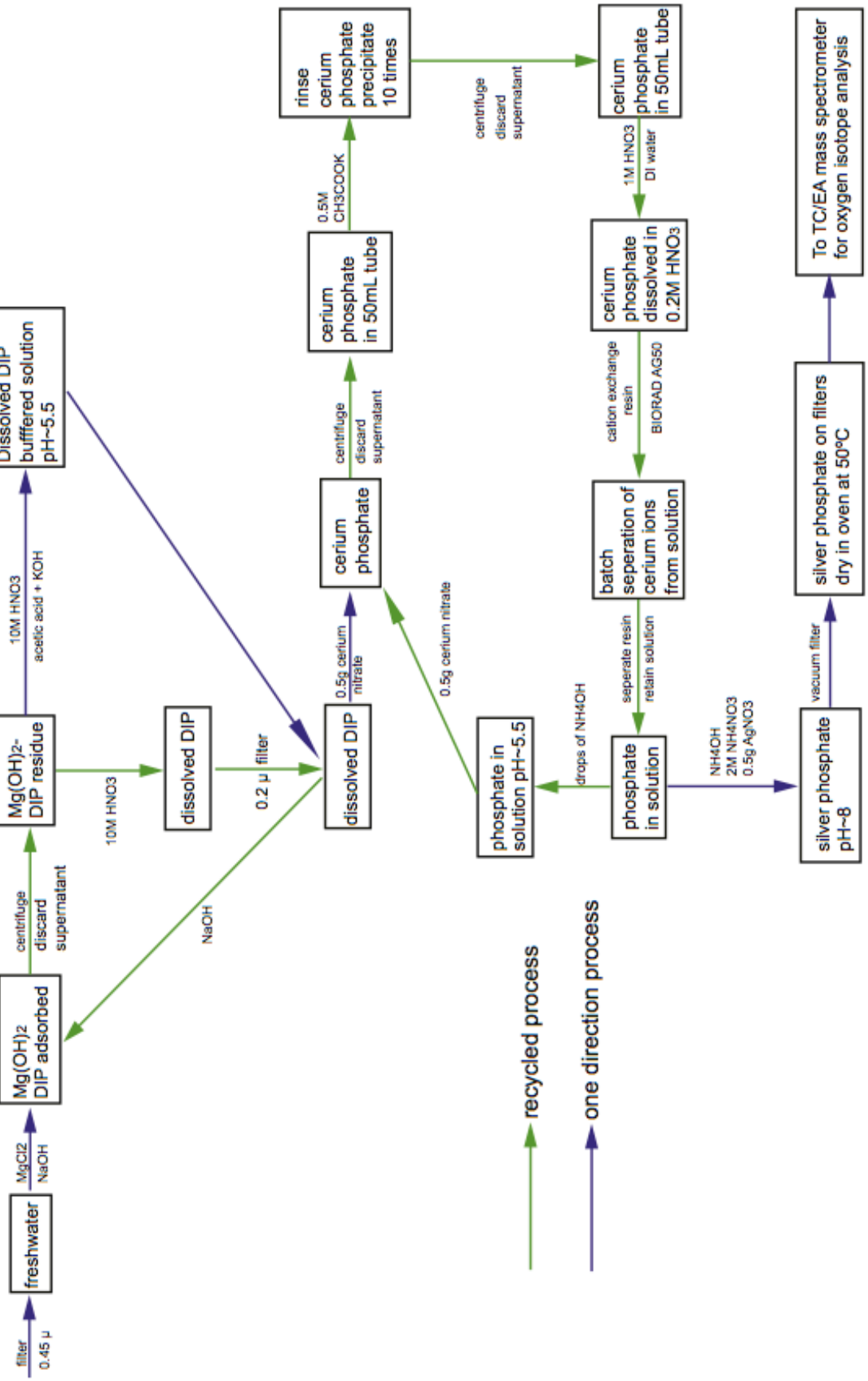

Fig 2.04: Modifications incorporated in Li (2009) for the removal of organic matter. Modifications include increased number of rinses of $CePO_4$ samples, as well as repeating the $CePO_4$ precipitation step.

McLaughlin et al. (2004) describes the use of 4 mL of BioRad AG-50X8 resin per sample. The volume of cation exchange resin was adjusted to 20 mL per sample to ensure Ce^{3+} removal, and the use of this resin was repeated for each $CePO_4$ sample, on two consecutive days. Following this, 1 mL of 2-M ammonium nitrate (NH_4NO_3) was added to each sample, and they were brought to a neutral pH through the use of concentrated ammonium hydroxide (NH_4OH) and 3-N HNO_3. The fast Ag_3PO_4 precipitation method of McLaughlin et al. (2004) was used, through the addition of 0.5 g silver nitrate ($AgNO_3$) dissolved in 2 mL of Millipore water. The pH was adjusted to 7 and samples were left overnight to precipitate. The following morning the pH was read using a pH probe, and any samples not at pH 7 underwent further pH adjustments, and were left another night to prevent incomplete precipitation.

Cleaning of the Ag_3PO_4 crystals was then carried out through the addition of 1 mL of 15% H_2O_2 (Tamburini et al., 2010). Samples were left to react for a day, allowing for OM oxidation, followed by a day of repeated rinses and centrifugation with Millipore water. They were each rinsed a minimum of 3 times, pipetted into small vials, and left to dry in the oven at 60^0C. Samples with high SRP concentrations, and therefore greater amounts of precipitate, were not rinsed through centrifugation, but were instead vacuum filtered onto polycarbonate filters, and rinsed with 200 mL of Millipore water. The filters were also left in the oven to dry. Once dry, 0.3-0.5-mg samples were weighed into silver capsules along with 1.5-mg of baked, nickelized carbon (Ni-C) as a catalyst for pyrolysis. Samples were sent to the U.S. Geological Survey in Menlo Park, California, where $\delta^{18}O\text{-}PO_4$ was determined.

Errors in this method arise if incomplete precipitation in any of the steps occurs. A loss of PO_4^{3-} could allow fractionation effects, biasing the final results through the loss of isotopically distinct O (Paytan & McLaughlin, 2011). This was monitored through SRP analysis of the supernatant following the precipitation reactions.

2.3 Results

2.3.1 Physical and chemical measurements

Temperature was similar between the upstream (Bridgeport) and downstream (Victoria, Blair) sites on all sampling dates (Fig 2.05). Spring temperatures (May/June) for all three sites averaged 20.9^{0}C, with a summer average of 22.8^{0}C (July-September). SRP concentrations ranged from 1.4 to 4.0 μg P L^{-1} at Bridgeport, 1.9 to 6.0 μg P L^{-1} at Victoria, and from 5.3 to 116 μg P L^{-1} at Blair (Fig 2.05). The $\delta^{18}O\text{-}H_2O$ values increased from June to September with a range from -7.7 to -9.8‰ and an average of -8.8‰ (Fig. 2.05). The $\delta^{18}O\text{-}H_2O$ rose over the sampling period, with the highest values observed in September. The calculated $\delta^{18}O\text{-}PO_4$ equilibrium values throughout the spring and summer were similar, with an average value of 12.1‰ (SD ± 1.0) using Eq. 2.2.

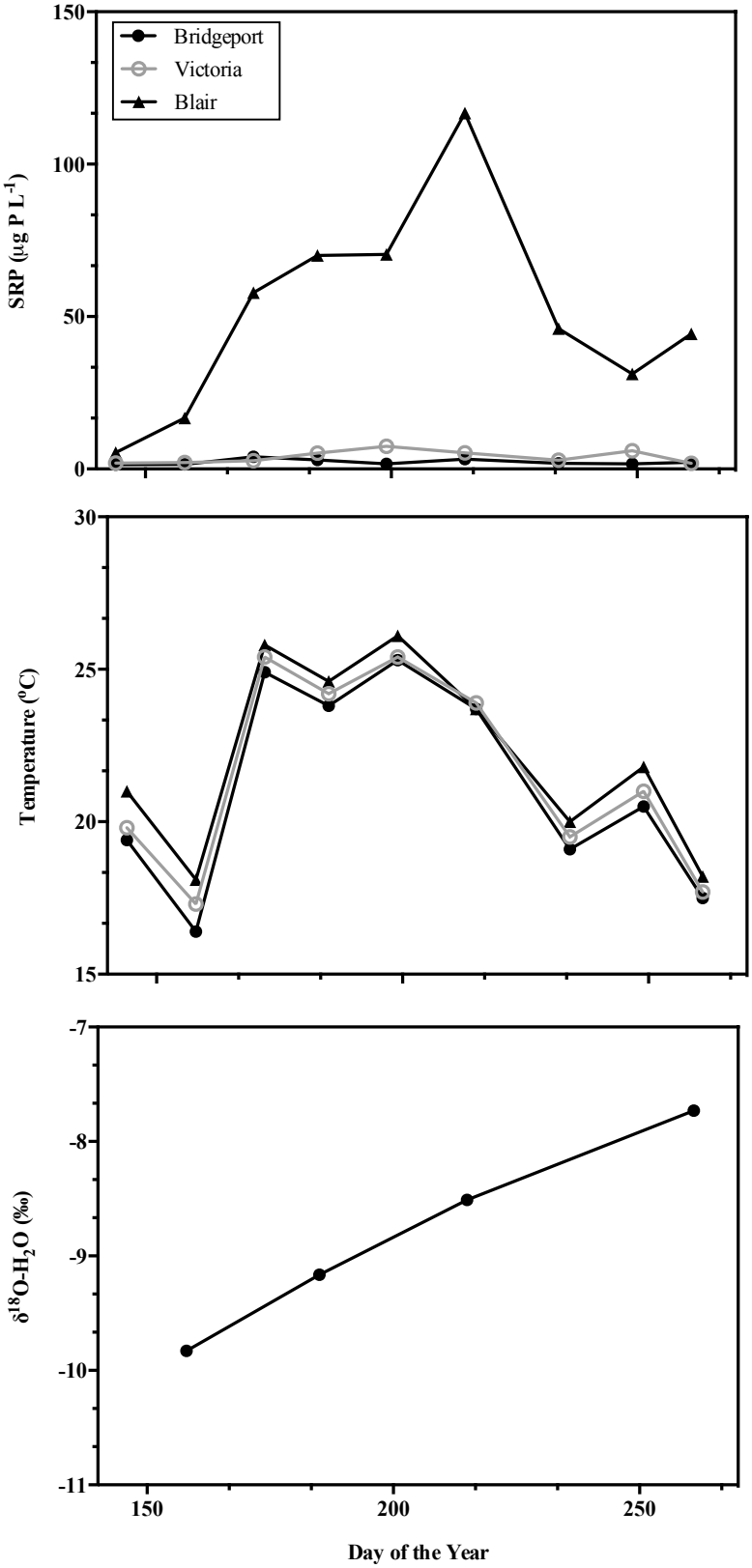

Figure 2.05: SRP, and temperature data for the Grand River for all sampling dates over the summer of 2012. Also included are the $\delta^{18}O$-H_2O signatures obtained from Bridgeport from each sampled month.

2.3.2 Method effectiveness for the removal of contaminants and reproducibility

MagIC precipitation allowed approximately 50% of the DOC to be discarded with the supernatant (Table 2.01). This left 3.5-4.1 mg C L^{-1} of DOC after the initial precipitation reaction. Three different methods were tested for DOM removal effectiveness by measuring the DOC removed from whole water Bridgeport samples collected on May 9th (Table 2.02). The DAX-8 resin removed approximately 40% of the DOC and 20% of the SRP. This method by Tamburini et al. (2010) also includes the use of a H_2O_2 pre-treatment of the Ag_3PO_4 crystals, which was not accounted for in this test. The addition of 1-mL of 10% H_2O_2 to the DOM-contaminated Ag_3PO_4 crystals was observed to cause a visual reduction in the dark brown shade of the precipitate, consistent with the removal of DOM. Samples that had the resin added directly to them had SRP recoveries of 75-85%. The resulting solution was lighter in colour, having lost some, but not all, of the yellow discolouration.

Table 2.01: DOC results following filtration and MagIC for the Grand River sites, collected on June 20th. The DOC remaining represents the amount of organic matter left over in the $Mg(OH_2)$ precipitate.

Site	Step	DOC (mg C L^{-1})	DOC Remaining (mg C L^{-1})	% DOC Remaining
Bridgeport	Unfiltered	6.9		
	Filtered to 0.7	6.8		
	MagIC Supernatant	3.3	3.5	52
Victoria	Unfiltered	7.4		
	Filtered to 0.7	7.4		
	MagIC Supernatant	3.3	4.1	55
Blair	Unfiltered	7.9		
	Filtered to 0.7	7.6		
	MagIC Supernatant	4.3	3.6	46

Table 2.02: Assessing the effectiveness of DOM removal methods using whole water Bridgeport samples, collected on May 9th.

Method	% DOC Removal	% SRP Recovery
Charcoal	87	3.3
Ultrafiltration (3000 Dalton)	33	65
DAX-8 Resin (column)	40	82

Samples processed using the DAX-8 resin method alone generated a dark brown to black Ag_3PO_4 precipitate, with the average percent O at 20.5% (SD ± 9.5). The percent O yield for pure Ag_3PO_4 is 15.3%, with higher percentages reflecting contamination by other O-containing species. Two samples in this batch were also found to possess low O yields (5.9%, 4.9%), representing a contaminant that possesses less than 15% O. It was determined through ICP analysis that the 4.5 mL of cation exchange resin was failing to remove all cations, including Ce^{3+}, from the samples prior to Ag_3PO_4 precipitation. One concern associated with lingering cations includes leftover Ce^{3+} reacting with PO_4^{3-}, causing incomplete Ag_3PO_4 precipitation, inducing fractionation. Since $CePO_4$ (O yield: 27.2%), possesses a higher O yield than Ag_3PO_4, it was unlikely that this had occurred in the low O yield samples. Another concern is associated with excess $Ce(NO_3)_3$ or $AgNO_3$ from the final two precipitation reactions. Lingering NO_3^- could contribute to the measured O signatures, resulting in increased O yields. Several samples in the initial batches possessed O yields above 30%, which could be explained by DOM or residual reagent O. These high O yields were only observed among samples collected prior to June 20th, 2012. All samples run after June 20th included the Li-modifications, which appeared to eliminate most of the high O yields. Samples possessing low O yields remained prevalent among all subsequent batches, representing a persistent low O-bearing contaminant (Fig. 2.06 A, B). Although contaminants possessing little to no O should not contribute to the observed $\delta^{18}O\text{-}PO_4$ signature, they can cause O yields that are too low for reliable detection when analyzed on a mass spectrometer.

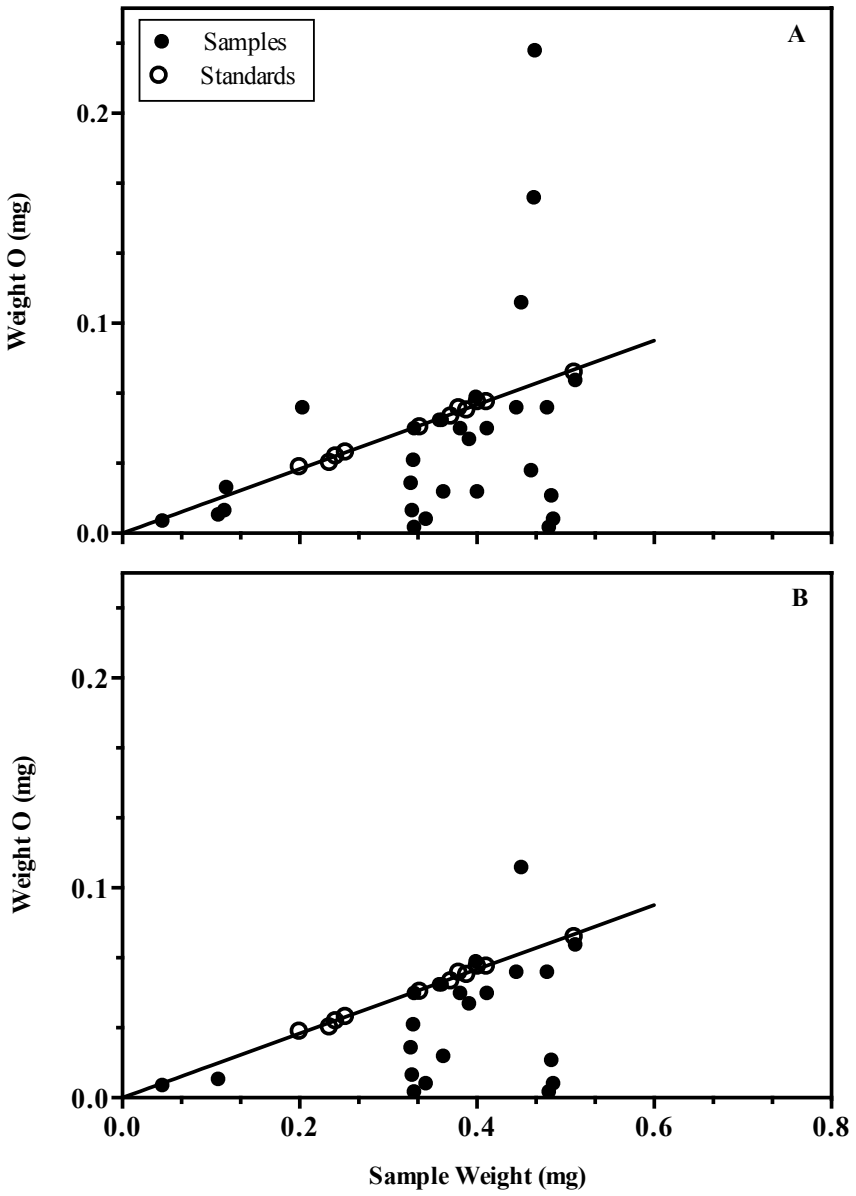

Figure 2.06: O yields for a) all samples analyzed, and b) samples run after June 20th only (using the Li-modified method) from the Grand River sites, and from Waterloo and Kitchener WWTP effluent over the summer of 2012. Included are data for pure Ag_3PO_4 standards possessing 15.3% O by weight, and the theoretical line for pure Ag_3PO_4 samples.

Natural river samples, with lower SRP, possessed a wider range of O yields than samples collected from the WWTPs, with higher SRP. These samples usually possessed O yields closer to 15% (Fig. 2.07 A, B). To determine the effect of the Li-modified method and lingering cations on the O signature of real river water, two samples were collected from Bridgeport on December 19th 2012 for $\delta^{18}O\text{-}PO_4$ determination. These samples were filtered and carried through MagIC, as described in section 2.2.4, however the $Mg(OH_2)$ precipitate was discarded and the supernatant was kept for analysis. It was then was spiked with potassium phosphate (K_2HPO_4) possessing a known $\delta^{18}O\text{-}PO_4$ signature (12.9 SD ± 0.2‰), and was carried through the MagIC procedure again. These samples were processed, and resulted in $\delta^{18}O\text{-}PO_4$ signatures of 13.0 ± 0.0‰ and 14.4 ± 1.4‰. This represents an offset from the real value of +0.1‰ and +1.5‰ respectively. The spiked samples had SRP concentrations between those observed at the Kitchener WWTP and those observed at the downstream site at BLA, with concentrations of 178 μg P L^{-1} and 211 μg P L^{-1}. This corresponded to average O yields of 14.4% and 15.5% respectively, which is similar to the ideal of 15.3%. These samples illustrated the success of the Li-modified method for samples possessing high SRP.

Several river samples showed N peaks when analyzed, representing a contaminant of the Ag_3PO_4 which was likely derived from one of two sources. Either N was present as NO_3^-, left over from one of the final two precipitation steps ($AgNO_3$ or $Ce(NO_3)_3$), or it resulted from organic matter contamination. Based on the discolouration of many of the upstream samples, it was concluded that organic matter persisted in some samples even after inclusion of several DOM removal steps. This problem was greatest among samples from the river sites (Bridgeport, Victoria and Blair), compared to the WWTP samples. A positive relationship between O isotopic composition and percent O yield was observed among river samples ($r = 0.78$, $p < 0.0001$, Fig. 2.08), which was particularly evident amongst samples possessing low O yields (<10%). This suggests the presence of a contaminant possessing little to no O potentially causing unreliable mass spectrometric analysis at these low O yields. No correlation was observed between these two parameters for WWTP effluent samples ($r = -0.04$, $p = 0.89$).

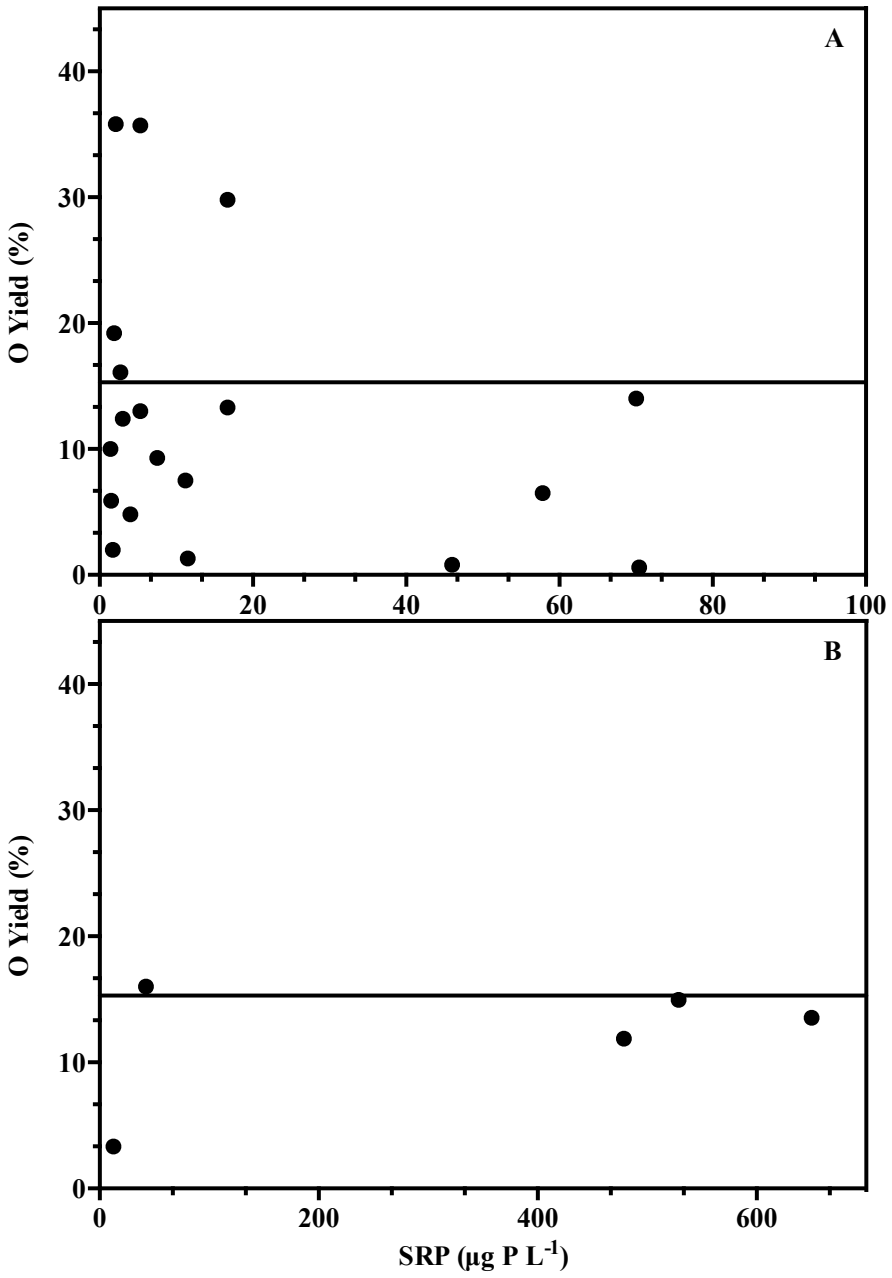

Figure 2.07: Relationship between SRP and % O yield for a) all samples from the Grand River sites at Bridgeport, Victoria, and Blair, and b) the Waterloo and Kitchener WWTPs for the summer of 2012. Also included at 15.3% O by weight is a line representing pure Ag_3PO_4.

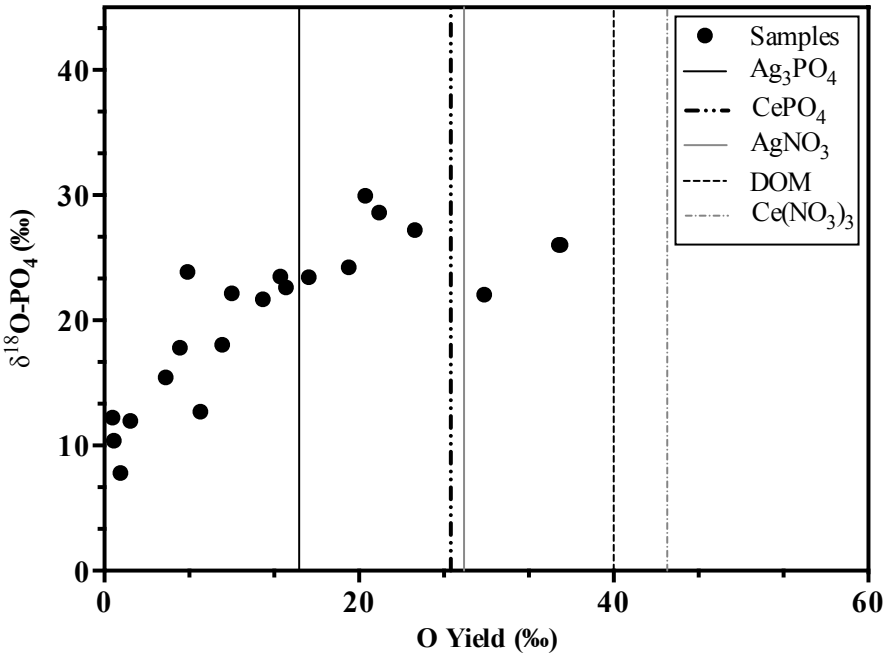

Figure 2.08: Observed relationship between O isotopic composition and % O yield for all samples from the Grand River sites at Bridgeport, Victoria, and Blair for the summer of 2012. Also included are lines representing the possible sources of contamination that could alter the observed O isotopic composition. The line representing DOM assumes that DOM is approximately 40% O by weight.

Method reproducibility was tested at the Blair site, which possessed the highest SRP among the river sites, and where an extra carboy was filled with river water on each sampling date. When sufficient SRP was present, the carboys collected at Blair were run separately allowing for an evaluation of experimental reproducibility. This was also done at the Kitchener WWTP where 10 L of sample were collected on each sampling date, and split into two 5-L replicates. These samples were run through the method separately, and were often analyzed on the mass spectrophotometer on different dates (Table 2.03). Blair samples showed poorer reproducibility than WWTP effluent, with a large range in $\delta^{18}O$ values between replicates on June 6th (22.1, 35.2‰), and June 20th (30.6, 17.9‰). Good reproducibility was however observed among the May 23rd samples, where sample replicates were within 2.4‰ despite possessing very different O yields. Similarly, good reproducibility was observed for the July 3rd samples for both O yield and isotopic composition.

The PO_4^{3-} yields from the first two precipitation reactions ranged from 65 – 85% with 15-35% of the PO_4^{3-} lost through analysis. Greatest amounts were lost through modifications to the method for organic matter removal, particularly the DAX-8 resin filtering, and repeated rinses of $CePO_4$. These were deemed acceptable losses, as these steps were unlikely to cause fractionation. Further sample loss was incurred due to the final precipitate adhering to the glass vials when left to dry. This resulted in some samples being present in quantities too small to analyze.

Sample analysis was most difficult for samples possessing low SRP, which affected the river samples to a greater degree than the WWTP effluent. Low SRP occasionally caused insufficient Ag_3PO_4 for analysis, and led to incomplete data sets for some of the sampling dates. Lower concentrations of SRP also necessitated larger sample sizes, causing greater amount of DOM to be concentrated into the river samples. More sample rinsing and cleaning steps were required for the river samples and caused further PO_4^{3-} losses through these steps. No samples possessing O yields higher than 20% will be included in this analysis. Care must also be taken when interpreting samples possessing very low O yields. At very low O yields even well-conditioned nickelized carbon,

added to the samples to aid in pyrolysis, can significantly contribute to the O content of these samples. Correcting for this effect can be difficult when samples possess O weights lower than the smallest standard that can be analyzed (O weight: 0.008 mg). Samples possessing O yields below 5% will not be included in this analysis. Almost all of the effluent samples possessed O yields close to pure Ag_3PO_4. Only one effluent sample possessed O yields outside of this range, from the Waterloo WWTP on July 30th (O yield: 50%) and is excluded from this analysis.

Table 2.03: Reproducibility among replicate samples with high SRP (Kitchener WWTP effluent) and low SRP (Blair). Also included are the results for the method evaluation tests on whole water Bridgeport samples spiked with PO_4^{3-}. $\delta^{18}O$ values are expressed as the mean ± SD for sample duplicates run through the mass spectrophotometer when sufficient sample was present.

Sample	SRP (μg P L^{-1})	% O Yield	$\delta^{18}O$ (‰ VSMOW)	Average $\delta^{18}O$ for Replicates (‰ VSMOW)	σ (‰ VSMOW)
K_2HPO_4 spiked Bridgeport #1	178	14.4	14.4 ± 1.4		
K_2HPO_4 spiked Bridgeport #2	211	15.5	13.0 ± 0.0	13.7	1.0
Kit. WWTP (23 Aug 2012) #1	528	15.0	13.7 ± 0.1		
Kit. WWTP (23 Aug 2012) #2	528	15.1	12.5 ± 0.4	13.1	0.8
Kit. WWTP (19 Sept 2012) #1	479	11.9	20.0		
Kit. WWTP (19 Sept 2012) #2	479	11.0	18.1	19.0	1.3
Blair (23 May 2012) #1	5.3	35.7	26.0 ± 0.2		
Blair (23 May 2012) #2	5.4	13.0	28.4 ± 0.6	27.2	1.7
Blair (6 June 2012) #1	16.7	29.8	22.1 ± 1.9		
Blair (6 June 2012) #2	16.7	13.3	35.2 ± 0.7	28.6	9.3
Blair (20 June 2012) #1	57.8	4.9	30.6		
Blair (20 June 2012) #2	57.8	8.1	17.1	23.9	9.6
Blair (3 July 2012) #1	70.0	14.3	22.6 ± 0.4		
Blair (3 July 2012) # 2	70.0	13.8	23.5	23.1	0.6

2.3.3 $\delta^{18}O - PO_4$ in the Waterloo and Kitchener WWTPs

Effluent samples displayed a range of $\delta^{18}O$ -PO_4 signatures from 10.4 to 22.8‰ (Table 2.04). Most of the variation in isotopic composition was observed at the Kitchener plant, which had a range of 12.5 to 22.9‰ (n = 3). The Kitchener plant possessed the larger $\delta^{18}O$ -PO_4 values on both days where the Kitchener and Waterloo effluent were analyzed. Equilibrium values were calculated using temperature and the $\delta^{18}O$ –H_2O values from the river site at Bridgeport. Expected equilibrium was calculated using Eq. 2.2 and only differed by 1.4‰ for all three sampling dates. The Kitchener plant possessed an $\delta^{18}O$-PO_4 value of 22.8‰, representing an offset from equilibrium of +11.9‰. This was the largest offset observed amongst the WWTP samples, and corresponded to the highest measured SRP, 650 μg P L^{-1}. A suggestive (r = 0.80) but non-significant (p = 0.10, n = 5) correlation between the offset from equilibrium and SRP was observed among the WWTP samples (Fig. 2.09). On August 23rd however, both the Kitchener and Waterloo plants possessed $\delta^{18}O$ values close to the theoretical river equilibrium (Fig. 2.10). The other two sampling dates showed the Kitchener WWTP to have large offsets from river equilibrium. No significant difference between the river equilibrium and the mean $\delta^{18}O$ was observed for all effluent samples over all sampling dates (paired t-test, p = 0.32, n = 5), but a large range was observed at the Kitchener WWTP.

Table 2.04: Waterloo and Kitchener WWTP $\delta^{18}O$ values for the summer of 2012. Included are the SRP values, % O yields, and the sample replicates for the Kitchener WWTP. $\delta^{18}O$ values are expressed as the mean ± SD for sample duplicates, when sufficient Ag_3PO_4 was present.

Plant/ Sample #	Date	SRP (μg P L^{-1})	% O Yield	$\delta^{18}O$ (‰ VSMOW)	Offset from Equilibrium (‰ VSMOW)
Kitchener	30-Jul-12	650	13.6	22.8 ± 0.1	12
Waterloo	23-Aug-12	12.6	3.42	10.6 ± 0.4	-2.2
Kitchener #1	23-Aug-12	528	15.0	13.7 ± 0.1	0.9
Kitchener #2	23-Aug-12	528	15.1	12.5 ± 0.3	-0.3
Waterloo	19-Sep-12	42.3	16.4	12.1 ± 0.5	-1.0
Kitchener #1	19-Sep-12	478	11.89	20.0	6.9
Kitchener #2	19-Sep-12	478	10.98	18.1	5

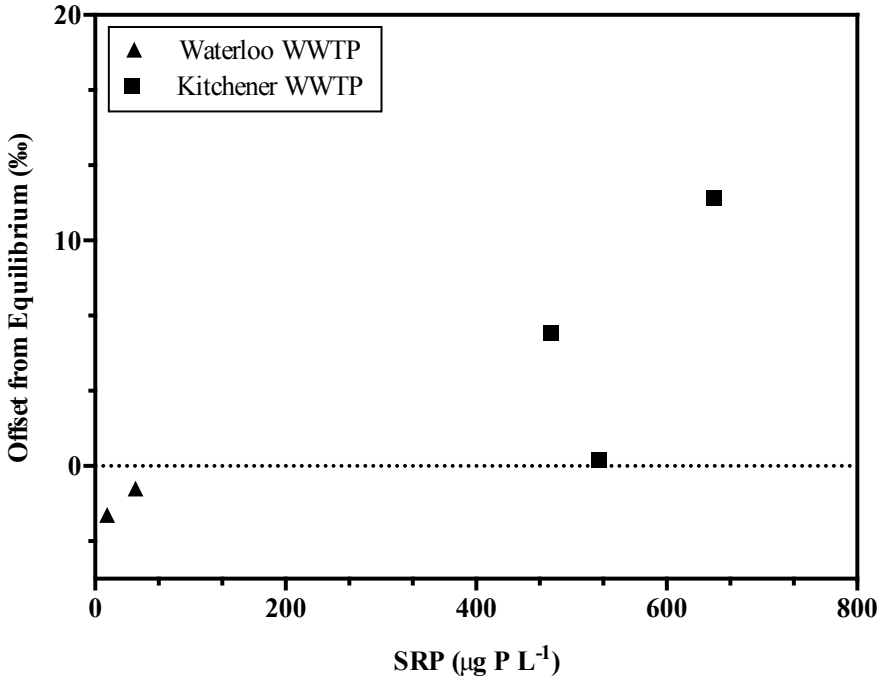

Figure 2.09: Offset from equilibrium as a function of SRP, for the Kitchener (■) and Waterloo (▲) WWTPs for the summer of 2012. The Kitchener WWTP values represent an average of two replicate samples for August 23rd, and September 19th.

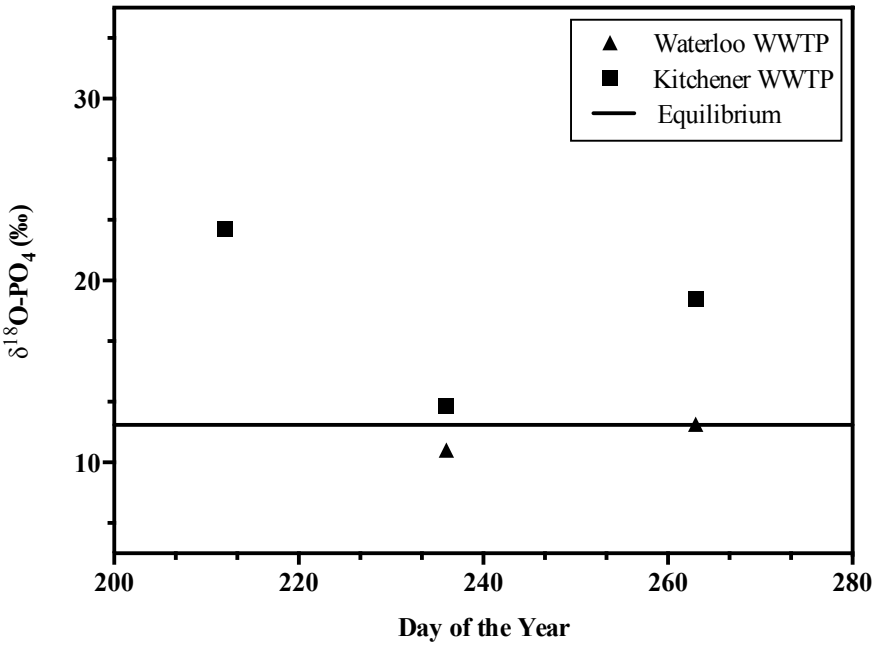

Figure 2.10: $\delta^{18}O$ -PO_4 values for the Kitchener (■) and Waterloo (▲) WWTPs over the summer of 2012. Also included is a line representing the average river equilibrium. The Kitchener WWTP values represent an average of two replicate samples for August 23rd, and September 19th.

2.3.4 $\delta^{18}O - PO_4$ in the Grand River

Samples collected from Bridgeport, upstream of the Waterloo WWTP, possessed a range of $\delta^{18}O\text{-}PO_4$ values between 13 and 22‰, with a mean of 19‰ (SD ± 4.4, n = 4) corresponding to an offset from equilibrium between -0.2 and 11‰ (Table 2.05). The relationship between $\delta^{18}O\text{-}PO_4$ and percent O yield at Bridgeport was not significant ($r = 0.68$, $p = 0.32$), but the two samples possessing the highest O yields (May 23rd and July 3rd) also possessed the highest $\delta^{18}O$ values and the largest offsets from the theoretical equilibrium (approximately 11‰). Elevated $\delta^{18}O\text{-}PO_4$ values are often ascribed to an isotopically enriched PO_4^{3-} source. Bridgeport is located downstream of the Conestogo River, delivering largely agriculturally derived nutrients. A Conestogo River sample from June 20th possessed an $\delta^{18}O$ value of 27‰, with a SRP of 5.9 μg P L^{-1}. Correlation analyses found no relationship between SRP and the offset from equilibrium for all samples from all river sites using the Pearson's Correlation Coefficient ($r = 0.19$, $p = 0.55$, Fig. 2.11a). Eliminating the two Blair samples with the highest SRP and intermediate offsets from equilibrium (June 20th and July 3rd) result in a significant positive relationship between SRP and the offset from equilibrium using the Pearson Correlation Coefficient ($r = 0.68$, $p < 0.05$, Fig 2.11b).

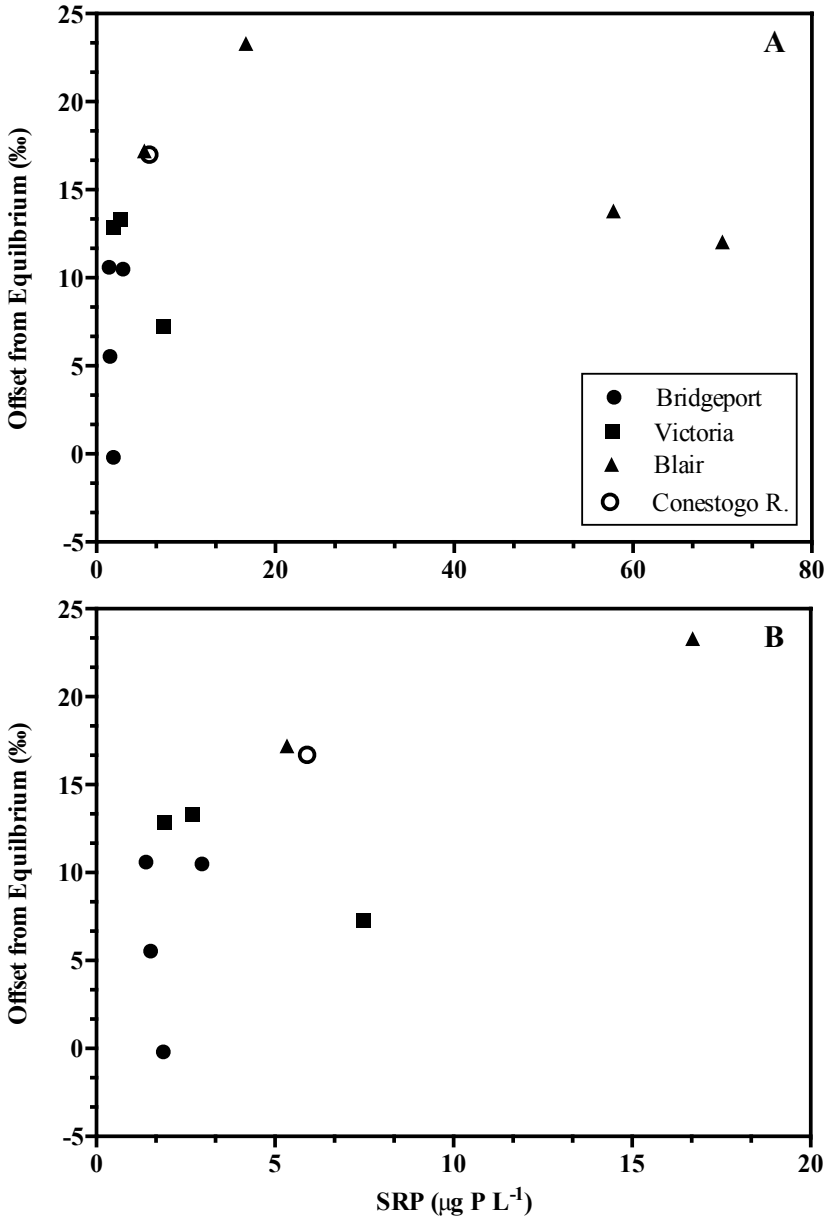

Figure 2.11: Offset from equilibrium (observed $\delta^{18}O$ – equilibrium $\delta^{18}O$) as a function of SRP for a) all river sites over the summer of 2012 and b) the low SRP river samples (excluding the June 20th and July 3rd Blair samples).

Table 2.05: $\delta^{18}O$ values for the river sites over the summer of 2012. Included are the SRP values, % O yields, temperature, conductivity, offset from the theoretical equilibrium, and sample replicates for Blair. $\delta^{18}O$ values and % O are expressed as the mean ± s.d for sample duplicates, when sufficient Ag_3PO_4 was present. Only samples possessing less than 20% O and greater O content than the lowest O bearing standards are included in this table.

Site	Date	SRP (μg P L^{-1})	% O Yield	$\delta^{18}O$ (‰ VSMOW)	Temperature (°C)	Conductivity (μS cm^{-1})	Offset from Equilibrium (‰ VSMOW)
Bridgeport	23-May-12	1.4	10.0	22.2	19.4	458	11
Bridgeport	6-Jun-12	1.5	5.9	17.8	16.4	526	5.5
Bridgeport	3-Jul-12	3.0	12.4 ± 2.8	21.7 ± 2.9	23.8	448	11
Bridgeport	21-Aug-12	11.2	7.5 ± 0.1	12.7 ± 0.3	19.1	401	-0.2
Victoria	23-May-12	1.9	19.2	24.3	19.8	626	13
Victoria	20-Jun-12	2.7	16.1 ± 1.1	23.5 ± 0.3	25.0	621	13
Victoria	17-Jul-12	7.5	9.3 ± 2.0	18.0 ± 0.2	25.4	582	7.2
Blair	23-May-12	5.3	13.0 ± 1.4	28.4 ± 0.6	21.0	660	17
Blair	6-Jun-12	16.7	13.3 ± 0.8	35.2 ± 0.7	18.1	728	23
Blair #1	20-Jun-12	57.8	4.9	30.6	25.8	751	21
Blair #2	20-Jun-12	57.8	8.1	17.0	25.8	751	7.0
Blair #1	3-Jul-12	70.0	14.2 ± 0.2	22.6 ± 0.4	24.6	638	12
Blair #2	3-Jul-12	70.0	13.8	23.5	24.6	638	12
Conestogo R.	20-Jun-12	5.9	13.0 ± 0.4	26.6 ± 0.1	26.8	444	17

The Victoria site had an average $\delta^{18}O$-PO_4 value of 22‰ (SD ± 3.4, n=3). These three dates had offsets from equilibrium of 13, 13, and 7.2‰. No relationship was observed between the offset from equilibrium and SRP at Victoria, where the sample with the highest SRP (7.5 μg P L^{-1}) had the lowest deviation from equilibrium (7.2‰). There were too few data to assess the relationship between $\delta^{18}O$-PO_4 and percent O yield at Victoria.

Since the Waterloo WWTP possessed $\delta^{18}O$-PO_4 values showing less variability than the Kitchener plant, I used an average of the two values from the Waterloo plant (11.35‰) to estimate the contribution of this plant on the Victoria site. Source apportionment was carried out for the May 23rd Victoria value (24.3‰), as this was the only date when a corresponding upstream value, at Bridgeport (22.2‰), was available. A two end-member linear mixing model was used based on the following mass balance equations:

$$\delta^{18}O - PO_4\, mix = (\delta^{18}O - PO_{4\ WWTP} \bullet fPO_{4\ WWTP}) + (\delta^{18}O - PO_{4\ Up} \bullet fPO_{4\ Up})$$

$$1 = fPO_{4\ WWTP} + fPO_{4\ Up} \quad (2.4)$$

where f is the proportion of each source to the mixture. The above equations resulted in greater than 100% of the PO_4^{3-} at Victoria to be derived from the upstream site at Bridgeport (119%). The Victoria site possessed a higher $\delta^{18}O$-PO_4 value than either Bridgeport or the Waterloo WWTP, causing a greater than 100% contribution from Bridgeport.

As discussed, Blair possessed the highest SRP among the three river sites allowing for sample reproducibility to be assessed. Only one of the sample replicates from both May 23rd and June 6th possessed O yields below 20%, and are included in Table 2.05. The sample collected for Blair on July 3rd displayed an $\delta^{18}O$ value very similar to that of Bridgeport from this same date. Blair however possessed a much higher SRP concentration than Bridgeport on this date. The average $\delta^{18}O$ at Blair was 28‰ (SD ± 5.6, n = 4), with offsets from equilibrium ranging from 7 to 23‰. Once again no significant relationship was found between O yield and $\delta^{18}O$-PO_4 at Blair ($r = 0.38$, $p = 0.61$).

At all river sites, $\delta^{18}O$-PO_4 decreased over the summer, with values closer to equilibrium later in the summer (Fig. 2.12). This trend is not consistent with that observed amongst the WWTP effluent samples, however the limited dataset makes it difficult to assess the effluents' temporal trends. The decline in $\delta^{18}O$-PO_4 with day of the year was not however significant at any of the sites (ANCOVA, $p > 0.05$). There was also no significant difference in the slope or elevation of the change in $\delta^{18}O$-PO_4 with day of the year between the sites (ANCOVA, $p < 0.05$).

There was also no relationship between $\delta^{18}O$-PO_4 and SRP among all of the river samples ($r = 0.18$, $p = 0.60$). Removing the two Blair samples with the highest SRP (June 20th, July 3rd) however, did result in a positive relationship between these two parameters amongst the low SRP samples ($r = 0.70$, $p < 0.05$). Blair was found to possess a significantly higher mean $\delta^{18}O$-PO_4 value than Bridgeport (un-paired t-test, $p < 0.05$) while the mean at Victoria was not significantly different than either of the other two sites (t-test, Bridgeport: $p = 0.21$, Blair: $p = 0.18$).

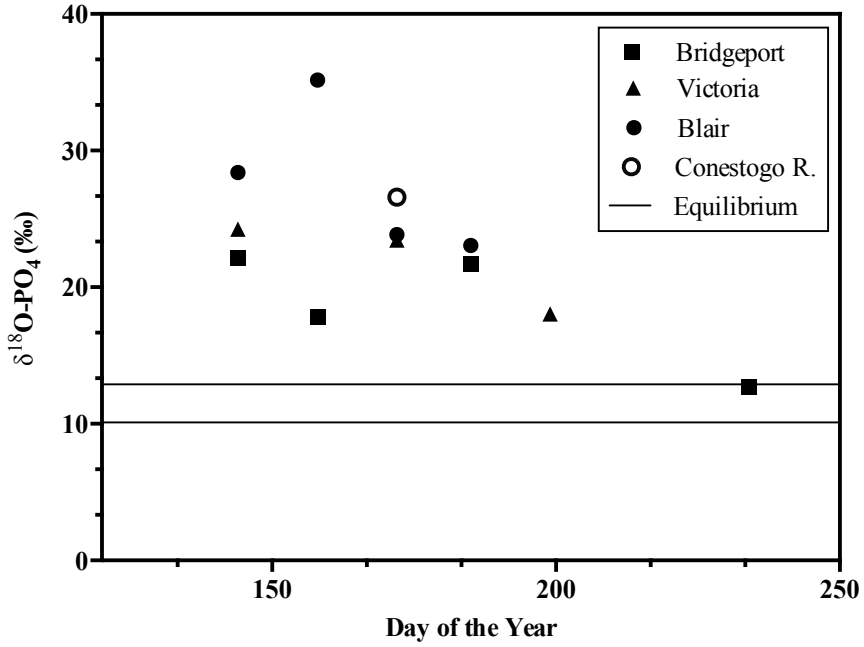

the river sites. Also included are two lines representing the range of calculated equilibrium $\delta^{18}O$ -PO_4 values for the river over the summer of 2012.

2.4 Discussion

Sample processing was most difficult for water taken from the river sites, as opposed to WWTP effluent. This was evident in the river data, in both the failure to produce reproducible Blair values at times, and the large range of O yields. PO_4^{3-} concentrations were lower in the river than the WWTPs, causing greater matrix effects amongst river samples due to the necessary difference in sample volumes. The cleanest precipitates, as shown by percent O yield, were generated from Kitchener WWTP effluent, where only 5 L of water was required. There was also a positive relationship between O yield and $\delta^{18}O\text{-}PO_4$ for the river data, but this relationship was not evident among samples taken from the WWTPs. One explanation for this relationship is a volume effect at low O yield that affects the operation of the mass spectrometer during sample analysis. This appears to be the most likely explanation given the strong positive relationship between O yield and $\delta^{18}O\text{-}PO_4$ at low O yields. This trend was not significant amongst the river samples after samples possessing percent O yields below the detection limit were excluded from the data set. Alternatively, a contaminant possessing high O content with elevated $\delta^{18}O\text{-}PO_4$ could cause a positive relationship between percent O yield and $\delta^{18}O\text{-}PO_4$. This however, would fail to explain the relationship between $\delta^{18}O\text{-}PO_4$ and O yield amongst samples possessing low O content, and would only explain samples possessing high percent O and elevated $\delta^{18}O\text{-}PO_4$.

The $\delta^{18}O$ signatures observed at Bridgeport displayed offsets from equilibrium that are much greater than what one might expect at a site located above the WWTPs. Bridgeport has low SRP during the summer months, which may create conditions of rapid recycling of the PO_4^{3-} pool, drawing the values down towards equilibrium. The signatures at Bridgeport could also reflect Conestogo River inputs that have high SRP and may be more reflective of source signatures. If Bridgeport reflects these two controls, deviations from equilibrium would be expected to increase as SRP increases. That is, as SRP increases, the reduced DIP requirements would result in slower uptake and decreased recycling of the PO_4^{3-} pool towards equilibrium. Reduced DIP cycling would cause $\delta^{18}O$ values to reflect source inputs, over equilibrium driven fractionation effects. However,

SRP was not found to correlate with the deviation from equilibrium at Bridgeport. A positive correlation between the offset from equilibrium and SRP was found however, when all of the low SRP samples were considered, from all sites. Potentially there are two few data points at the river sites to observe this relationship at any one site.

The Conestogo River delivers largely agriculturally derived nutrients. The $\delta^{18}O\text{-}PO_4$ signatures of fertilizer samples in other studies were found to be elevated compared to equilibrium (15.5 to 23.1‰; Young et al., 2009, Gruau et al., 2005) but not as high as the value from the Conestogo River (27‰). The previously published range of fertilizer values is similar to the $\delta^{18}O\text{-}PO_4$ signatures collected at Bridgeport (range: 13 to 22‰, mean: 19‰).

Another explanation for samples possessing disequilibrium values in PO_4^{3-} depleted environments is isotopic fractionation accompanying extracellular enzyme activity during DOP hydrolysis. These extracellular enzymes impart negative fractionation effects on the freed $PO_4^{3-,}$ causing lower observed $\delta^{18}O\text{-}PO_4$, while the residual DOP is left enriched. This process affects low PO_4^{3-} sites because a greater fraction of the PO_4^{3-} has come from the hydrolysis of DOP. Fractionation effects from DOP hydrolysis cannot explain the $\delta^{18}O\text{-}PO_4$ signatures at Bridgeport or the Conestoga River, where samples were elevated relative to equilibrium.

The $\delta^{18}O\text{-}PO_4$ values observed at Bridgeport are not significantly different than those collected at Victoria, despite the WWTP located between these two sites. The Waterloo WWTP had lower $\delta^{18}O\text{-}PO_4$ values than those collected at Victoria. Source apportionment led to none of the $\delta^{18}O\text{-}PO_4$ at Victoria explainable by the mean Waterloo WWTP signature. The only $\delta^{18}O\text{-}PO_4$ values for Victoria however are early summer samples (May to July) for which there is no corresponding Waterloo effluent value.

Blair consistently possessed the highest SRP among the three sites. The $\delta^{18}O\text{-}PO_4$ values obtained at Blair were elevated relative to Bridgeport and Victoria throughout the early summer.

The variations in $\delta^{18}O\text{-}PO_4$ at Blair could indicate the changing $\delta^{18}O\text{-}PO_4$ of the Kitchener WWTP effluent for those sampling dates. Even the lowest SRP values at Blair corresponded to large, positive deviations from equilibrium. Similarly, samples at Bridgeport and Victoria showed large positive deviations despite lower SRP concentrations. These large deviations indicate that even at the lowest observed SRP values, the $\delta^{18}O$ signatures were not experiencing rapid P cycling towards equilibrium, but were instead controlled by source inputs. The decline in $\delta^{18}O\text{-}PO_4$ in the river sites throughout the summer could indicate increased rates of biological cycling later in the summer (July, August). Higher biomass accumulation is expected during the warmer summer months potentially leading to higher rates of PO_4^{3-} cycling.

It is difficult to draw conclusions about the source of the elevated $\delta^{18}O\text{-}PO_4$ values found at all of the river sites without further information on the $\delta^{18}O\text{-}PO_4$ signatures from the Waterloo and Kitchener WWTPs, which appear to be quite variable. Given that both the Conestogo River and the Kitchener WWTP showed elevated $\delta^{18}O$ signatures, $\delta^{18}O\text{-}PO_4$ analysis could be a valuable tool to assess the contribution of these sources in future PO_4^{3-} studies.

Interpreting $\delta^{18}O$ values from WWTP effluent is complicated due to the mixing of multiple PO_4^{3-} sources entering the plant (i.e., human waste, detergents) and biological cycling towards equilibrium (Gruau et al., 2005). $\delta^{18}O\text{-}PO_4$ values have been found to vary between treatment stages and WWTPs, with variation potentially caused by differences in source water, temperature, and residence time in the plant (Young et al., 2009). The $\delta^{18}O\text{-}PO_4$ values obtained for the Waterloo and Kitchener plants fall within the range of $\delta^{18}O$ values observed in previous studies (Gruau et al., 2005: 16.6 to 18.2‰, Young et al., 2009: 8.4 to 14.2‰, Breaker, 2009: 25.2‰). These plants possess a wider range than has been previously observed in final effluent samples. The Waterloo plant possessed signatures very close to the theoretical equilibrium on both occasions. This may indicate that these $\delta^{18}O$ values are not displaying source values, but instead reflect a reset of the DIP pool within the WWTP through microbial processing. This conclusion was also drawn in the study

conducted by Gruau et al. (2005) where WWTP $\delta^{18}O$ values appeared to indicate rapid biological cycling. It is also interesting to note that the Waterloo WWTP possesses a significantly lower mean SRP concentration than the Kitchener plant (paired t-test, $p < 0.05$), and exhibited equilibrium-like $\delta^{18}O$-PO_4 values. The Kitchener plant however showed large offsets. This could indicate that the Waterloo effluent $\delta^{18}O$-PO_4 signatures are controlled primarily by equilibrium-driven fractionation, while the Kitchener plant is largely controlled by a PO_4^{3-} source with elevated $\delta^{18}O$-PO_4. Determining what controls the WWTP's signatures would be impossible without characterizing the O isotopic compositions of all the major PO_4^{3-} sources entering these plants. Differences in plant signatures could also be attributed to differences in treatment processes.

On two dates, the Kitchener WWTP possessed values that were not controlled by equilibrium-driven biological cycling. The $\delta^{18}O$ values (19‰, 23‰) appear to represent an isotopically enriched PO_4^{3-} source contributing to the DIP pool. The values reported here are almost as high as the WWTP effluent analyzed in the Illinois River watershed, which possessed a value of 25.2‰ (Breaker, 2009). Among the likely sources, PO_4^{3-} builders from detergents were analyzed by Gruau et al. (2005) and possessed $\delta^{18}O$ signatures of 17.9‰. Likewise, Young et al (2009) analyzed the signatures of PO_4-containing detergents and found a mean value of 16.8‰, with a range of 13.3 to 18.6‰. Since the PO_4^{3-} present in detergents are produced from the same phosphorite rocks used to create fertilizers, the signatures are expected to be similar (Young et al., 2009). The range in $\delta^{18}O$ values among fertilizers observed by Gruau et al. (2005) was between 19.6 and 23.1‰. The mean among all fertilizer data compiled by Young et al. (2009) was 20.2‰. Assuming detergents are the dominant source to the Kitchener WWTP, the results obtained in this study would corroborate these values.

Aside from variable source signatures, a major controller of WWTP values would be the residence time of the water in the plant. This would control the degree to which microbial processing drives the return to equilibrium $\delta^{18}O$ values. During the summer and fall of 2012 the

Kitchener WWTP was undergoing major upgrades (Region of Waterloo, 2012) resulting in variations in residence time and effluent quality (Eduardo Cejudo, Earth and Environmental Sciences, University of Waterloo, personal communication). Longer residence times should result in $\delta^{18}O$ values closer to the theoretical equilibrium, which is one possible explanation for the large range of $\delta^{18}O$-PO_4 values observed at the Kitchener WWTP.

2.5 Conclusions

The objective of this work was to determine if $\delta^{18}O$- PO_4 analysis was a useful tool for the study of effluent impacts on surface waters. This was done through the use of this tool in the Grand River watershed. In order for this to be accomplished, a method capable of removing DOM while preserving PO_4^{3-} concentration is required. I determined that much of the variation initially observed among river samples was caused by incomplete removal of O-bearing contaminants; either NO_3^{3-} from reagents or DOM from the river. Modifications to the McLaughlin method, including those of Li (2009), resulted in cleaner precipitates and eliminated most of the O-bearing contaminants. Even after the inclusion of this method however, some samples still possessed high O yields, suggesting persistent contamination of Ag_3PO_4 samples by DOM or another O containing contaminant. In addition, I hypothesize that samples possessing low O yields were plagued by a contaminant possessing little to no O (e.g., Ce^{3+}, Cl^-), potentially reducing their reliability when analyzed on a mass spectrometer. This was observed though the poor reproducibility amongst Blair samples, and the strong positive relationship between O yield and $\delta^{18}O$- PO_4, particularly amongst samples possessing very low O yields. Further work is required to find other modifications that allow for the convenient analysis of samples possessing low SRP.

The river samples showed $\delta^{18}O$- PO_4 values that were elevated relative to equilibrium. This indicates that these sites are not equilibrium-controlled, and instead possess $\delta^{18}O$ signatures controlled by either source inputs or fractionation effects. Both the Conestogo River and the

Kitchener WWTP were shown to deliver PO_4^{3-} that was elevated relative to equilibrium, and could explain the $\delta^{18}O$- PO_4 values observed at Bridgeport and Blair, respectively.

The successful isolation of clean Ag_3PO_4 precipitates from Kitchener WWTP effluent suggests that the Kitchener WWTP is supplying the Grand River with isotopically distinct PO_4^{3-}. This could be used to establish the effect of the WWTP inputs on the downstream PO_4^{3-} pool, provided a more effective method for samples with low SRP and DOM concentrations typical of temperate rivers in developed. The range in $\delta^{18}O$-PO_4 values observed in the Kitchener WWTP suggests that both equilibrium-driven fractionation and unique source inputs are contributing to these signatures. Characterization of the source inputs to the WWTPs would be useful for determining what influences these signatures, and why they exhibit such varied $\delta^{18}O$-PO_4 values. Future studies using $\delta^{18}O$-PO_4 analysis in riverine environments will need to be coupled with WWTP effluent analysis given the variability of the plant signatures.

Chapter 3: Use of ^{32}P-PO_4^{3-} to estimate sestonic and periphytic phosphate kinetics in the Grand River

3.1 Introduction

3.1.1 Nutrient spiraling

The term nutrient spiraling describes the cycling of nutrients in lotic environments. It includes the assimilation of a nutrient into the benthos, its utilization and temporary storage, and eventual remineralization into the water column (Ensign & Doyle, 2006). Uptake length, or spiraling length (S_w), is used as an index for nutrient spiraling, and provides a relative measure of the distance travelled by a nutrient molecule that enters a system in its inorganic phase prior to uptake (Mulholland et al., 1990). Calculation of S_w uses the turnover rate, or the uptake rate coefficient (k_r, time^{-1}), and the average stream velocity (v; distance x time^{-1}) as shown:

$$S_w = v/k_r \quad (3.1)$$

Uptake length is used to assess the nutrient retention efficiency of a stream environment, or the system's efficiency in utilizing an available nutrient pool (Mulholland et al., 1990). It offers a comparative tool that takes into account both the downstream transport of the nutrient as well as the biological transformations it undergoes after entering a stream (Marti et al., 1997). Both of these factors control the river's ability to retain the nutrients and materials it receives from the surrounding environment.

The majority of studies that have been carried out to determine uptake length have used one of two methods. The most commonly employed methods are whole-stream additions of PO_4^{3-} pulses, or radioisotope labeling of the PO_4^{3-} pool in chambers or enclosed experiments. The stable PO_4^{3-} approach involves the use of a conservative tracer (e.g., Cl^-), and short experimental run times, in order to minimize taxonomic changes, and prevent increases in plant or periphytic biomass (Mulholland et al., 1990). The major limitation is the change to uptake rates that can accompany

elevated PO_4^{3-} concentrations, with the PO_4^{3-} addition method found to consistently overestimate uptake length (Mulholland et al., 1990).

Due to the unsuitability of these experiments to assess uptake rates at ambient PO_4^{3-} concentrations, the radioisotope method may be preferred for observing natural P kinetics (Barlow-Busch et al., 2006). This method involves enclosing water and benthic communities taken from the river and placing them in continually circulating chambers or beakers. These chambers undergo additions of carrier-free ^{32}P- or ^{33}P-labelled PO_4^{3-}, allowing for measurements of gross uptake. The term gross uptake is used to describe what these radiotracer experiments reveal about P kinetics because they ignore the simultaneous PO_4^{3-} release that is occurring (Barlow-Busch et al., 2006). Although these experiments allow for calculations of uptake rates at ambient PO_4^{3-} concentrations, they impose significant perturbations to the enclosed biological communities (Barlow-Busch et al., 2006). Because of concerns regarding additions of radioactive tracers to natural systems, incubations are nevertheless used to estimate rates of uptake and simulate steady-state conditions. Steady state refers to the PO_4^{3-} concentration where PO_4^{3-} uptake equals PO_4^{3-} regeneration, and there is no net change in concentration with time (Barlow-Busch et al., 2006).

A previous study was carried out in the Grand River using ^{33}P-PO_4^{3-} to determine PO_4^{3-} turnover times, and estimate uptake length (Barlow-Busch et al., 2006). This study was carried out on a site upstream of both the Kitchener and Waterloo WWTPs, approximately 30 km downstream of the Shand Dam. PO_4^{3-} turnover was found to be rapid, when measured SRP was low. To determine the effect of the two WWTP on P kinetics, sites were chosen downstream of both plants where SRP concentrations are elevated due to the effluent inputs.

3.1.2 Research objectives

The objective of my study is to observe gross and net PO_4^{3-} uptake rates by seston and epilithon below two WWTPs within the Grand River watershed, in the Region of Waterloo. The chosen method involves radiolabelling the PO_4^{3-} pool in recirculating stream microcosms with

seston and epilithon from the river. This study ignores PO_4^{3-} uptake from the water column by macrophytes, and their associated epiphytes, as well as the interactions between macrophytes and the studied communities (seston and epilithon). My goal is to determine the effect of effluent inputs on uptake, release and steady state PO_4^{3-} concentrations. These measurements allow me to calculate the uptake length of PO_4^{3-} in an impacted stream ecosystem. A second objective is to determine estimates of V_{max} and K_s for predicting Michaelis-Menten uptake kinetics, at two sites on the Grand River. These values will lay the foundation for a predictive model capable of determining the effect of increasing PO_4^{3-} inputs on downstream PO_4^{3-} concentrations, and $\delta^{18}O$-PO_4 signatures. Along with the determination of these rates, I will address the following questions:

1) What are the PO_4^{3-} uptake and release rates downstream of two WWTPs and how do these compare with the rates observed by Barlow-Busch et al. (2006) at a site upstream of these plants?
2) What can this tell us about the ability of the river to assimilate PO_4^{3-} following point source enrichment?

3.2 Materials and Methods

3.2.1 Research sites

Sampling was carried out in the Grand River basin, in the Region of Waterloo. For a full watershed description, refer to the Materials and Methods section in chapter 2. The chosen research sites were Freeport, approximately 5 km upstream of the Kitchener WWTP, and Blair, located 6 km downstream of the same plant (Fig. 3.01). Freeport is downstream of both the confluence of the Conestogo River, a major tributary of the Grand River, and approximately 15 km downstream of the Waterloo WWTP. TP concentrations have been found to increase as the river moves downstream (Cooke, 2006), however a large increase in SRP has been noted at Blair. Summer SRP concentrations for the upstream site at Freeport are typically below 10 µg P L^{-1}. Typical SRP concentrations for the downstream site at Blair are often above 20 µg P L^{-1}, but can

reach concentrations of 100 µg P L^{-1}. Samples were collected from both sites within an hour of each other on five occasions: June 4th, June 6th, July 15th, August 6th, and September 25th, 2013.

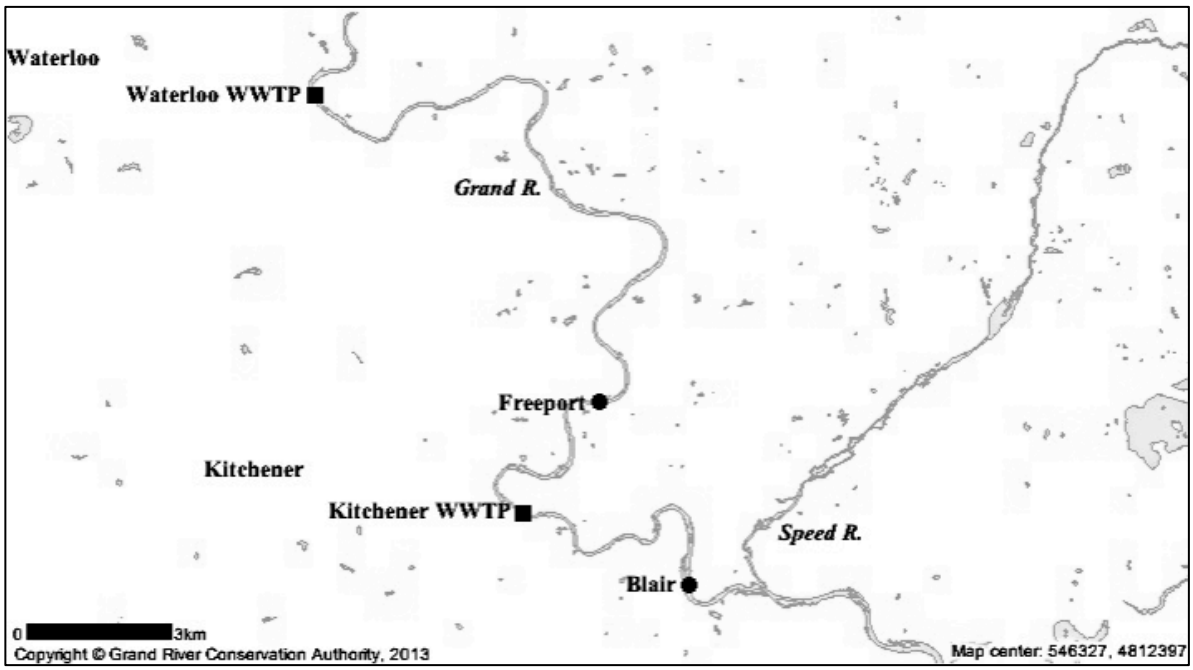

Figure 3.01: The Grand River watershed, showing the locations of the Waterloo and Kitchener WWTP and the two sampling sites (GRCA, 2013).

3.2.2 Sample collection and analysis

Sampling at Freeport and Blair over the summer of 2013 involved the collection and analysis of water samples for SRP, TP, and sestonic PO_4^{3-} uptake, as well as the collection of rocks for assessing periphytic PO_4^{3-} uptake and periphyton P. Gross uptake, net uptake, and PO_4^{3-} release experiments will be described in section 3.2.3. Collection and analysis of SRP samples was carried out as described in section 2.2.3. Collection of 40 mL of unfiltered water for TP analysis was done in 100-mL glass bottles using graduated syringes rinsed three times in river water prior to sample collection. All glassware was cleaned in 10% HCl, rinsed three times with deionized water, and air dried prior to use. TP samples were digested in hot 2.5% persulphate solution for 1 h. PO_4^{3-} analysis used the ascorbic acid - phosphomolybdate spectrophotometric method discussed previously.

Seston samples were collected in 2-L HDPE acid-washed bottles, which were rinsed three times in unfiltered river water prior to sample collection. Approximately 6 L of water was collected from each site with 500 mL of river water used in each ^{32}P experiment. Rocks of a similar size, approximately 10 cm in diameter, were collected from both sites in acid-washed plastic containers. I transported these containers as carefully as possible to prevent epiphytes from rubbing off the rock during transport. Water and rock samples were transported back to the lab, and uptake experiments began immediately upon return.

Rock surface area was determined several days after measurements for gross and net uptake were taken. The aluminum foil - weight method was used, where the exposed, upper surface of the rock (including top and sides) was wrapped in aluminum foil with the foil trimmed to fit the uneven rock surfaces. The foil was rinsed with water, and dried in the 60^{o}C oven overnight. After cooling, all foil pieces were weighed, and rock surface area was calculated as the product of the foil weight and the average ratio of foil area to foil weight from three 10 x 10 cm pieces of foil.

The rock surfaces were scraped and measurements of TP and ash free dry weight (AFDW) were taken. The rocks were rinsed and three sections of known area from each rock were scraped. The scrapings from each rock were filtered onto ashed GF/F glass fiber filters. The rocks were

stored frozen in plastic bags. Filters containing rock scrapings, or rinse water, were dried overnight (65^{o}C) and weighed. Filters were then ashed for 4 h at 500^{o}C, and AFDW was calculated as the difference between the dried and ashed weight. The subsample values were extrapolated to the rock's area, with the rinse water value added to the total weight. These values were expressed in units of mg AFDW cm^{-2}. The rock surface area, calculated using the tin-foil method, was used to determine the biomass per unit rock area. This method relies on the assumption that all biomass is present on the exposed rock surface, being the top and sides of the rock. The same method was used for finding seston biomass with whole water samples filtered onto GF/F filters, and the AFDW collected. This method allowed for a volumetric expression of seston biomass that was converted to units of μg P cm^{-2} using the river's depth. Areal units were chosen in order to compare epilithon and seston biomass. All AFDW determinations were corrected using the change in weight of a dried and ashed blank filter.

TP of the epilithon was found using the ashed filters. Each filter was placed into a 100 mL glass bottle with 100 mL of Millipore water. TP samples were analyzed using the protocol described above for whole water, but these values were corrected using bottles possessing unused ashed filters.

3.2.3 Methods for measuring gross uptake, net uptake, and PO_4^{3-} release

In order to estimate gross PO_4^{3-} uptake, the disappearance of carrier-free $^{32}PO_4^{3-}$ from solution was measured with time in stirred beakers enclosing periphytic and sestonic communities as in Barlow-Busch et al. (2006). To measure gross uptake, a rock was placed into a 1-L polypropylene beaker with 500 mL of river water. Eight to twelve gross uptake experiments were run on each sampling date. The sampling on June 4th included two replicate seston-only beakers, and two seston plus epilithon beakers for each site, which were all at ambient PO_4^{3-} concentrations. The gross uptake experimental setup for the other four days involved one ambient concentration beaker for each site, while the remaining beakers were spiked with different amounts of a 5 mg L^{-1} stock solution of K_2HPO_4 (Table 3.01). Experiments were carried out under laboratory lighting.

Table 3.01: Gross uptake experimental setup for the summer of 2013. Includes a list of PO_4^{3-} additions using 5 mg L^{-1} K_2HPO_4. Beakers containing samples from both Freeport and Blair were run under the described conditions.

Sampling Date	Concentration of PO_4^{3-} Added (µg P L^{-1})	Communities Present
June 4th	0 (with replicates)	Seston
	0 (with replicates)	Seston + Epilithon
June 6th	0, 2, 5, 8, 10, 80	Seston + Epilithon
July 15th	0, 2, 5, 10, 30, 80	Seston + Epilithon
August 6th	0, 2, 5, 10, 30, 80	Seston + Epilithon
September 25th	0, 2, 5, 10, 30, 200	Seston + Epilithon

Additions of 10^5 dpm mL^{-1} carrier- free ^{32}P-PO_4 were carried out in three beakers at a time. At 1, 5, 10, 15, 20, and 30 minutes following radiolabel addition, two 1-mL aliquots were taken from each of the three beakers. One aliquot was filtered through a 0.2-µm polycarbonate membrane filter and the filter was placed into a scintillation vial, while the other was left unfiltered and placed directly into a vial. After 30 min the next batch of three beakers was radiolabeled and this process was repeated. This method was carried out until all samples had been labeled and undergone the first 30 minutes of sampling. Aliquots were also taken at 1, 2, 3, 4, 5, and 24 h from each beaker. Additional sampling from the ambient concentration beakers occurred at the 30-min time point, where aliquots were filtered to 0.2, 2, and 20 µm. These aliquots allowed uptake to be partitioned between picoplankton, nanoplankton, and microplankton, respectively (Barlow-Busch et al., 2006). 10 mL of scintillation fluor was added to all vials prior to determining their ^{32}P content in a scintillation counter. The percentage of ^{32}P remaining in solution was calculated for each time point. The rate of decline of unfiltered "total" ^{32}P was used to estimate uptake by the epilithon, while the amount retained by the filters was used to estimate uptake by the seston.

Net PO_4 uptake was estimated in a similar manner to gross uptake however it involved eight beakers that had no ^{32}P or K_2HPO_4 additions. Upon return to the laboratory four beakers per site were set up containing two seston- only, and two seston plus epilithon experiments. This experimental setup allowed for replicate measurements of the net uptake carried out by both community types, with epilithon uptake being calculated as the difference between the beakers with and without rocks. Net uptake was found by measuring the change in SRP over time using the same time points as the gross uptake experiments.

Release rates were estimated in several ways. The first way involved calculating the difference between gross and net uptake. Assuming SRP is a suitable proxy for PO_4^{3-}, this difference should provide an estimate of the rate at which PO_4^{3-} is released back into solution. It further assumes there had been no release of the recently assimilated and ^{32}P- labeled PO_4^{3-}.

I also estimated release using a competitive inhibitor (unlabeled $^{31}PO_4$) to block the re-assimilation of $^{32}PO_4^{3-}$ in the gross uptake experiments (Hudson and Taylor, 1996). These release measurements were taken from the ambient concentration beakers, where the system was flooded with 5 mg P L^{-1} as K_2HPO_4. Then 0.5-mL aliquots were taken at 0, 1, 2, 3, and 4 h. Aliquots were filtered to 0.2 μm, placed in scintillation vials, and the filters were discarded, allowing for measurements of the re-appearance of the radiolabelled PO_4^{3-} in the dissolved pool. Release rates were determined as the slope of the released ^{32}P over time. This method will be referred to herein as the "Hudson method".

The purpose of carrying out multiple experiments to observe PO_4^{3-} release comes from the uncertainty that SRP is a suitable proxy for PO_4^{3-}. In the previous study of PO_4^{3-} release in the Grand River, negative release rates were calculated on several occasions using the difference between net and gross uptake. These negative values were likely due to the unsuitability of SRP to measure PO_4^{3-} (Barlow-Busch et al., 2006). The sites chosen for this study, however, possess higher SRP

concentration than those observed in most lakes as well as in the previous Grand River study. This could mean that SRP is a better estimate of PO_4^{3-} but that has not been determined.

3.2.4 Calculating gross uptake, net uptake, and PO_4^{3-} release

Gross uptake rate constants were found as the initial slope of the linear regression of ln(%^{32}P remaining) versus time. For epilithon this was calculated from the % total ^{32}P versus time, while seston was calculated from the % ^{32}P retained on 0.2 µm filters. These values represent the first order rate constants, expressed in units of time^{-1}. The total rate constant (seston + epilithon) is calculated by adding these two values, and the reciprocal of this value gives an estimate of turnover time (TT). Epilithon uptake rate constants required conversion from beaker- specific values (K_b), to areal estimates in the river (K_r) using the equation:

$$K_r = (K_b \times V)/(A \times D) \quad (3.2)$$

Where V represents the volume of river water used (500 mL), D is the depth of the river (cm), and A represents the surface area of the rock (cm^2) (Barlow-Busch et al., 2006).

Rate constants were converted to PO_4^{3-} uptake velocities (U: µg P cm^{-2} h^{-1}) using SRP (µg P L^{-1}) measured in the field, depth of the river (D) and the equation:

$$U = K_c \times SRP \times D/1000 \quad (3.3)$$

Net uptake velocities (U_N) were calculated as the slope of the line for change in SRP with time, where negative slopes represented positive net uptake rates. Epilithon rates were calculated as the difference between beakers with and without rocks, and were corrected by dividing by the area of the rock and multiplying by the beaker volume. These were also expressed in units of µg P cm^{-2} h^{-1} in order to compare them to the gross uptake velocities.

As previously described, release was calculated in multiple ways. The first allowed for regeneration to be expressed as a rate (R: µg P cm^{-2} h^{-1}), using the equation:

$$R = U_{Gross} - U_{Net} \quad (3.4)$$

The second calculation of release involved using the slope of the line for ^{32}P released into the dissolved pool (< 0.2 μm) versus time, following saturation with the ^{31}P competitive uptake inhibitor. This calculation provides a release rate in units of DPM mL^{-1} h^{-1}, which was converted to a release rate constant (K_r: d^{-1}) using the equation:

$$K_r = (^{32}P \text{ release}/\text{Initial } ^{32}P \text{ in Beaker}) \times 24 \quad (3.5)$$

The reciprocal of this value provides a measure of the turnover time for the particulate P pool, which can be converted to units of μg P cm^{-2} h^{-1} using the specific activity ($^{32}P/^{31}P$):

$$P \text{ release} = ^{32}P \text{ release} \times (\text{total P}/\text{total } ^{32}P) \quad (3.6)$$

The use of this equation involves several assumptions that are outlined in Hudson & Taylor (1996) and include: incubation conditions do not affect release, the ratio of ^{31}P:^{32}P is the same between the epilithon and the released material, ^{31}P addition does not lead to increased rates of ^{32}P release, and the amount of ^{31}P is sufficient to block re-uptake of ^{32}P.

Finally, release can be calculated using the observed steady state PO_4^{3-} conditions, found at the 24 h time point in the net uptake experiments. As discussed, steady state conditions refer to the PO_4^{3-} concentration where uptake equals regeneration (Barlow-Busch et al., 2006). Previous work carried out to model the controls on PO_4^{3-} concentrations use Michaelis-Menten kinetics to describe the relationship between uptake and nutrient concentration until saturation. The equation used to express this relationship is shown here:

$$U = (V_{max} \times [PO_4^{3-}])/(K_s + [PO_4^{3-}]) \quad (3.7)$$

Where U is the uptake rate (units in $[PO_4^{3-}] \times time^{-1}$), V_{max} is the maximum uptake rate (units in $[PO_4^{3-}] \times time^{-1}$), and K_s is the half saturation constant (units in $[PO_4^{3-}]$; Dodds, 1993). Using estimates of V_{max} and K_s allows for the uptake rate at steady state PO_4^{3-}concentration to be

calculated, providing an estimate of regeneration (μg P cm^{-2} h^{-1}). These three methods will be compared to bracket estimates of PO_4^{3-} regeneration for both sites.

3.2.5 Uptake length

Uptake length was calculated using Eq. 3.1, and the rate constants (K_r) from the ambient concentration beakers. River velocity was found for each date using flow data collected by the GRCA at the monitoring station at Brantford accessed via Environment Canada's hydrometric database. Travel times were previously estimated for several Grand River reaches, under different flow regimes, by the GRCA. Travel times were found through hydraulic modeling calibrated with dye tracer studies (Mark Anderson, GRCA, personal communication). The relationship between travel time and river discharge was found, and converted to river velocity using the distance between the two sites. The sites chosen to calculate travel time were from the Waterloo WWTP to the GRCA monitoring site at Brantford.

3.2.6 River Depth

In order to compare seston and epilithon uptake velocities, river depth was required to express seston uptake in areal units. Depth was estimated using the daily average flow obtained from the GRCA monitoring stations for the downstream site at Doon (close to the sampling site used in this chapter at Blair), and upstream site at Bridgeport. Estimates of river depth were found using the discharge- hydraulic radius relationship established for the sites at Bridgeport and Blair in Jamieson (2010). The relationship for Blair was found using a series of cross-sectional stream gauging events carried out by the GRCA that resulted in an equation that describes the relationship between hydraulic radius (mean depth) and flow rate.

$$R\ (Blair) = 0.1788 \times Q^{0.3071} \quad (3.8)$$

Jamieson (2010) also developed an equation for the sampling site at West Montrose (upstream of Bridgeport) based on a topographic survey where two cross sections were surveyed above her chosen sampling site. The mean of the curves (discharge-depth) obtained for West Montrose and

Blair were used to calculate this relationship for Bridgeport, located approximately at the mid-point of these two sites:

$$R\ (\text{Bridgeport}) = 0.155 \times Q^{0.45} \quad (3.9)$$

An average of the depth calculated using these two equations was used to estimate the river depth at Freeport.

3.2.7 Statistical analysis

Parameters describing Michaelis-Menten kinetics (V_{max} and K_s) were estimated using non-linear least squares regression. Michaelis-Menten model fit was assessed using the coefficient of determination (R^2) All statistical analysis was carried out in GraphPad Prism 6.

3.3 Results

3.3.1 Physical and chemical measurements

SRP and TP were found to covary ($r = 0.97$, $p < 0.001$) over all sampling dates and at both sites (Fig. 3.02). The average SRP and TP concentrations at Blair were 28.2 and 102.0 µg P L^{-1} respectively. Average SRP and TP concentrations at Freeport, were 20.3 and 92.7 µg P L^{-1} respectively. SRP was significantly higher at Blair than Freeport (paired t-test, $p < 0.05$), as was TP (paired t-test, $p < 0.05$). The measured depth at the two sampling sites for all dates ranged from 30 to 50 cm. The estimated river depth for all dates and both river sites ranged from 45 to 75 cm, using equations 3.8 and 3.9 as described above.

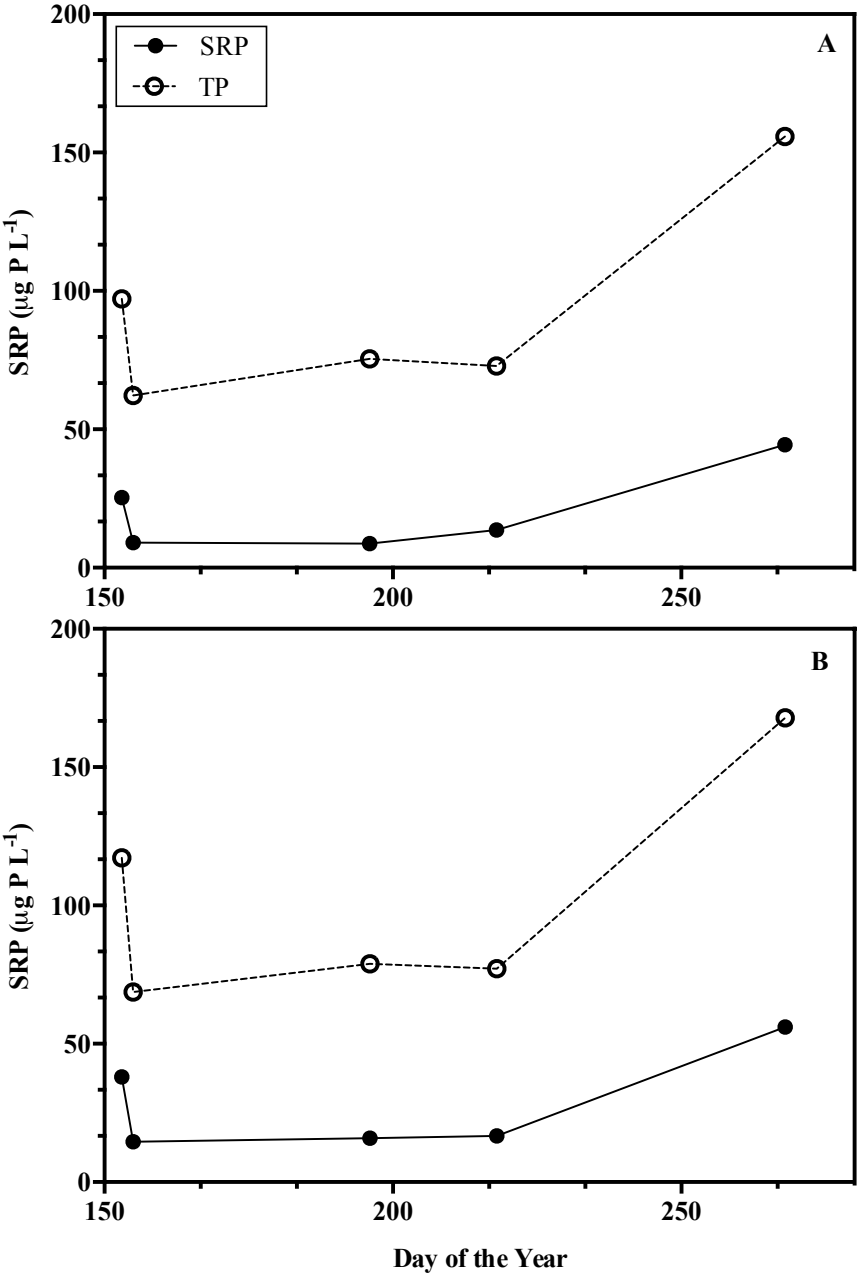

Figure 3.02: SRP and TP concentrations for the Grand River from a) Freeport and b) Blair for all sampling dates over the summer of 2013.

3.3.2 Gross uptake by seston and epiphytes

The combined (seston + epilithon) uptake rate coefficients (K_r) ranged from 0.03 to 0.08 h^{-1} for Freeport, and from 0.03 to 0.06 h^{-1} for Blair, with a mean of 0.05 for Freeport and a mean of 0.04 h^{-1} for Blair (Table 3.02). These K_r values equate to turnover times ranging from 12.0 to 39.8 h, with mean values of 23.0 and 25.2 h for Freeport and Blair, respectively. No significant difference was found in turnover times between the two sites (paired t-test, p = 0.51), however PO_4^{3-} turnover was longer at Blair for every sampling day except June 4th and 6th. Uptake constants for the epilithon, with areal corrections, were greater than for seston at Blair on all but one date (June 4th), with the mean K_r for the epilithon at 0.02 h^{-1} and 0.03 h^{-1} for Freeport and Blair, respectively. Seston, however, possessed the larger rates constants at Freeport on all but one date (September 25th), with the average seston K_r values at 0.03 h^{-1} and 0.02 h^{-1} for Freeport and Blair, respectively.

Table 3.02: Gross uptake rate constants for epilithon and seston in the Grand River, collected over the summer of 2013. Included are the SRP concentrations from the field, and the net uptake experiments, as well as the calculated turnover time (TT). Also included is the range of values collected at Winterbourne (Barlow-Busch et al., 2006).

Date	Site	SRP_{Field} (µg P L^{-1})	SRP_{Lab} (µg P L^{-1})	K_r Seston (h^{-1})	K_r Epilithon (h^{-1})	Total K_r (h^{-1})	TT (h)
June 4th	Freeport	25.4	27.8	0.03	0.01	0.04	24.6
	Blair	38.0	38.0	0.03	0.02	0.05	20.9
June 6th	Freeport	9.1	N/M	0.02	0.01	0.03	34.3
	Blair	14.5	N/M	0.01	0.02	0.03	29.1
July 15th	Freeport	8.7	8.4	0.05	0.02	0.07	15.1
	Blair	15.9	17.5	0.01	0.05	0.06	16.9
August 6th	Freeport	13.6	13.9	0.05	0.04	0.08	12.0
	Blair	16.7	16.6	0.02	0.03	0.05	19.4
September 25th	Freeport	44.4	44.0	0.01	0.02	0.03	29.2
	Blair	56.1	57.9	0.01	0.01	0.03	39.8
	Winterbourne	5 to 20	-	0.01 to 0.28	0.05 to 2.1	0.07 to 2.2	0.7 to 15

N/M = not measured

Gross uptake velocities (U) were calculated using the river SRP values from the field collected samples. Little change in SRP was detected between field-filtered samples and those taken at time zero in the net uptake experiments (Table 3.02) indicating that preservation of field PO_4^{3-} conditions was not a problem. The mean uptake velocity for Freeport at an ambient nutrient concentration was 0.06 µg P cm^{-2} h^{-1} with a range of 0.02 to 0.10 µg P cm^{-2} h^{-1}. Blair had an average U of 0.05 µg P cm^{-2} h^{-1}, with a range of 0.02 to 0.09 µg P cm^{-2} h^{-1}. PO_4^{3-} uptake by the epilithon was not significantly different between the two sites (paired t-test, $p = 0.64$) and had a mean value of 0.03 µg P cm^{-2} h^{-1}. Likewise seston uptake was not significantly different between the sites (paired t-test, $p = 0.22$), and possessed a mean of 0.03 µg P cm^{-2} h^{-1}. Seston was found to be the major contributor (> 50%) to total uptake on four out of the five sampling dates at Freeport, and once at Blair. At Freeport, seston contributed between 28 to 74% to total uptake, while at Blair seston contributed 20 to 57% (Fig. 3.03). The average contribution of sestonic uptake was 59% and 38% for Freeport and Blair, respectively. The contribution by the seston was greatest on June 4th at both sites. The mean seston uptake among all experiments (including PO_4^{3-} addition experiments) was significantly greater at Freeport than Blair (unpaired t-test, $p < 0.05$). No difference was found between the two sites for epilithon uptake (unpaired t-test, $p = 0.88$). Similarly, total uptake velocities (seston + epilithon) at the two sites for all experiments (including PO_4^{3-} addition experiments) were not significantly different (unpaired t-test, $p = 0.09$). Freeport, however, possessed the higher mean value of 0.12 µg P cm^{-2} h^{-1}, with a mean at Blair of 0.08 µg P cm^{-2} h^{-1}.

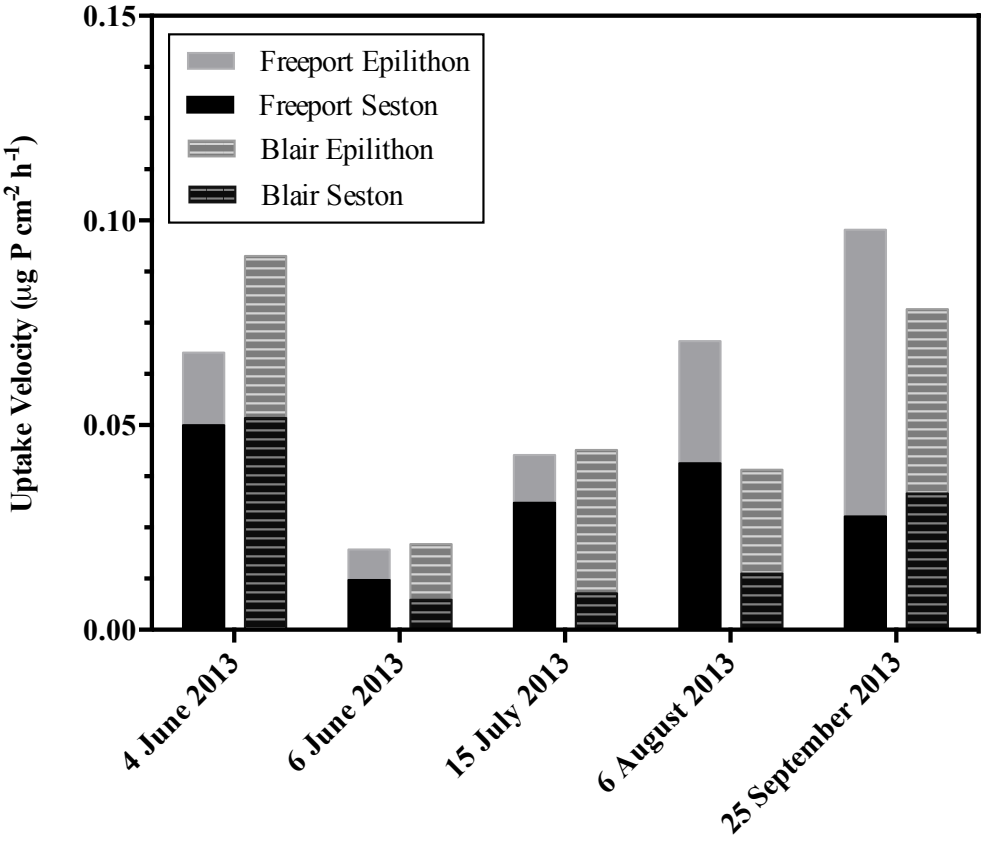

Figure 3.03: PO_4^{3-} uptake by seston and epilithon in the Grand River for all sampling dates over the summer of 2013.

The mean epilithon biomass at Freeport was significantly lower than that observed at Blair (paired t-test, $p < 0.05$), with mean values of 5.35 and 13.04 mg AFDW cm^{-2}, respectively. Epilithon biomass appeared to peak in July at Blair with a large reduction between the sampling dates in July and August. Epilithon biomass at Freeport was highest in August (Fig. 3.04). Mean biomass corrected uptake velocities for the epilithon were 0.005 and 0.002 µg P mg $AFDW^{-1}$ h^{-1} for Freeport and Blair, respectively. On a biomass basis the epilithon-only uptake velocities at Freeport and Blair were not significantly different among the ambient concentration beakers (paired t-test, $p = 0.09$). They were however higher at Freeport on all but one date (July 15th). The mean seston biomass was significantly less than that of the epilithon (paired t-test, $p < 0.001$), with average values of 0.28 and 0.20 mg AFDW cm^{-2} for Freeport and Blair respectively. Seston biomass was not significantly different between the two sites (paired t-test, $p = 0.12$). The biomass-specific seston uptake velocities were also not significantly different between the two sites (paired t-test, $p = 0.52$), but were higher at Freeport on all but one day (September 25th; Fig. 3.05). Mean seston uptake velocities of 0.12 and 0.10 µg P mg $AFDW^{-1}$ h^{-1} were obtained for Freeport and Blair respectively. On a biomass basis, the uptake of PO_4^{3-} by seston was significantly greater than the epilithon at both sites (paired t-test, $p < 0.001$). Although seston biomass was similar between the two sites, the seston was more active at Freeport. Thus, despite the significantly lower epilithon biomass at Freeport, uptake velocities (µg P cm^{-2} h^{-1}) were not significantly lower than those at Blair.

Increased depth can largely explain the higher seston uptake velocities at Freeport. Estimated river depth was greater at Freeport than Blair on every sampling date. Comparing seston uptake velocities expressed volumetrically shows no significant difference between sites (paired t-test, $p = 0.82$) with average velocities of 0.49 and 0.46 µg P L^{-1} h^{-1} for Freeport and Blair respectively. Once again the difference in seston uptake velocities between the two sites is greater when the PO_4^{3-} addition experiments are included. On a volumetric basis, seston uptake velocities are significantly larger at Freeport than Blair when these experiments are included ($p < 0.05$).

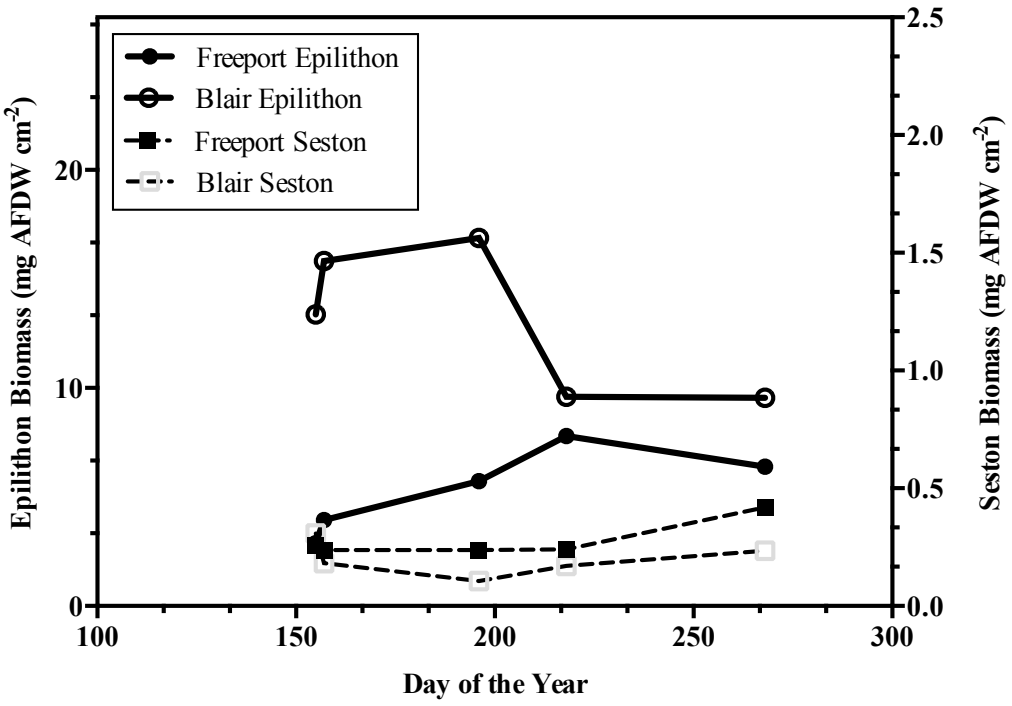

Figure 3.04: Variations in epilithon and seston biomass as estimated by AFDW for the river sites at Freeport and Blair over the summer of 2013. Note the difference in scales for the epilithon and seston.

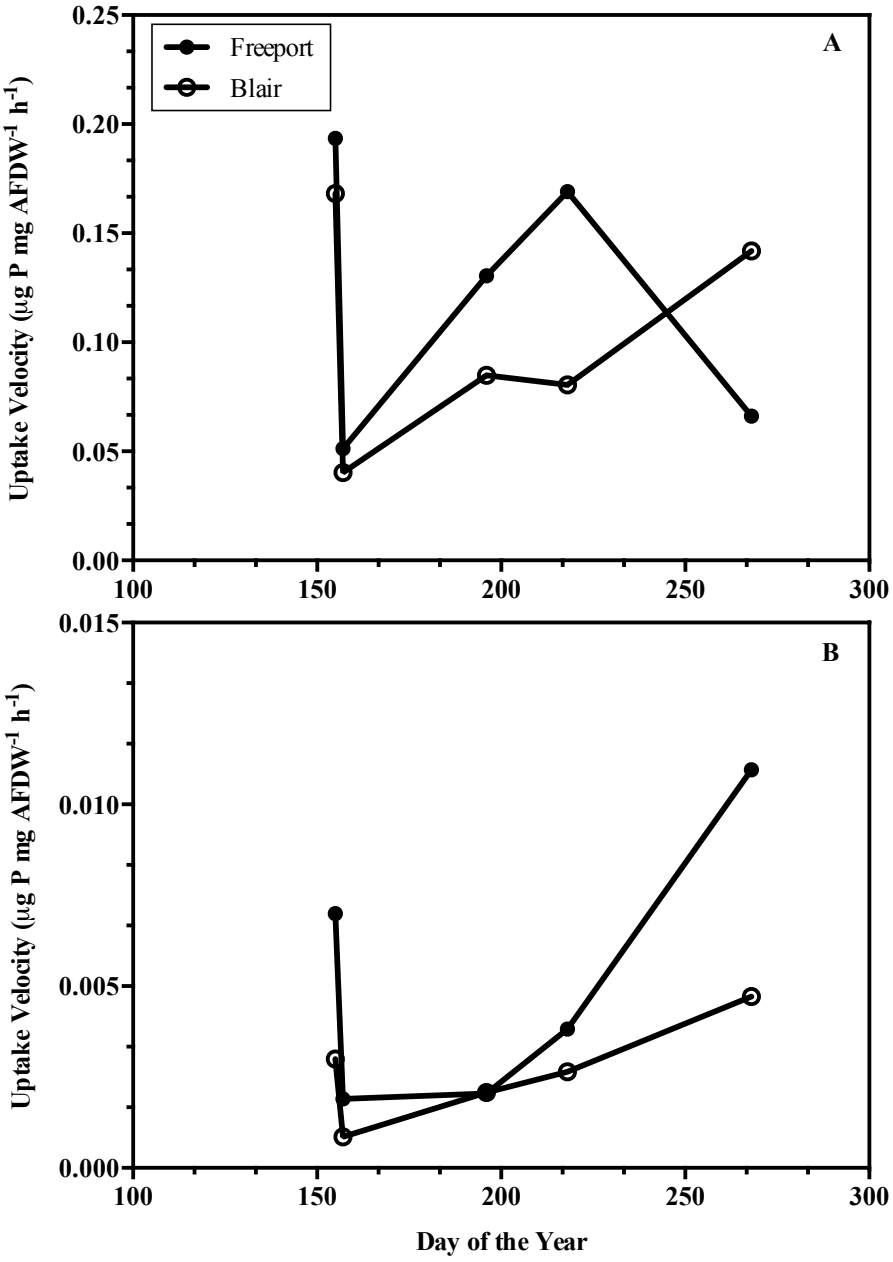

Figure 3.05: Biomass-specific PO_4^{3-} uptake by the a) seston, and b) epilithon over the summer of 2013.

River flow was found to have a significant impact on both the seston and epilithon contribution to uptake at Winterbourne, with high flow thought to reduce epilithon biomass and increase seston biomass (Barlow-Busch et al., 2006). Using river flow data accessed via Environment Canada's hydrometric database for the GRCA monitoring sites at Victoria and Doon allowed an assessment of the effect of flow on the two communities contribution to uptake (Fig. 3.06). Average river flow for 24 h prior to sampling was used to assess this correlation. Ambient seston uptake velocities were positively correlated to mean river flow using data from both sites ($r = 0.83$, $p < 0.05$). River flow was however used to calculate the depth estimates that allowed these velocities to be expressed in areal units. Comparing volumetric seston uptake velocities to river flow also resulted in a significant positive correlation ($r = 0.81$, $p < 0.05$). No relationship was found for the epilithon ($r = 0.12$, $p = 0.73$). Similarly no relationship was noted between SRP and flow at either site ($r = 0.23$, $p = 0.51$; Fig. 3.07). There was also no relationship observed between ambient uptake velocity and biomass for the seston ($r = 0.53$, $p = 0.10$) or the epilithon ($r = 0.25$, $p = 0.42$; Fig. 3.08). Although the relationship between seston uptake velocity and biomass was not significantly positive this was largely due to the sampling at Freeport on September 25th, 2013. On this date one of the smallest seston uptake velocities was observed and the largest seston biomass. Excluding this point results in a significant positive relationship between the two ($r = 0.81$, $p < 0.05$). Epilithon uptake was more strongly related to the river's SRP ($r = 0.78$, $p < 0.05$) however this relationship is much stronger at Freeport ($r = 0.89$, $p < 0.05$), than Blair ($r = 0.75$, $p = 0.14$). Seston-only uptake was not significantly related to SRP at either site ($r = 0.42$, $p = 0.22$, Fig. 3.09).

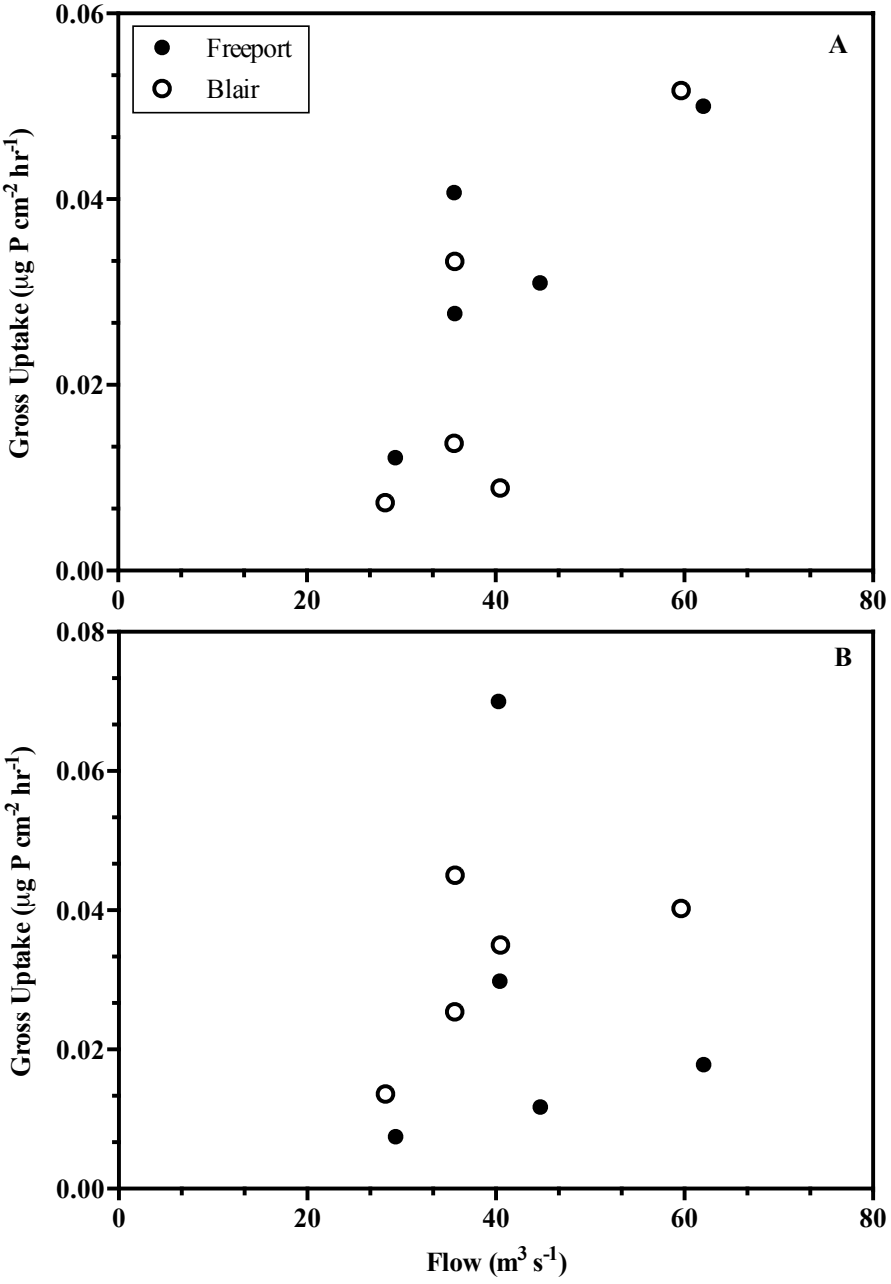

Figure 3.06: Gross uptake velocity vs. river discharge at an ambient PO_4^{3-} concentration for the a) seston, and b) epilithon over the summer of 2013.

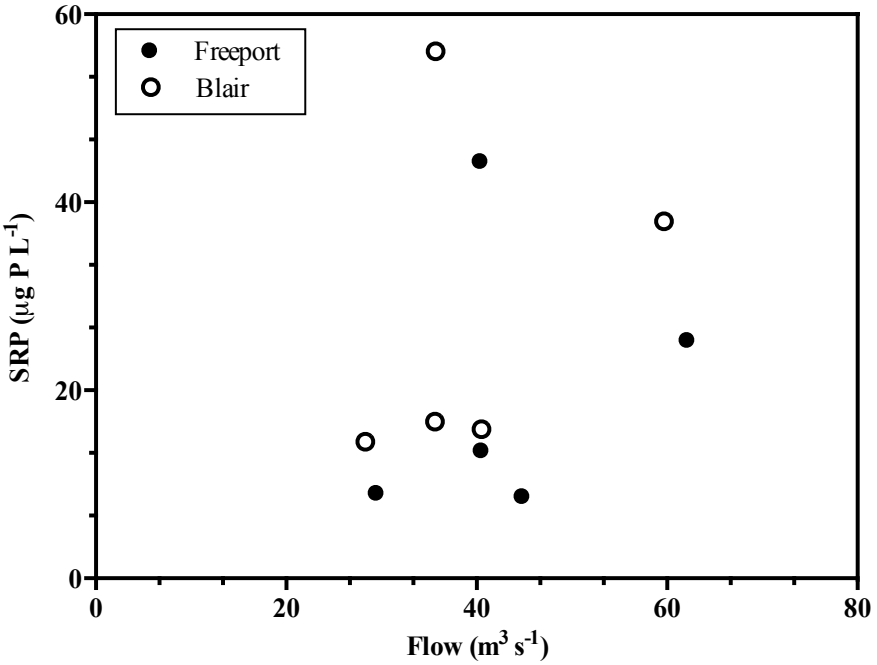

Figure 3.07: River SRP vs. river discharge over the summer of 2013.

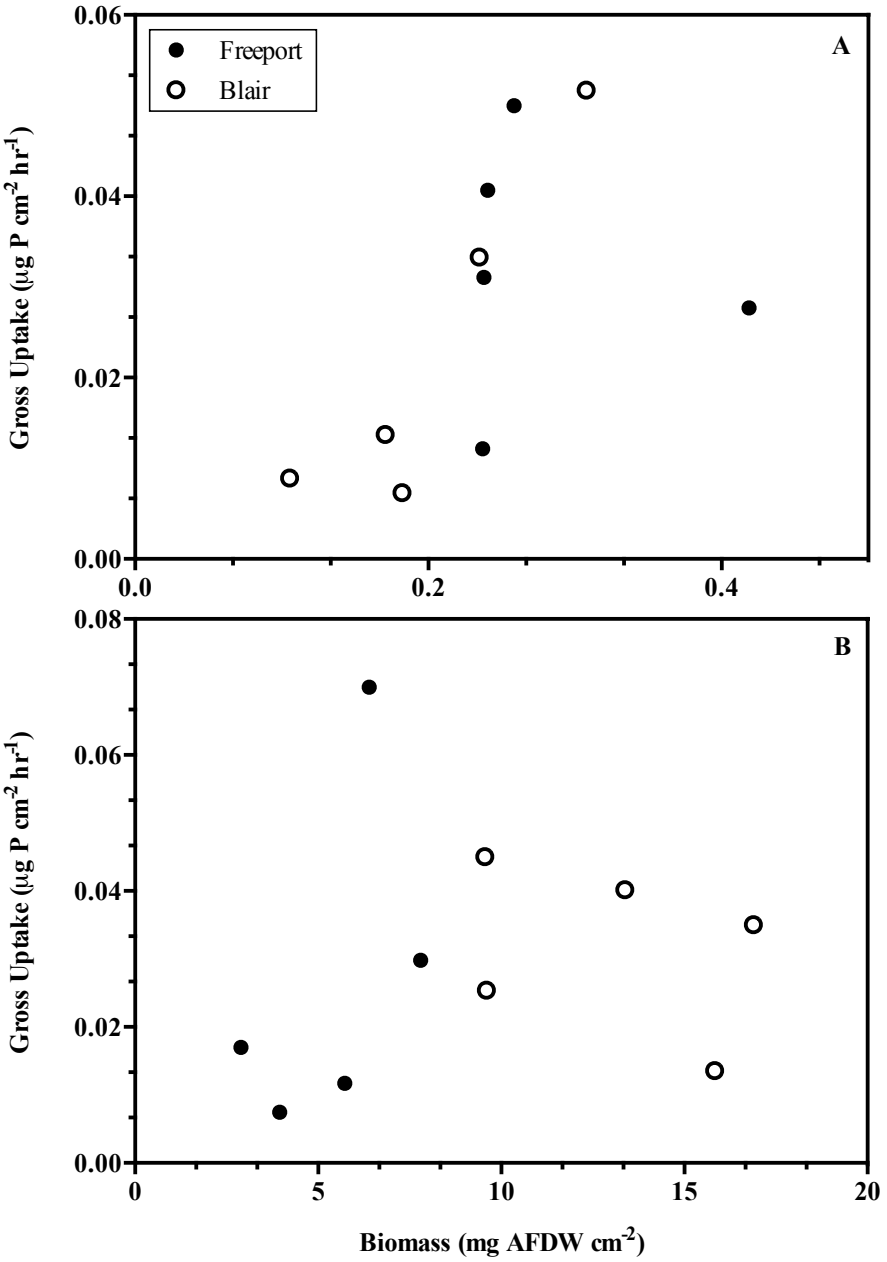

Figure 3.08: Gross uptake velocity in the ambient concentration beakers vs. community biomass for the a) seston, and b) epilithon over the summer of 2013.

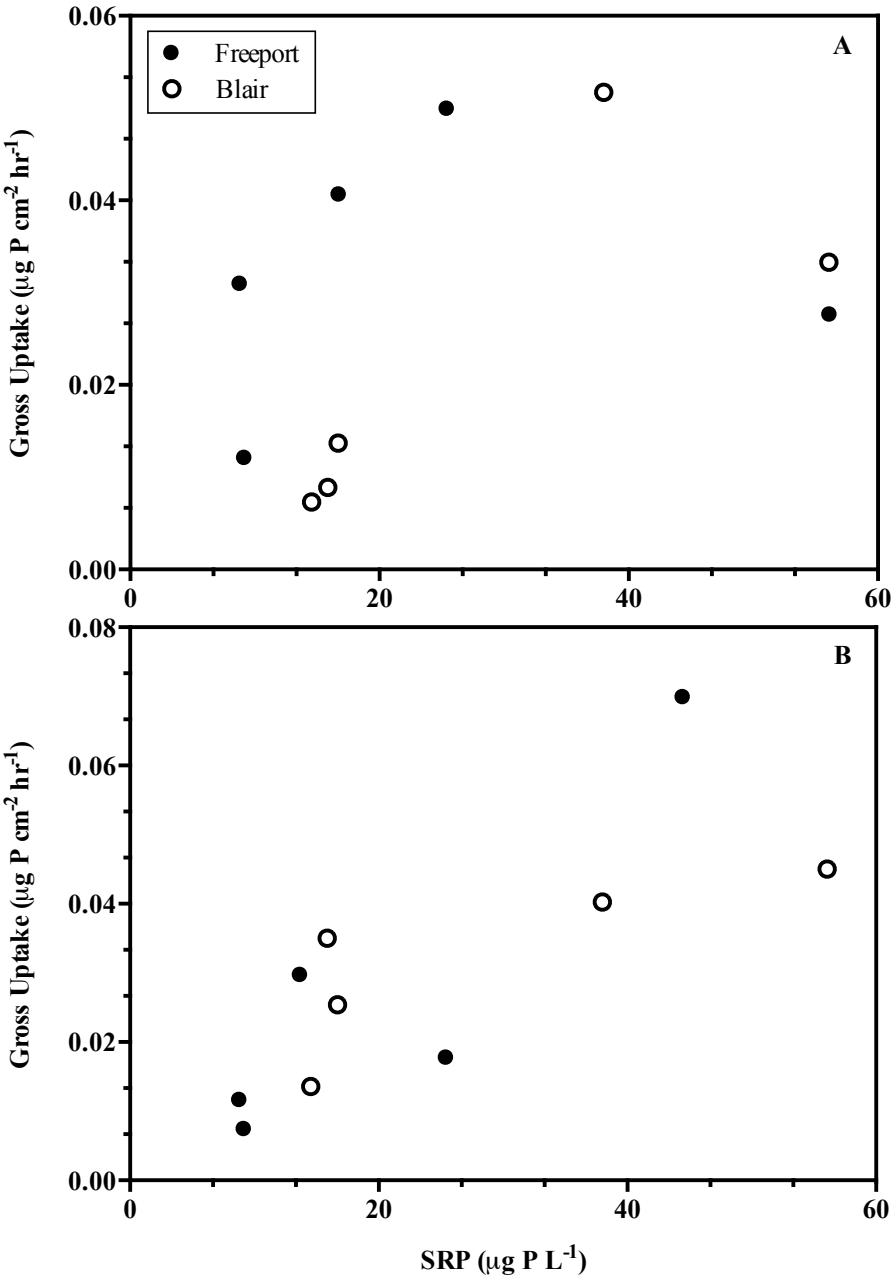

Figure 3.09: Gross uptake velocity in the ambient concentration beakers vs. SRP concentration for the a) seston, and b) epilithon over the summer of 2013.

Another factor that was found to affect epilithon biomass at Winterbourne were storm events capable of scouring epilithon off of the river's substrata (Barlow-Busch, 1997). The summer of 1996 was noted to be a summer of unusually frequent rain (Barlow-Busch et al., 2006). The summer of 2013 also experienced high rainfall, with several large storm events. Using the GRCAs discharge values for both summers, accessed via Environment Canada's hydrometric database, showed 2013 to possess flow rates exceeding those of 1996 with mean daily flow rates of 16.4 and 11.2 $m^3 s^{-1}$ for 2013 and 1996 respectively (June 1st to October 1st for both years; Fig. 3.10).

The mean contributions of seston size-fractions to PO_4^{3-} uptake at Freeport were 47, 21, and 32%, for picoplankton (0.2 - 2 μm), nanoplankton (2-20 μm), and microplankton (> 20 μm) respectively (Fig. 3.11). Similarly, at Blair the mean percent uptakes for all sampling dates were 52, 22, and 26% respectively. The smallest size-fraction dominated uptake on all occasions at both sites, except on June 4th, 2013, at Freeport when the >20 μm size class dominated. This date also corresponded to the highest seston uptake velocity (0.76 μg P $L^{-1} h^{-1}$). The percent contribution of uptake by picoplankton and microplankton were not however correlated to total uptake (picoplankton: $r = -0.27$, $p = 0.52$; microplankton: $r = 0.33$, $p = 0.42$). Fluctuations in the major contributors to sestonic P-uptake throughout the summer appeared to be much greater at Freeport, where a larger range was observed for all size fractions (0.2 – 2 μm: 2 to 92%, 2-20 μm: 7 to 30%, >20 μm: 1 to 69%), than Blair (0.2 – 2μm: 38 to 75%, 2 – 20 μm: 13 to 33%, >20 μm: 10 to 29%).

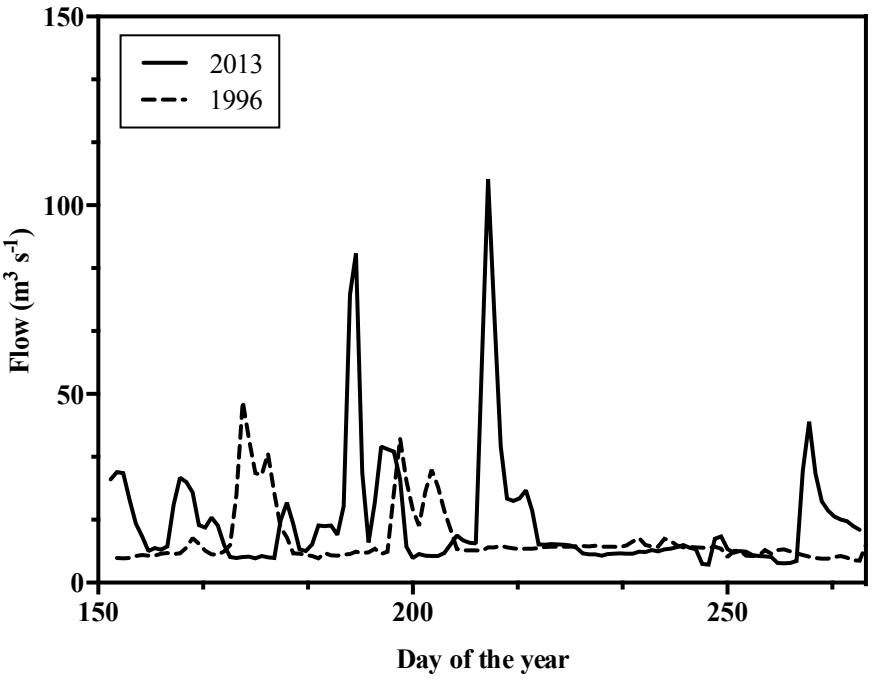

Figure 3.10: River discharge over the summers (June 1st to October 1st) of 1996 and 2013 collected by the GRCA at West Montrose (near Winterbourne). The lines are made up of daily averages taken from the GRCA website for 2013 and Environment Canada's hydrometric database for 1996.

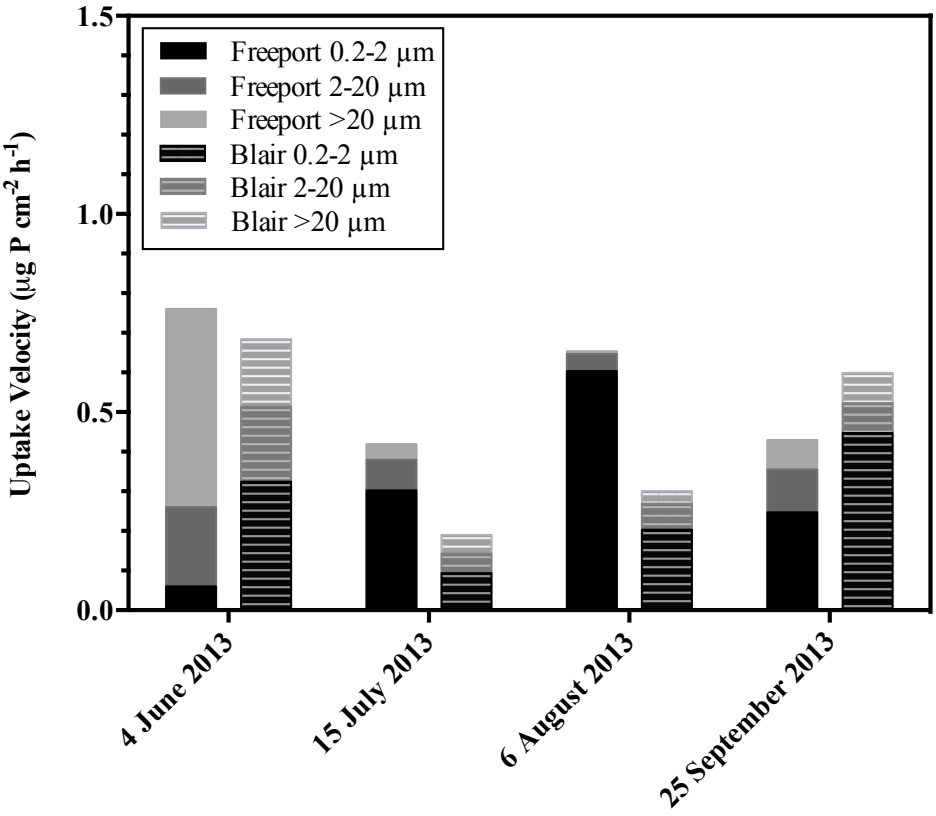

Figure 3.11: Size fractionated seston-only uptake using filter sizes: 0.2, 2, and 20 µm. Partitioning of the seston-only uptake occurred 30 minutes into the gross uptake experiments, and was carried out in beakers possessing ambient PO_4^{3-} concentrations. The June 4th, 2013 values are an average of the replicate seston-only beakers.

3.3.3 Net uptake and release by seston and epiphytes

The range of total (seston + epilithon) net uptake velocities (U_N) for Freeport was 0.03 to 0.07 μg P cm^{-2} h^{-1}, with a mean of 0.05 μg P cm^{-2} h^{-1}. Total net uptake rates were always positive (i.e., negative slope for [SRP] with time), meaning more PO_4^{3-} was assimilated than released in all beaker experiments. The range of U_N values for Blair was 0.02 to 0.05 μg P cm^{-2} h^{-1} with a mean rate of 0.04 μg P cm^{-2} h^{-1}. Seston was assimilating PO_4^{3-} in all incubations, with a range of U_N values from 0.01 to 0.05 μg P cm^{-2} h^{-1}, and a mean value of 0.03 μg P cm^{-2} h^{-1}. The epilithon was assimilating PO_4^{3-} on all dates except the June 4th, which had average U_N values of -2×10^{-3} and -2×10^{-3} μg P cm^{-2} h^{-1} for Freeport and Blair, respectively. In these beakers, the seston-only replicates possessed higher rate constants than the seston + rock incubations. The range of U_N values for the epilithon alone was from 0 to 0.03 μg P cm^{-2} h^{-1}, with a mean of 0.01 μg P cm^{-2} h^{-1}. Seston had the largest net uptake velocities on all dates except September 25th, likely suggesting that although the epilithon are acquiring SRP (as seen in the gross uptake experiments) it also plays a larger role in SRP release.

The decline in SRP during all net uptake experiments was significant (ANCOVAs, $p < 0.05$) except on June 4th (Fig. 3.12, 3.13, 3.14, 3.15). On this date, both seston only and seston + epilithon at Blair, and seston + epilithon beakers at Freeport possessed non-significant slopes. The presence of the rock always had a significant effect on the slope except for June 4th, at both sites. There was no significant difference in the slopes of the seston-only beakers between Freeport and Blair for any date except July 15th. On this date Blair possessed the significantly larger slope. Similarly, comparing the epilithon-only conditions resulted in only the July 15th beakers being significantly different between the two sites, with Blair possessing the larger slope.

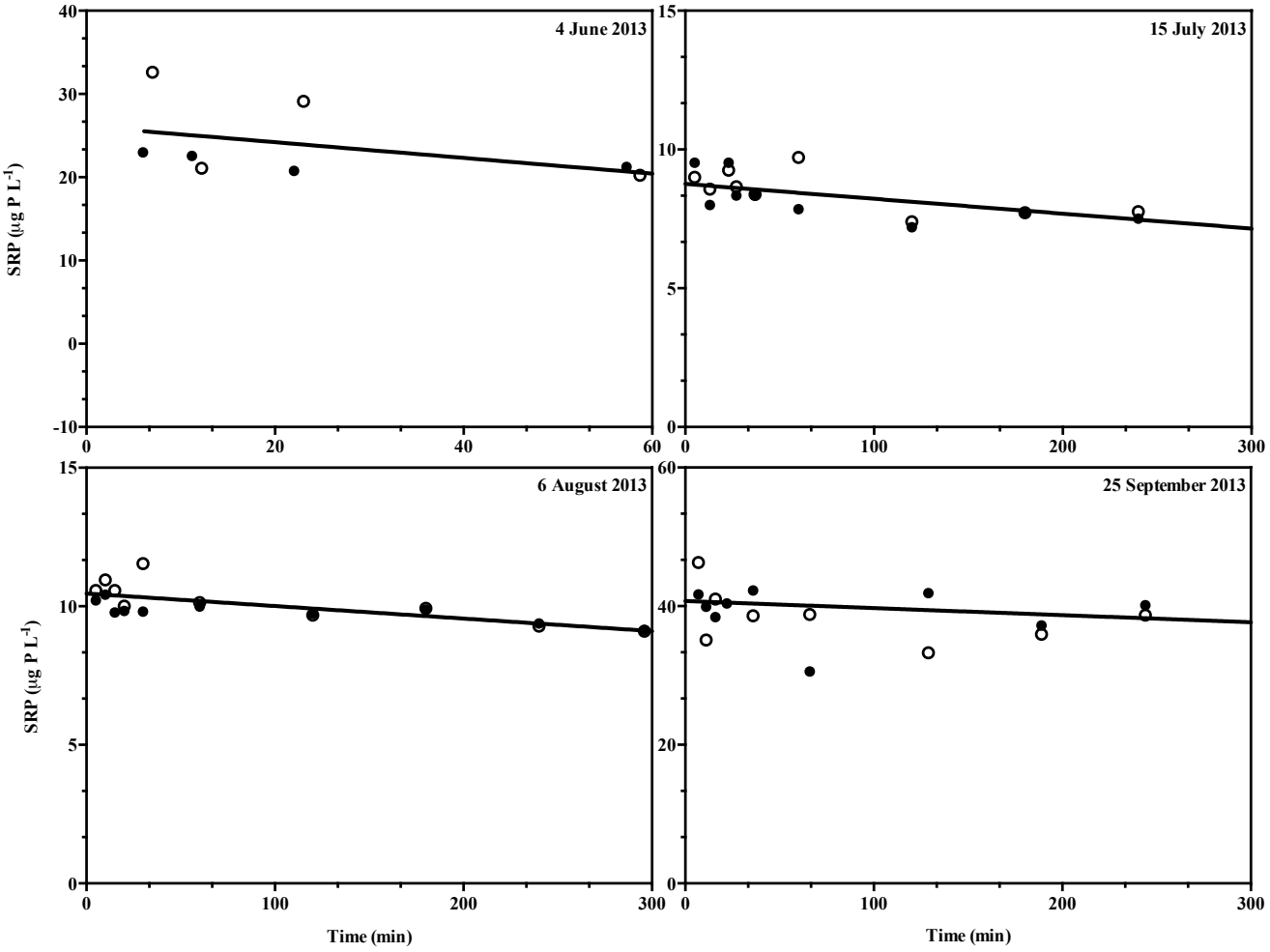

Figure 3.12: Freeport seston-only net uptake for the summer of 2013, from the Grand River. Different symbols represent replicate samples with the slope taken from an average of the replicates. The slope value was calculated using the first 5 h of SRP collection for all days except June 4th where hourly samples were not collected and the slope is based on the first 60 min.

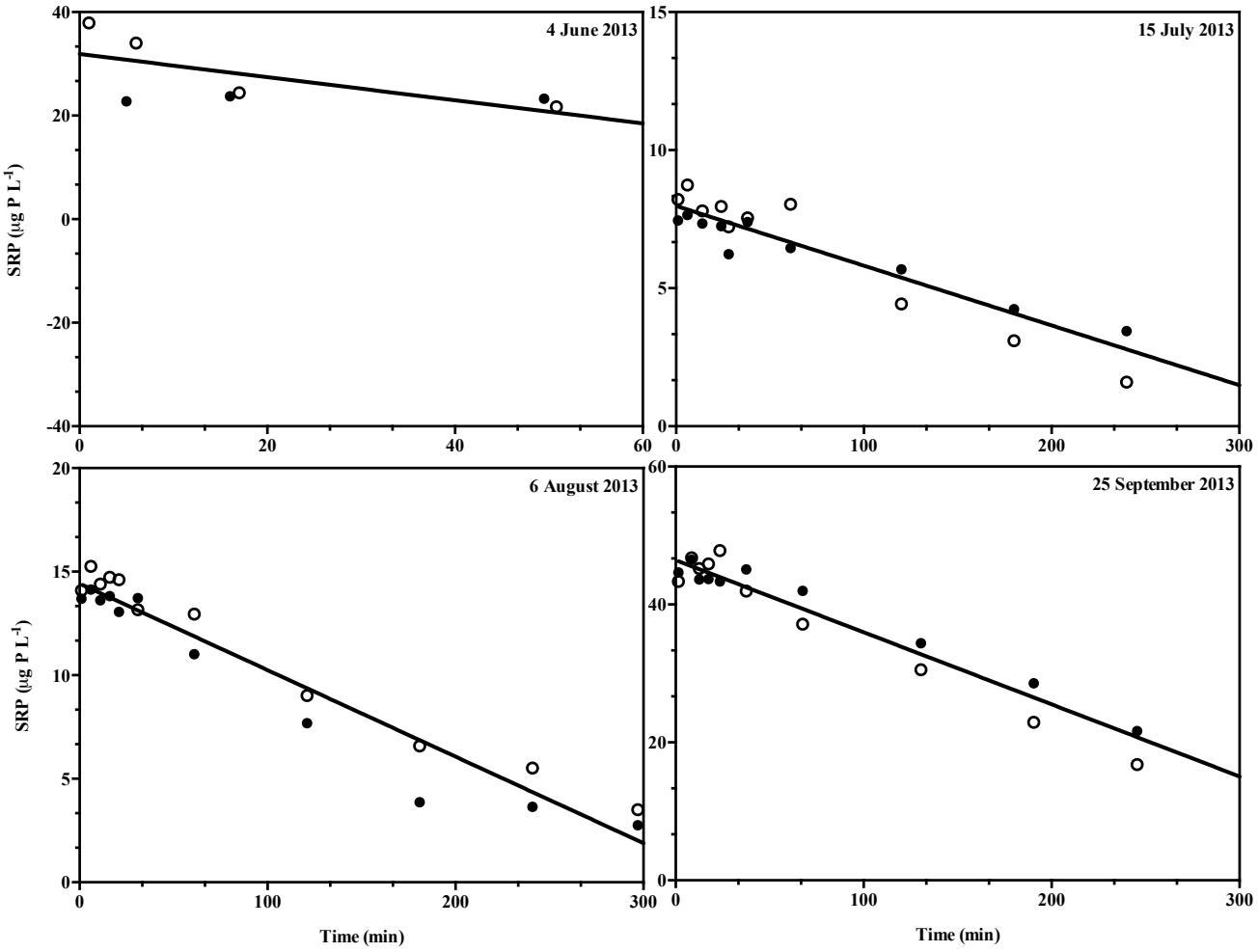

Figure 3.13: Freeport seston + rock net uptake for the summer of 2013 from the Grand River. Different symbols represent replicate samples with the slope taken from an average of the replicates. The slope value was calculated using the first 5 h of SRP collection for all days except June 4th where hourly samples were not collected and the slope is based on the first 60 min.

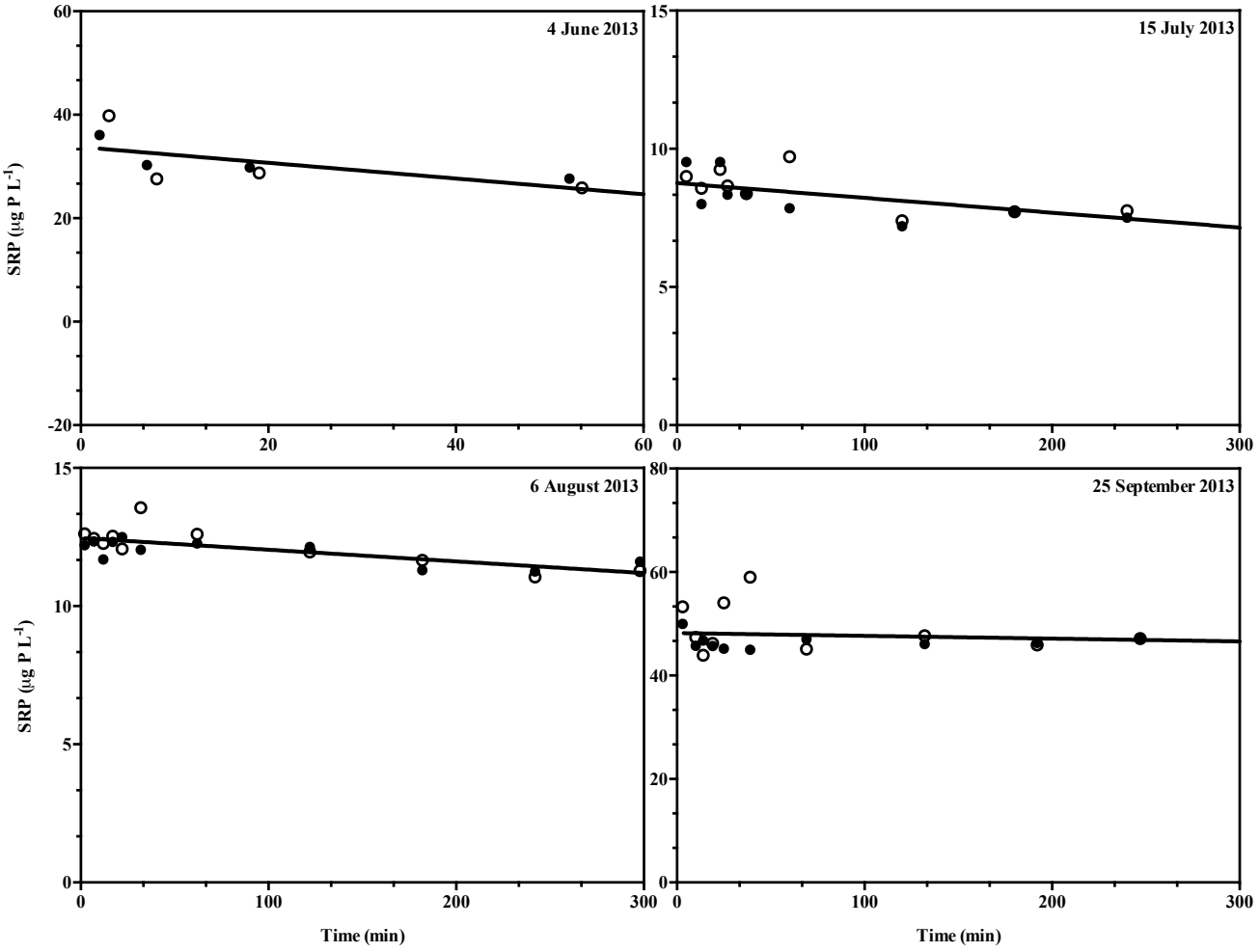

Figure 3.14: Blair seston-only net uptake for the summer of 2013 from the Grand River. Different symbols represent replicate samples with the slope taken from an average of the replicates. The slope value was calculated using the first 5 h of SRP collection for all days except June 4th where hourly samples were not collected and the slope is based on the first 60 min.

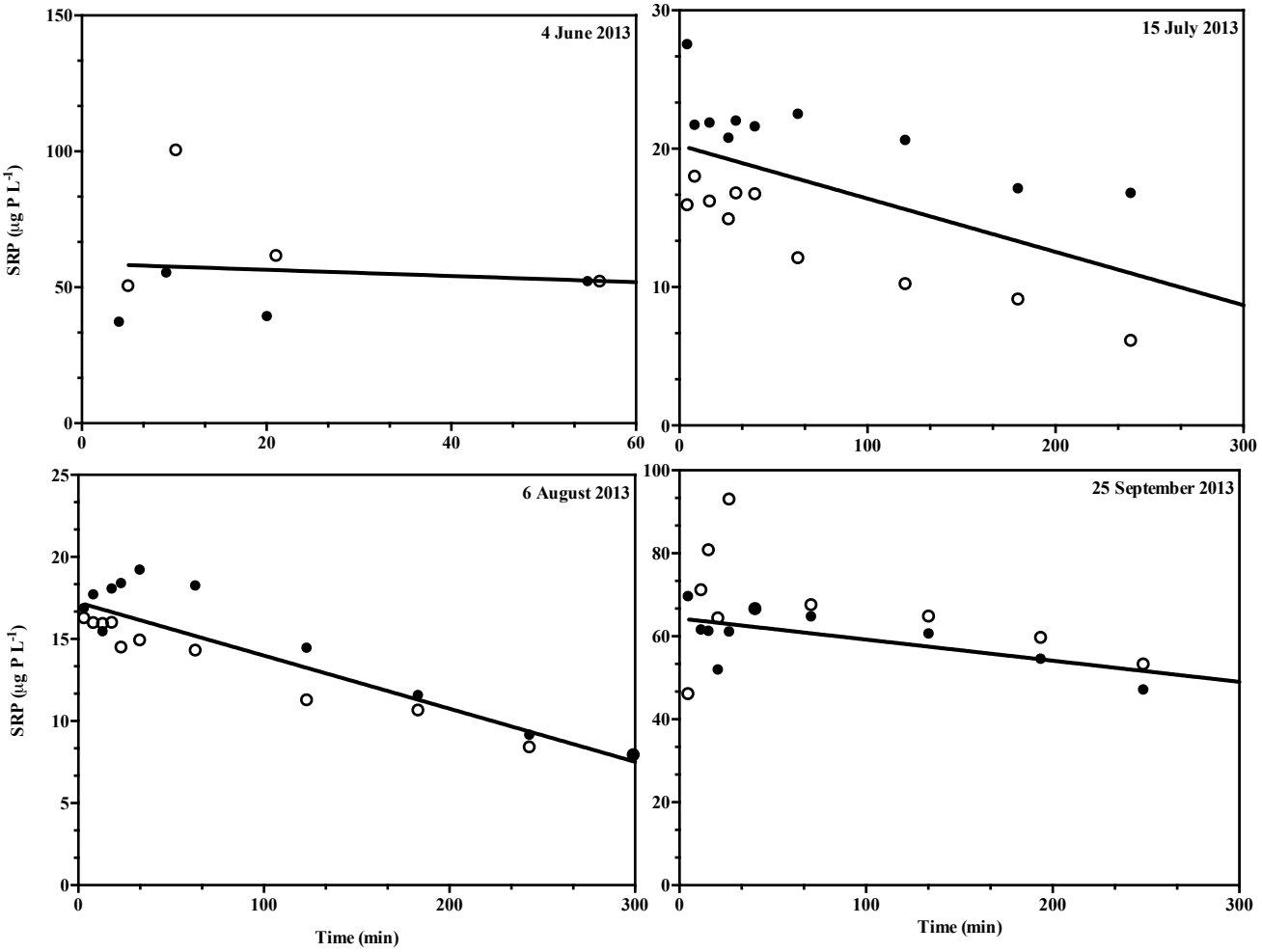

Figure 3.15: Blair seston + rock net uptake for the summer of 2013 from the Grand River. Different symbols represent replicate samples with the slope taken from an average of the replicates. The slope value was calculated using the first 5 h of SRP collection for all days except June 4th where hourly samples were not collected and the slope is based on the first 60 min.

Assuming SRP is a suitable proxy for PO_4^{3-}, the difference between the gross and net uptake velocities provides an estimate for the PO_4^{3-} regeneration rate (Table 3.03). Seston-only regeneration appeared to be negative on three sampling dates, however total regeneration was positive on all dates except July 15th at Blair. A negative release rate could suggest that SRP overestimates PO_4^{3-} even in the downstream reaches of the river at times. The negative value for total regeneration was obtained at Blair when the lowest SRP concentration was observed (July 15th), but there was no correlation between regeneration rate and SRP concentration ($r = 0.58$, $p = 0.12$). The average rates of release were 0.02 and 0.03 μg P cm^{-2} h^{-1} for Freeport and Blair, respectively. Excluding the negative value at Blair on July 15th resulted in a mean release for Blair of 0.04 μg P cm^{-2} h^{-1}.

Steady-state SRP concentrations were also estimated through these experiments. The SRP concentrations following 24 h of incubation estimate steady-state conditions, where PO_4^{3-} release equals PO_4^{3-} uptake. Steady-state SRP at Freeport and Blair were 4.5 μg PL^{-1} and 19.6 μg P L^{-1} respectively (Table 3.04). Blair possessed higher steady-state SRP concentrations on all sampling dates, with the highest observed concentrations for both sites occurring on June 4th. These values of 12.6 and 51.6 μg P L^{-1} were higher than those observed on the other sampling dates, and corresponded with the second highest field collected SRP concentrations. Potentially 24 h of incubation time was insufficient to capture the steady-state conditions on this day, given the large initial SRP concentrations. Likewise, the September 25th Blair steady-state value of 21.6 μg P L^{-1} was higher than those of the other beaker experiments, and corresponded with the highest measured SRP concentration. The steady-state SRP concentrations were used to estimate PO_4^{3-} release using the Michaelis-Menten parameters discussed in Section 3.3.3.

Table 3.03: Net and gross seston and epilithon uptake velocities for Freeport and Blair over the summer of 2013 measured in the ambient concentration beakers. Also shown are seston, epilithon and total PO_4^{3-} regeneration rates, calculated as the difference between gross and net uptake, and the biomass (BM) of the seston and epilithon. All uptake and regeneration rates are presented in units of μg P cm^{-2} h^{-1}, and biomass is expressed in mg AFDW cm^{-2}. Also included is the range of values collected at Winterbourne as stated in the text or illustrated in figures (Barlow-Busch et al., 2006). The Winterbourne epilithon and seston net and regeneration ranges are taken from Table 1 in Barlow-Busch et al. (2006).

Date	Site	Seston Net	Epilithon Net	Seston Gross	Epilithon Gross	Seston Regen.	Epilithon Regen.	Total Net	Total Gross	Total Regen.	Epilithon BM	Seston BM
June 4th	Freeport	0.05	-1.5×10^{-3}	0.05	0.02	-2.6×10^{-3}	0.02	0.05	0.07	0.02	2.9	0.26
	Blair	0.04	-1.7×10^{-3}	0.05	0.04	0.01	0.04	0.04	0.09	0.06	13	0.30
July 15th	Freeport	0.02	0.01	0.03	0.01	0.01	3.2×10^{-3}	0.03	0.04	0.01	5.7	0.24
	Blair	0.04	0.01	0.01	0.04	-0.03	0.03	0.05	0.04	-6.6×10^{-3}	17	0.11
August 6th	Freeport	0.02	0.01	0.04	0.03	0.02	0.02	0.03	0.07	0.04	7.7	0.24
	Blair	0.01	0.01	0.01	0.03	2.2×10^{-3}	0.02	0.02	0.04	0.02	9.6	0.17
September 25th	Freeport	0.04	0.03	0.03	0.07	-0.01	0.04	0.07	0.10	0.03	6.3	0.41
	Blair	0.02	0.02	0.03	0.05	0.02	0.03	0.04	0.08	0.04	9.5	0.23
	Winterbourne	-0.02 to 0.11	-0.03 to 0.12	0.01 to 0.23	0.01 to 1.79	-0.11 to 0.02	-0.06 to 0.06	-	0.06 to 1.83	-	1.0 to 22	0.01 to 0.54

Table 3.04: Measured field and steady-state SRP data for Freeport and Blair over the summer of 2013. Steady-state SRP was measured after 24 h of incubation. Also included are the calculated release rates using Eq. 3.7.

Date	Site	SRP_{Field} (µg P L^{-1})	Steady-state SRP (µg P L^{-1})	Release (µg P cm^{-2} h^{-1})
June 4th	Freeport	25.4	12.6	0.06
	Blair	38.0	51.6	0.08
July 15th	Freeport	8.7	1.9	0.01
	Blair	15.9	2.6	0.01
August 6th	Freeport	13.6	1.2	0.01
	Blair	16.7	2.4	0.01
September 25th	Freeport	44.4	2.4	0.01
	Blair	56.1	21.6	0.03

In order to calculate release, V_{max}, and K_s values for each site and date (Table 3.07) were used in Eq. 3.7. This calculation resulted in uptake rates that could be related to release based on the assumption that at steady-state PO_4^{3-} uptake equals release. The average release rates calculated using this method were 0.02 and 0.03 µg P cm^{-2} h^{-1} for Freeport and Blair respectively. These values can be compared to the release rates calculated as the difference between gross and net uptake of 0.02 and 0.04 µg P cm^{-2} h^{-1}. No significant difference was found between the mean release rates calculated using either method (paired t-test, $p = 0.94$). It should be noted that the steady-state release rates, like those derived as gross minus net uptake, rely on the use of SRP to estimate PO_4^{3-}. Therefore, the steady-state release rates could be poor estimates of actual PO_4^{3-} release. This method for estimating release also assumes that after 24 h of incubation time the beakers were at steady state, which was already determined to be unlikely on some dates. This may mean that the gross minus net estimates are superior.

The third method to estimate release involved the addition of a ^{31}P competitive inhibitor to block re-uptake of ^{32}P-PO_4^{3-} following 24 h of incubation. This method resulted in release rate

constants in units of time^{-1} that could be converted to turnover times for the particulate P pool (Table 3.05). This method resulted in mean turnover times of 3.9 and 2.9 days for Freeport and Blair, respectively, with a significantly longer mean turnover time for Freeport than Blair (paired t-test, $p < 0.05$). Using Eq. 3.6 and the total TP in the beakers (water TP + epilithon TP) these turnover rates equate to mean release rates of 0.39 and 1.33 μg P cm^{-2} h^{-1} for Freeport and Blair, respectively. These values are an order of magnitude larger than the values collected using either of the other two tested methods for calculating release. One critical assumption for use of this method is that the ratio of ^{31}P to ^{32}P is similar between the released P and the total P. The specific activity (^{32}P:^{31}P, dpm/μg P) of the water column was compared to that of the epilithon in order to determine if 24 h was sufficient to allow the ^{32}P to be evenly distributed. The specific activity of the ^{32}P present in the rocks was significantly lower than the ^{32}P in the water column (paired t-test, $p < 0.05$). The mean ratios of the specific activity (total P) to specific activity (water column) were 0.20 and 0.15 for Freeport and Blair respectively. These reduced specific activities lead to overestimates of P release using Eq. 3.6 because the ratio of ^{31}P to ^{32}P is greater than what would be expected in the released material. Another approach would be to use the specific activity of the water column P prior to the onset of the release experiments. This approach assumes that the water P has a specific activity that is closer to that of the released material. The specific activity of the water column is likely higher than that of the released material, meaning that these values could be underestimates of true PO_4^{3-} release. The mean values for Freeport and Blair calculated using the water column specific activity are 0.08 and 0.18 μg P cm^{-2} h^{-1} (Table 3.05).

The results obtained using the Hudson method were significantly larger than those obtained using the gross minus net approach (paired t- test, $p < 0.05$), and the steady-state assumption (paired t-test, $p < 0.05$; Fig. 3.16). All three methods appear to show a similar trend, at Blair, where decreased release rates were observed in July and August followed by a peak in September. This trend is similar to that observed for uptake velocity (Fig. 3.17). The gross minus

net approach, however, showed a lower rate in June at Freeport, while the Hudson method and steady-state approach showed a high rate on this date.

Table 3.05: Turnover rate constants, turnover times, and release rates for the combined particulate and periphytic P pool for the Grand River over the summer of 2013. The June 4th turnover rates are an average of two replicate samples. These values were obtained using the Hudson method and the specific activity of the water (as discussed in text). Also included is the mean turnover rate and time collected at Winterbourne on September 14th, 2012 (as discussed in section 3.4; W.D Taylor, unpublished).

Date	Site	Turnover Rate (d^{-1})	Turnover Time (d)	Release Rates ($\mu g\ P\ cm^{-2}\ h^{-1}$)
June 4th	Freeport	0.77	1.3	0.14
	Blair	1.21	0.8	0.42
July 15th	Freeport	0.22	4.5	0.02
	Blair	0.27	3.7	0.09
August 6th	Freeport	0.22	4.6	0.03
	Blair	0.31	3.2	0.05
September 25th	Freeport	0.19	5.3	0.14
	Blair	0.27	3.7	0.15
14-Sept-12	Winterbourne	0.12	8.5	-

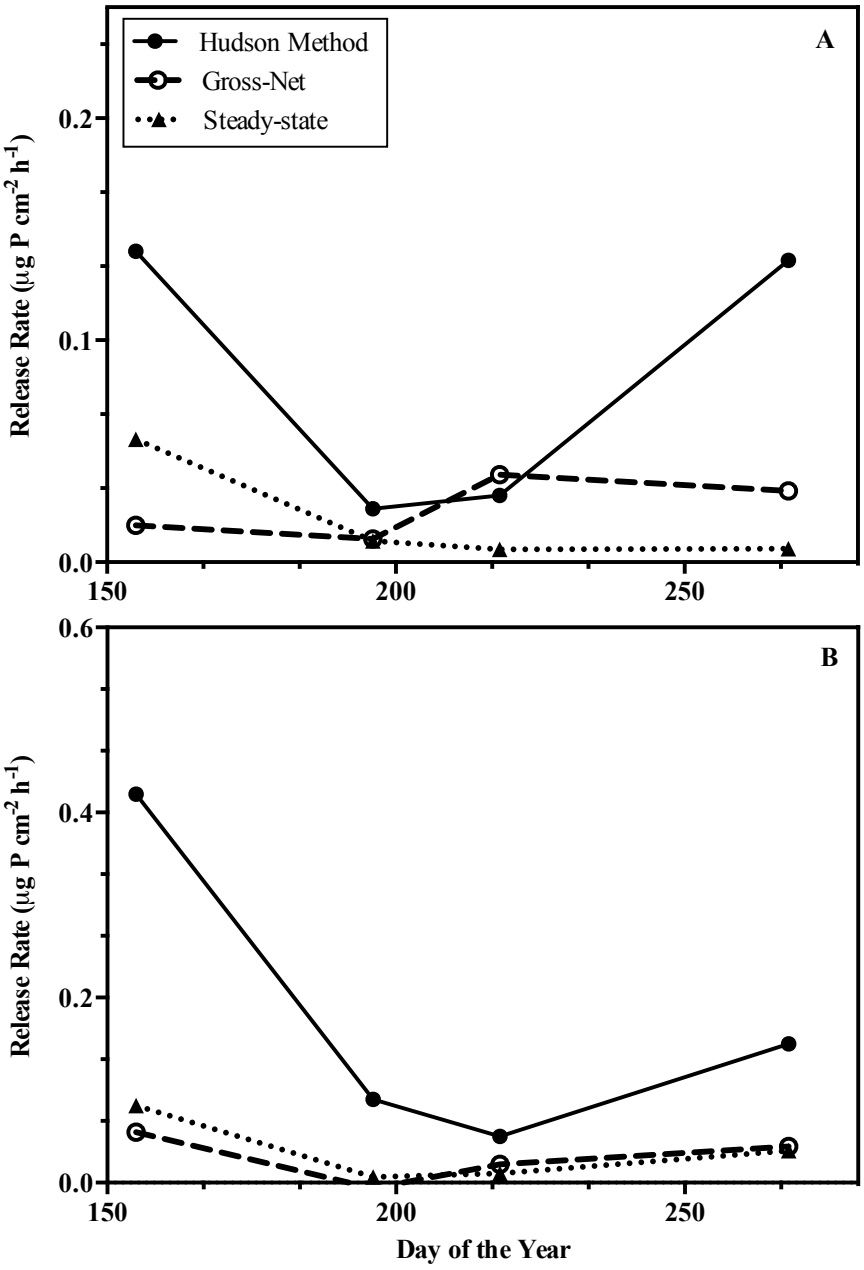

Figure 3.16: Release rates for a) Freeport and b) Blair for the summer of 2013. Release rates were calculated three ways: as gross minus net uptake, using the steady-state assumption, and using the Hudson method with the specific activity of the water (as discussed in text).

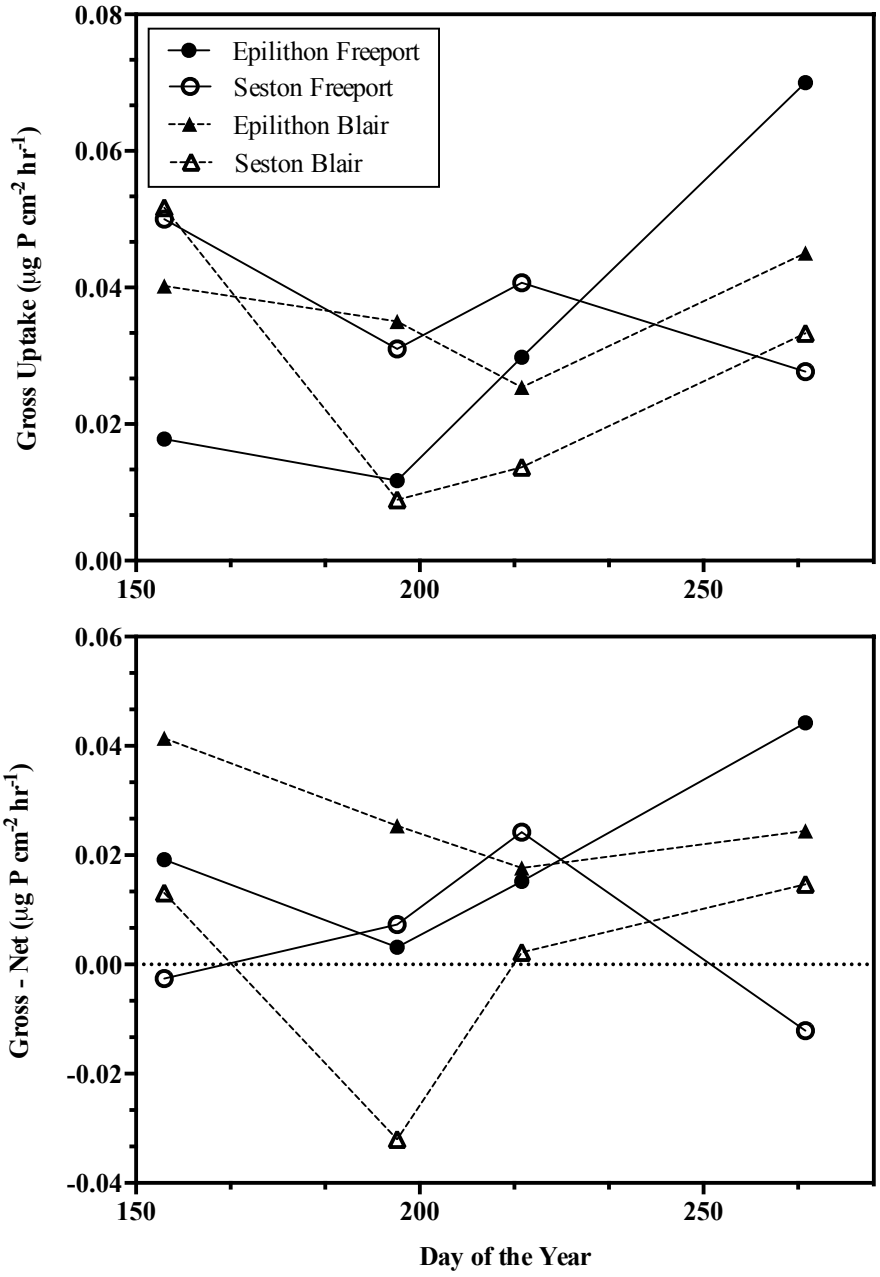

Figure 3.17: Seasonal variations in gross PO_4^{3-} uptake (with no added PO_4^{3-}) and release rates by the seston and epilithon at Freeport and Blair. PO_4^{3-} release rates are estimated as gross minus net uptake.

3.3.4 Determination of the Michaelis - Menten parameters

Fitting Michaelis-Menten curves for each date and site for the seston + epilithon (Fig. 3.18) yielded R^2 values of 0.7 to 1.0. The data from all four dates were compiled in Fig. 3.19, where a Michaelis-Menten curve was fit to all data collected. On June 6th and September 25th, Freeport had smaller V_{max} and K_s values than Blair (Table 3.06). On the two summer sampling dates (July 15th and August 6th) Blair had much lower values for both. Uptake velocity at Freeport did not reach V_{max} on the July and August sampling dates in the tested SRP range (0-100 μg P L^{-1}). Failure to approach the V_{max} at the maximum tested PO_4^{3-} concentration caused an approximately linear relationship between uptake velocity and PO_4^{3-} concentration at Freeport on August 6th. This linear relationship caused the estimates of V_{max} and K_s to be poorly defined, with a range of values producing the same line, and standard error values larger than the parameter estimates. In order to perform curve fitting at Freeport for this date for both the seston and epilithon combined, the V_{max} was set to the V_{max} obtained at Freeport on July 15th. It can be observed that the range and shape of the curve was similar for these two dates (Fig. 3.18), allowing an estimate of K_s to be found using the assumed V_{max}. The seston-only V_{max} and K_s values were consistently lower than the epilithon-only values at both sites (Table 3.07). The log transformed values showed significantly larger V_{max} and K_s values for the epilithon (paired t-test , $p < 0.05$).

Seston-only V_{max} values were always higher for Freeport than Blair (paired t-test on log-transformed data, $p < 0.05$). The data from all dates was compiled, and rectangular hyperbolas were fit to all seston and epilithon data separately (Fig. 3.20). Both the seston and epilithon at Blair possess lower V_{max} and K_s values than at Freeport. The model fit was far superior for the epilithon than the seston on several sampling dates.

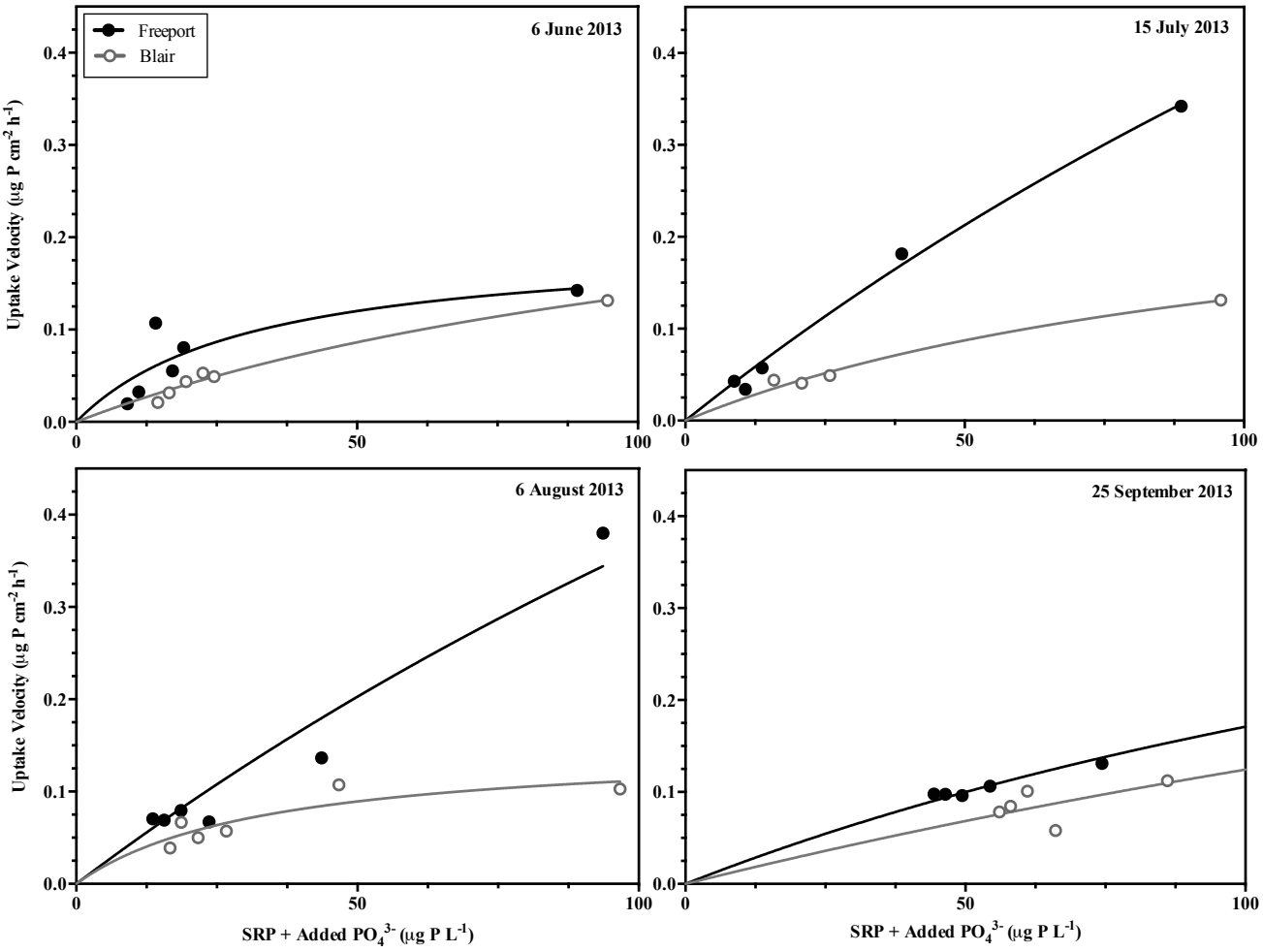

Figure 3.18: Uptake rate vs. initial SRP plus added PO_4^{3-} for Freeport and Blair (seston + epilithon) for the summer of 2013. The fitted line was estimated using non-linear least squares regression for each date. The highest concentration point (> 200 µg P L^{-1}) for both Freeport and Blair is excluded from the September 25th plot, but was used to calculate the Michaelis-Menten parameters.

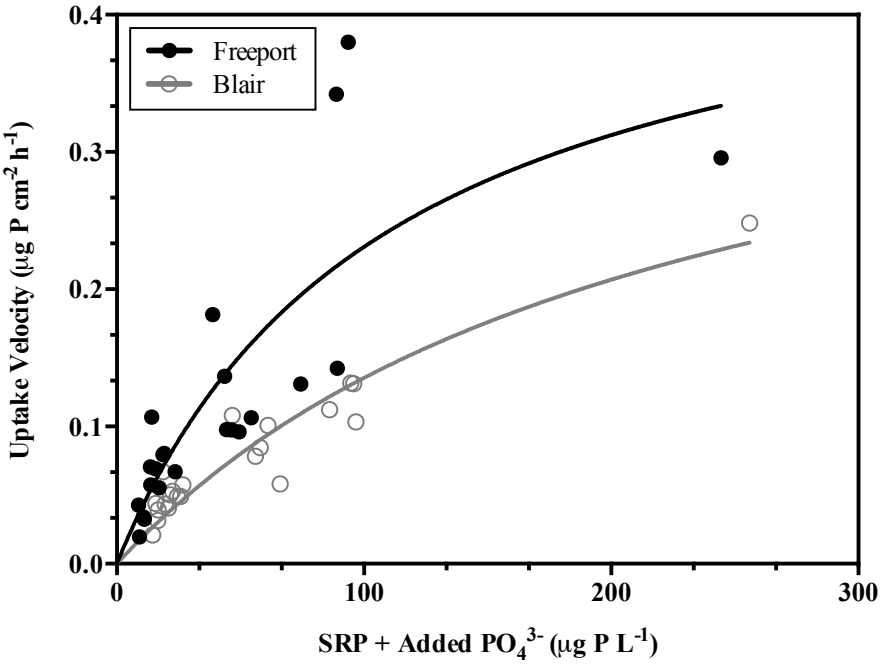

Figure 3.19: Uptake rate vs. initial SRP plus added PO_4^{3-} for Freeport and Blair (seston + epilithon) for the summer of 2013. The fitted line was estimated using non-linear least squares regression for all dates.

Table 3.06: Michaelis-Menten parameters calculated using non-linear least squares regression for the Grand River sites for both the epilithon and seston over the summer of 2013. Also included are the R^2 values for each regression analysis, and the calculated MM parameters using data from all of the samples. Parameters are expressed ± S.E. resulting from the fit curves, For comparison to V_{max}, V is included and represents the total gross uptake rate at ambient PO_4^{3-}.

Date	Site	V_{max} (µg P cm^{-2} h^{-1})	K_s (µg P L^{-1})	R^2	V (µg P cm^{-2} h^{-1})
June 6th	Freeport	0.19 ± 0.06	31.3 ± 21.7	0.69	0.02
	Blair	0.32 ± 0.07	139 ± 44.4	0.98	0.02
July 15th	Freeport	1.71 ± 0.86	353 ± 216	0.99	0.04
	Blair	0.28 ± 0.06	114 ± 42.8	0.98	0.04
August 6th	Freeport	1.71*	372 ± 31.5	0.94	0.07
	Blair	0.14 ± 0.03	33.9 ± 18.1	0.77	0.04
September 25th	Freeport	0.59 ± 0.03	247 ± 22.7	1.00	0.10
	Blair	0.68 ± 0.25	449 ± 225	0.95	0.08
All	Freeport	0.48 ± 0.13	109 ± 53.5	0.66	-
	Blair	0.43 ± 0.08	224 ± 62.3	0.88	-

* Fixed V_{max} = approximately linear relationship between uptake velocity and $[PO_4^{3-}]$

Table 3.07: Michaelis-Menten parameters calculated using non-linear least squares for the epilithon and seston separately, from the Grand River sites over the summer of 2013. Also included are the R^2 values for each regression analysis and the regression for all seston and epilithon uptake velocities, from all three dates. Parameters are expressed ± S.E. resulting from the fit curves. For comparison to V_{max}, V is included and represents the gross uptake rate at ambient PO_4^{3-}.

Date	Site	Community	V_{max} (µg P cm^{-2} h^{-1})	K_s (µg P L^{-1})	R^2	V (µg P cm^{-2} h^{-1})
June 6th	Freeport	Seston	0.10 ± 0.05	17.6 ± 20.4	0.37	0.01
		Epilithon	0.15 ± 0.06	125 ± 74.3	0.94	0.01
	Blair	Seston	0.03 ± 0.01	27.4 ± 33.1	0.36	0.01
		Epilithon	0.55 ± 0.3	393 ± 283	0.98	0.01
July 15th	Freeport	Seston	0.63 ± 0.3	193 ± 139	0.98	0.03
		Epilithon	0.74*	381 ± 16.4	0.99	0.01
	Blair	Seston	0.05 ± 0.02	90.5 ± 69.1	0.90	0.01
		Epilithon	0.23 ± 0.07	122 ± 60.4	0.97	0.04
August 6th	Freeport	Seston	0.63*	230 ± 28.0	0.90	0.04
		Epilithon	0.74*	353 ± 31.0	0.94	0.03
	Blair	Seston	0.04 ± 0.02	16.5 ± 23.9	0.24	0.01
		Epilithon	0.12 ± 0.01	56.7 ± 12.4	0.97	0.03
September 25th	Freeport	Seston	0.10 ± 0.02	76.5 ± 44.3	0.68	0.03
		Epilithon	0.74 ± 0.38	605 ± 399	0.95	0.07
	Blair	Seston	0.06 ± 0.01	50.8 ± 32.6	0.50	0.03
		Epilithon	4.78 ± 20.34	$6.13 \times 10^3 \pm 2.69 \times 10^4$	0.96	0.05
All	Freeport	Seston	0.15 ± 0.04	44.3 ± 30.8	0.35	-
		Epilithon	0.53 ± 0.18	352 ± 160	0.85	-
	Blair	Seston	0.05 ± 0.01	41.3 ± 21.0	0.47	-
		Epilithon	0.54 ± 0.17	481 ± 191	0.89	-

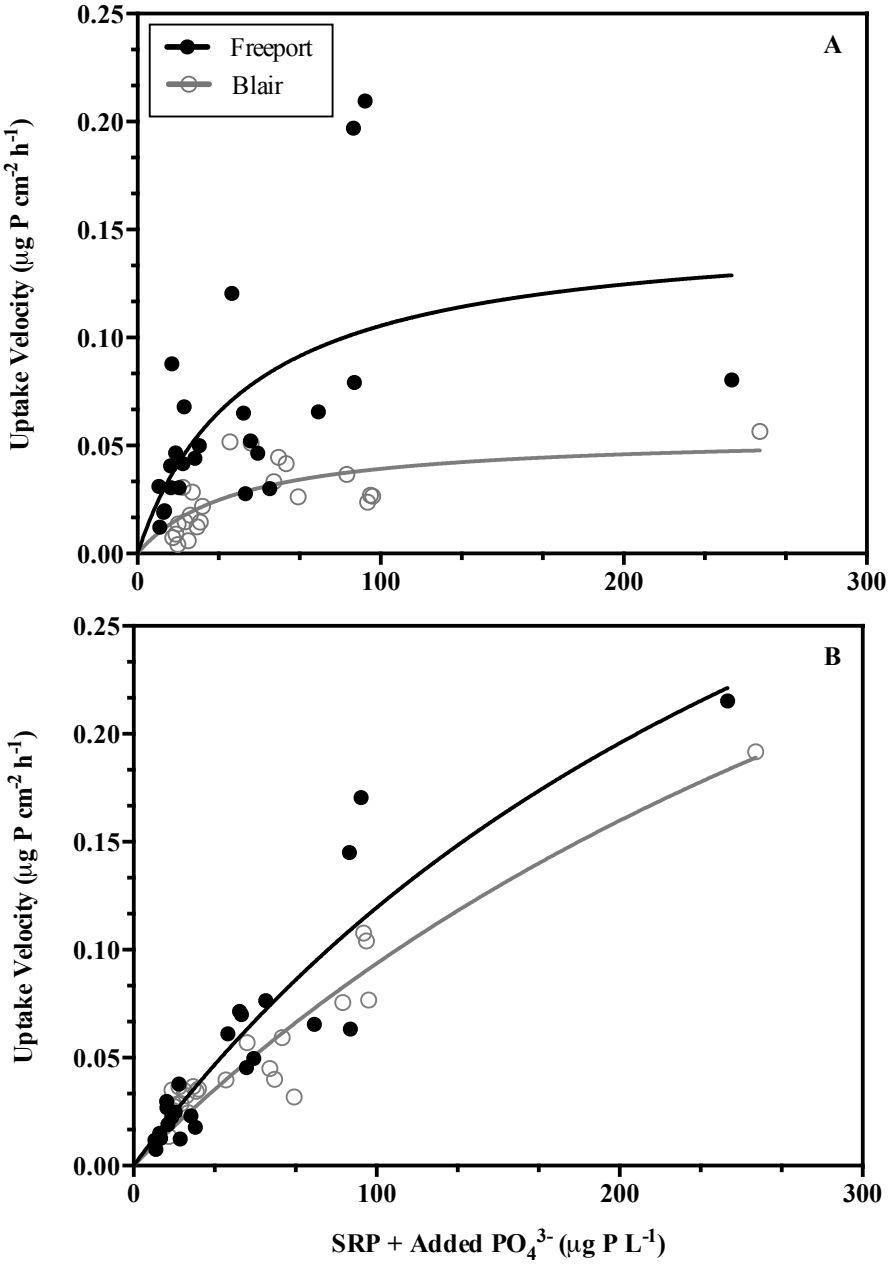

Figure 3.20: Uptake rate vs. initial SRP plus added PO_4^{3-} for the a) seston and b) epilithon at Freeport and Blair over the summer of 2013. The fitted lines were estimated using non-linear least squares regression for all dates.

3.3.5 Uptake lengths following point source enrichment

Uptake lengths (seston + epilithon) at Freeport ranged from 30 to 106 km with a mean of 70 km, and from 43 to 144 km at Blair, with a mean of 86 km (Table 3.08). The longest uptake lengths were observed in the spring (June) and autumn (September) at both sites, with reduced values in July and August (Fig. 3.21). Mean uptake lengths were not significantly different between the two sites (paired t-test, $p = 0.51$), and were significantly correlated with SRP ($r = 0.81$, $p < 0.05$; Fig. 3.22 a). The sampling point from Blair from September 25th affected the correlation between uptake length and SRP where the longest uptake length and largest SRP was obtained, and without this point the correlation between SRP and uptake length was not quite significant ($r = 0.63$, $p = 0.07$). The relationship between uptake length and river discharge was assessed for the Grand River using flow data provided by the GRCA monitoring program for the sites at Victoria (near Freeport), and Doon, (near Blair). No significant correlation between flow and uptake length was found for either site ($r = -0.04$, $p = 0.91$; Fig. 3.22 b).

Table 3.08: Uptake lengths (seston + epilithon) for the Grand River sites over the summer of 2013. SRP is included as well as the GRCA flow data measured at Victoria and Doon. Also included is the range of values collected at Winterbourne (Barlow-Busch et al., 2006).

Date	Site	SRP ($\mu g\ P\ L^{-1}$)	Flow ($m^3\ s^{-1}$)	Uptake Length (km)
June 4th	Freeport	25.4	62.0	89
	Blair	38.0	59.7	76
June 6th	Freeport	9.1	29.4	87
	Blair	14.5	28.3	73
July 15th	Freeport	8.7	44.7	38
	Blair	15.9	40.5	43
August 6th	Freeport	13.6	40.4	30
	Blair	16.7	35.6	49
September 25th	Freeport	44.4	40.3	106
	Blair	56.1	35.7	144
	Winterbourne	5 to 20	-	0.2 to 5.5

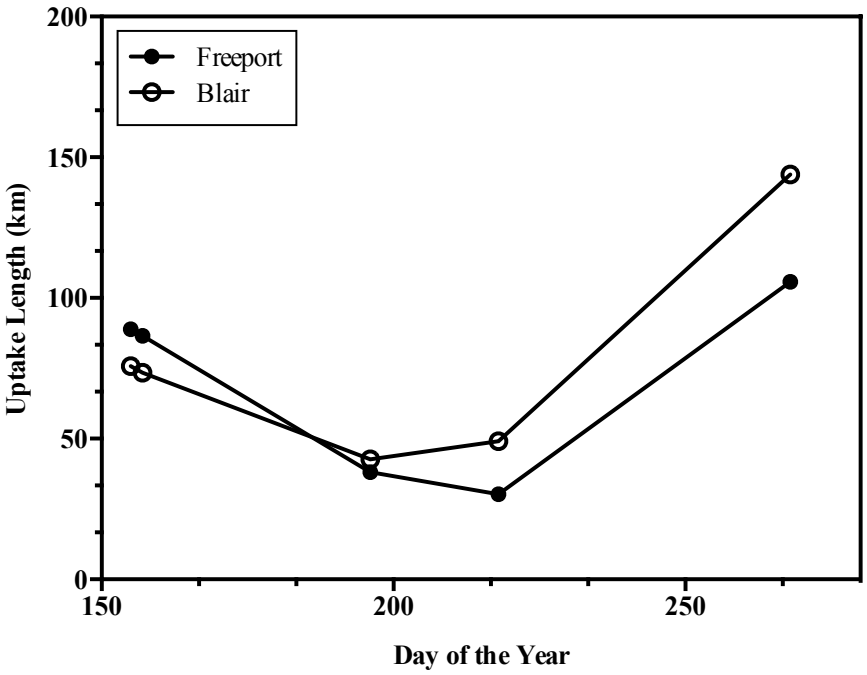

Figure 3.21: Uptake length (seston + epilithon) for Freeport and Blair over the summer of 2013.

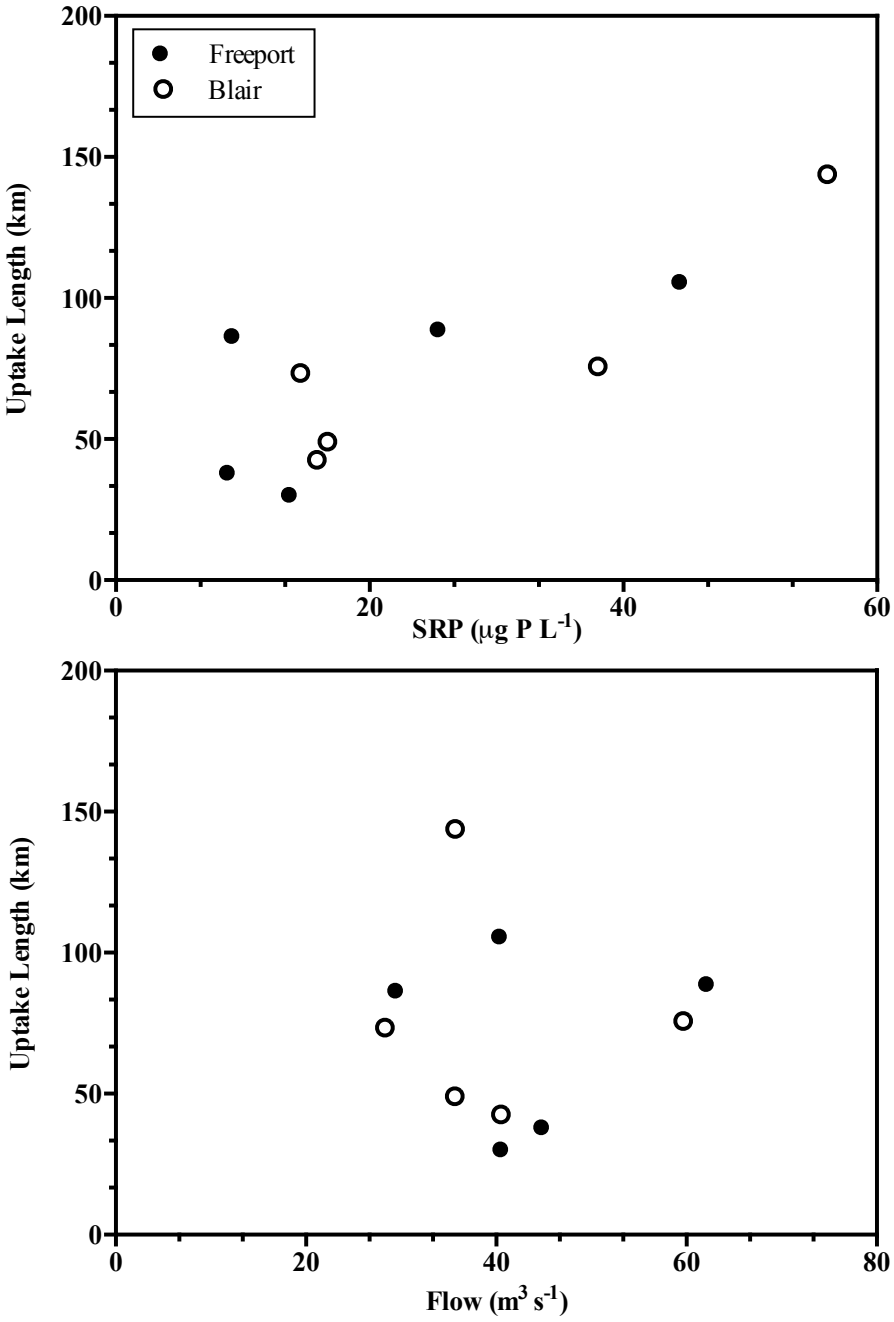

Figure 3.22: Uptake length (seston + epilithon) vs. a) SRP and b) river discharge for Freeport and Blair over the summer of 2013.

3.4 Discussion

3.4.1 Contribution of seston and epilithon to PO_4^{3-} uptake

At ambient PO_4^{3-} concentrations the epilithon contributed the major share of PO_4^{3-} uptake below the Kitchener WWTP (Blair). The average sestonic contribution to total uptake over all sampling dates was greater at Freeport (58%) than Blair (37%). The greater river depth at Freeport can explain most of the discrepancy between the sites sestonic uptake at an ambient nutrient concentration, with depth used to calculate areal sestonic uptake rates. Although uptake by the seston is expected to be low in smaller streams, large rivers have been found to possess significant seston uptake, particularly in rivers with developed phytoplankton communities (Newbold, 1992).

The contribution of these two communities to PO_4^{3-} uptake appears to be highly variable. This variability is observed not only between different river systems, but also between sites and dates along the same river. Storm events and periods of high flow positively correlated with high seston uptake velocities. High flow is known to increase seston biomass (to a limit) both aerially and volumetrically (Barlow-Busch et al., 2006). River conditions, including flow and depth, appear to satisfactorily explain much of the variation in seston uptake but fall short of explaining the range of uptake rates carried out by the epilithon. This was similarly observed in the Upper Grand River (Barlow-Busch et al., 2006). Only ambient SRP showed a positive correlation with epilithon uptake. Barlow-Busch (1997) examined the effect of light and river temperature on PO_4^{3-} uptake velocity, and found no relationship. Uptake velocities did however change over the course of the day but the relationship between time of day and uptake was not consistent, or predictable (Barlow-Busch, 1997). The environment of the epilithic-matrix can be different than what is measured within the river channel at the time of sampling, causing complicated relationships between epilithon uptake rates and field measured parameters, particularly amongst thick algal mats (Barlow-Busch, 1997).

It is not surprising that epilithon uptake was not correlated to epilithon biomass. It has been hypothesized that among benthic algal species the surface layer is responsible for the majority of PO_4^{3-} uptake from the overlying water (Horner et al., 1990). That is, as the rocks become covered in biofilm over the growing season only the outer layer is responsible for the majority of nutrient uptake, while the inner layer remains less active. The entire exposed rock surface however was scraped, and contributed to the biomass estimate, including the inner, less-active cell layers.

The average epilithon biomass in this study, 10.0 mg AFDW cm^{-2}, was lower than that of Winterbourne for June to October 1996, 15.0 mg AFDW cm^{-2}. The summer of 2013 experienced several prolonged periods of high flow and multiple storm events that exceeded those observed in 1996, potentially diminishing the epilithon biomass. These storm events may also be responsible for the lack of temporal trends in epilithon biomass over the sampling season. Barlow-Busch (1997) noticed low spring biomass followed by a peak in August that remained high until October. In the current study, the epilithon showed its highest biomass at Blair in the early summer, followed by a large reduction in August that was similarly low in September. Potentially the storm events that occurred throughout late July scoured the substrata prior to the August 6th sampling. The infrequency of the sampling trips also makes temporal trend analysis difficult.

Comparing the seston and epilithon ambient rates of gross PO_4^{3-} uptake to their community-specific V_{max} can establish how quickly they were taking up P relative to their potential. V_{max} and K_s can also be used to make inferences about the PO_4^{3-} demand at the two sites. V_{max} values are expected to increase in response to P limitation, while K_s values fall (Healey et al., 1980, Hwang et al., 1998). These high V_{max} and low K_s values offer organisms a competitive advantage when facing low nutrient concentrations (Healey et al., 1980). In fact the V_{max}/K_s ratio has been found to increase by several orders of magnitude in response to low ambient PO_4^{3-} concentrations (Hwang et al., 1998).

Grand River seston and epilithon did not reach their V_{max} under ambient nutrient concentrations for the dates studied. Ambient SRP at Blair is known to exceed the K_s values estimated in this study, thus the communities at Blair are expected to approach V_{max} within the ecologically relevant SRP range. Lower K_s values are interpreted as an increased ability to assimilate P at low concentrations (Scinto & Reddy, 2003). Grand River seston possesses lower K_s values (16.5 to 230 µg P L^{-1}) than the epilithon (56 to 6130 µg P L^{-1}), suggesting the seston possess a higher affinity for low SRP concentrations. Both the Grand River epilithon and seston however possess much lower PO_4^{3-} affinities compared to other studied planktonic (Taft et al.,1975; 2.8 to 52.3 µg P L-1, Hwang et al., 1998; 0.1 to 28.3 µg P L^{-1}) and periphytic algal species (Bothwell, 1985; 0.5 to 7.2, Hwang et al., 1998; 0.1 to 20.9 µg P L-1, Scinto & Reddy, 2003: 264 to 508 µg P L-1).

3.4.2 Reduced PO_4^{3-} uptake at Freeport and Blair

Maximum rates of uptake (V_{max}) were often lower at Blair than Freeport, particularly throughout the summer months when periods of low flow cause minimal dilution for point source inputs. It is at this time that the processes controlling P retention, i.e. sorption and biological uptake, are at their most important for reducing effluent concentrations. The low V_{max} values below the Kitchener WWTP suggest a limited capacity of the biota to reduce these concentrations.

Ambient rates of gross P uptake at Freeport and Blair (0.04 to 0.10 µg P cm^{-2} h^{-1}) are at the low end among the rates observed at Winterbourne (Barlow-Busch et al., 2006: 0.06 to 1.83 µg P cm^{-2} h^{-1}). The range of seston uptake velocities was similar between the studies, thus the difference in total uptake velocities is largely caused by lower epilithon uptake at Freeport and Blair (mean: 0.03 µg P cm^{-2} h^{-1}), than at Winterbourne (mean: 0.26 µg P cm^{-2} h^{-1}). The discrepancy in epilithon biomass between this study (mean: 10 mg AFDW cm^{-2}) and the previous study (Barlow-Busch et al., 2006; mean: 15 mg AFDW cm-2) does not appear large enough to account for the difference in uptake velocities. Biomass corrected epilithon uptake in this study averaged 0.003 µg P mg $AFDW^{-1}$ h^{-1}. Using the mean epilithon uptake velocity (0.26 µg P cm^{-2} h^{-1}) and mean epilithon biomass

provided in Barlow-Busch et al. (2006) equates to a velocity of 0.02 μg P mg AFDW^{-1} h^{-1}. The epilithon appear to be displaying much slower rates of uptake on both an areal and biomass basis than what was observed in the upper Grand River.

Despite being lower than what was previously observed at Winterbourne, the rates for gross uptake by the epilithon at Freeport and Blair (0.01 to 0.07 μg P cm^{-2} h-1) are similar to the uptake rates of epiphytes from the eutrophic La Platte River Vermont (0.02 to 0.10 μg P cm^{-2} h^{-1}; Pelton et al., 1998). These rates are in fact larger than those of the epilithon collected from several pristine, boreal streams (Corning et al., 1989) where uptake ranged from 0.01 to 0.02 μg P cm^{-2} h^{-1}. The latter is attributable to lower epilithon biomass than that observed in this study. Comparing the results from this study and the previous study at Winterbourne could suggest that effluent exposure correlates with reduced PO_4^{3-} uptake by the epilithon.

One hypothesis for the lower PO_4^{3-} uptake at Freeport and Blair is reduced PO_4^{3-} uptake efficiencies at enriched P concentrations (Mulholland et al., 1990). Marti et al. (2004) showed that long-term nutrient enrichment could saturate biological communities, and decrease their ability to retain available nutrient pools. This process was also discussed in Gibson & Meyer (2007) where SRP uptake velocities for the effluent-impacted Chattahoochee River were significantly lower than those of un-impacted streams.

Stream periphyton communities are predicted to become P saturated at PO_4^{3-} concentrations exceeding 6 μg P L^{-1} (Mulholland et al., 1990). Processes like abiotic sorption and luxury uptake may continue above this concentration but will not result in a clear relationship between PO_4^{3-} concentration and biomass (David & Minshall, 1999). Bothwell (1989) however discusses the existence of two levels of periphyton PO_4^{3-} saturation. The first is a cellular PO_4^{3-} limitation affecting the growth of individual algal cells or thin periphytic mats, which occurs at low P concentrations. The second is a community level saturation, caused by thicker layers of periphyton accrual. In this case, the internal cell layers receive less PO_4^{3-} than the surface layer, and

remain P-limited even when the outer layer reaches saturation. Community level saturation was observed at 30-50 μg P L^{-1} in experimental troughs filled with water from the South Thompson River, British Columbia, under varying levels of PO_4^{3-} enrichment (Bothwell, 1989). Horner et al. (1983) showed a biomass response amongst periphyton communities that continued to increase at concentrations above 50 μg P L^{-1}, but lost proportionality with PO_4^{3-}concentration above 25 μg P L^{-1}. Cessation of biomass response to PO_4^{3-} concentration indicates a secondary limitation to periphytic growth (Bothwell, 1989).

Declining rates of areal PO_4^{3-} uptake have also been found with increasing epilithon biomass (Horner et al., 1990). This relationship has been illustrated when increasing algal mat thickness, as opposed to increased rock coverage, causes an increase in biomass. As discussed, thick biofilms can possess an external P replete cell layer, and an internal P-limited layer that possesses much lower rates of areal uptake. Mean epilithon biomass was higher at Winterbourne than Freeport and Blair, thus thicker algal mats may be expected to be more prevalent during the study at Winterbourne. Other factors that can reduce or limit algal growth rates include: grazing pressure, changes to community structure (Sabater et al., 2002), reduced substratum stability, and limiting levels of other nutrients (Bothwell, 1989). Grazers, for example, have been found to significantly decrease periphyton biomass in stream environments (Winterbourn & Fegley, 1989, Hillebrand & Kahlert, 2001). When the effects of changing N and P concentrations in grazed and un-grazed conditions have been studied, increasing effects on periphyton biomass and composition by grazers were observed at high nutrient concentrations compared to more nutrient depleted environments (Rosemond et al., 2000, Hillebrand & Kahlert, 2001). Potentially grazers have a large impact on periphytic communities at the downstream, P –enriched sampling sites. Grazers are believed to impact the ability of periphyton to effectively remove compounds from the water column by altering the dominant taxa, the amount of growth, and the structure of the algal mats (Sabater et al., 2002).

An alternate hypothesis for the difference in uptake velocities between this study and that of Barlow-Busch et al. (2006) is the use of SRP in the calculation of gross uptake rates. Overestimation associated with SRP may be worse when SRP concentrations are low, with SRP found to significantly overestimate true PO_4^{3-} concentrations in lakes (Rigler, 1966, Tarapchak & Rubitschun, 1981). This overestimation could cause elevated estimates of uptake at Winterbourne, with reduced uptake at Freeport and Blair where PO_4^{3-} concentrations are higher. The mean SRP observed at Winterbourne was 14 µg P L^{-1}, with a range of 5 to 20 µg P L^{-1}. The mean SRP at Freeport was 20 µg P L^{-1} with a range from 8 to 44 µg P L^{-1}. This SRP difference may not appear large enough to explain the discrepancy in rates, but could offer a partial explanation.

For river management purposes, understanding the effect of changing P concentrations on downstream epilithon populations is important, both for determining how to decrease algal growth, and to elucidate the effect increasing P concentrations will have on downstream receiving waters. The ability of the river to reduce the bioavailability of excess PO_4^{3-} delivered via the WWTPs is of critical importance for maintaining downstream water quality (Gibson & Meyer, 2007). The reduced epilithon uptake velocities of Freeport and Blair could suggest this ability is alterable and impaired in the Grand River. Due to the slower epilithon uptake, increasing effluent P concentrations could be expected to result in longer distances of excessive periphytic and macrophytic growth, and increased concentrations of PO_4^{3-} travelling further distances without transformation or retention. Although there is an increase in periphytic biomass at Blair, this increase is not sufficient to compensate for the reduced PO_4^{3-} uptake velocities and increased P loads at Blair. Diminished retention capabilities could limit the role of the epilithon as a PO_4^{3-} sink in these downstream reaches.

The low rates of epilithon PO_4^{3-} uptake also increase the importance of seston for downstream P cycling, meaning the processes controlling sestonic P uptake and biomass could play a major role in the delivery of P downstream. The biomass of seston in large rivers, possessing

water residence times longer than 3 days, is thought to be strongly related to TP concentration. Rivers possessing shorter residence times (<3 d) possess a negative correlation between discharge and suspended algae biomass, caused by increased advective loss and insufficient time for phytoplankton development (Basu & Pick, 1994). The residence time of the Grand River is approximately 3 d (Rosamond, 2013) and the Grand River possesses the upstream Shand Dam that could provide the opportunity for phytoplankton development (Barlow-Busch et al., 2006). Other controls on seston biomass include: available light, predation, and interactions with benthic vegetation (Basu & Pick, 1994). The predicted positive relationship between TP and suspended algal biomass could cause suppression of periphytic communities at nutrient levels too high for the epilithon to control. This process has been noted in eutrophic systems, where high nutrient content leads to extensive phytoplankton blooms capable of shading benthic communities (Sand-Jensen & Borum, 1991).

Seston transport in streams is dependent on a variety of factors including discharge, particle size, streambed retention characteristics, and biological seston generation (Webster et al., 1987). It has been hypothesized that seston particles travel only short distances before they are retained by the streambed due to obstacles. Rough substrata reduce the distance travelled, but this is also dependent on the size of the particles (Webster et al., 1987). During periods of rapidly increasing flow rates, dislodgement of trapped particles will increase seston concentrations. Seston concentrations are expected to be highest in the summer months, particularly during periods of rapidly increasing flow (i.e. storm events) and lowest during the winter months. This trend may be due to higher accumulation of organic particulates during the warmer summer months (Meyers & Likens, 1979, Webster et al., 1987). Winter storms can also deplete the seston supply so that larger winter storms are required to produce similar quantities of seston delivered during smaller summer or autumn storms (Webster et al., 1987).

Seasonally, the increased occurrence of high flow events during the spring and autumn could result in increased seston transport. The spring and autumn will also be a period of reduced seston and epilithon biomass due to colder temperatures and lower light availability, but would still result in the entrainment of previously trapped particles (Webster et al., 1987). A peak in biomass in both seston and epilithon is expected during the warmer summer months, as well as reduced river discharge. Summer low flow will allow for greater seston retention in the streambed.

The greatest epilithon uptake rates would be expected during low flows, when the effect of depth, and seston shading do not reduce light availability. Low flows would also increase the association time between the epilithon and water column, further increasing PO_4^{3-} uptake. These factors could allow for the greatest reduction in water column PO_4^{3-} by the epilithon, which can act as transient storage increasing the P retained closer to the WWTPs. Thus, greater amounts of P retention may be expected during summer low flow. High amounts of summer P retention buffer the impacts of excessive P loading during the low flow periods when these loads could have the greatest impact on stream eutrophication (Withers & Jarvie, 2008). The low P uptake velocities of both the seston and epilithon at Blair in all studied months however could severely limit its abilities to reduce PO_4^{3-} concentrations even during these summer months. The ability of the river to reduce or alter the forms and concentration of P has implications for downstream water quality.

It is also interesting to note that on average, uptake velocity at Blair was lower than that of Freeport but epilithon biomass was significantly higher at Blair. Potentially the higher biomass at Blair indicates that a period of greater biomass accrual exists prior to the chosen sampling period (June to September), and higher rates of uptake could be observed during this time. Sampling carried out early in the summer may be required to capture the period of maximum biomass accrual below the Kitchener WWTP.

3.4.3 P turnover and retention in the Grand River

The PO_4^{3-} turnover times from Freeport and Blair, ranging from 12.0 to 39.8 h, are significantly greater than those presented in Barlow-Busch et al. (2006; $p < 0.05$ calculated from their Table 1 for July 1997 to July 1998). Turnover times at Blair were on average longer than those at Freeport, indicating slower PO_4^{3-} turnover at the more effluent-impacted site. The turnover times of the particulate and periphytic PO_4^{3-} pool at both Freeport and Blair (0.8 to 5.3 days) are comparable, but shorter, than those obtained for the Grand River in September of 2012 at Winterbourne. At Winterbourne, TT values ranging from 8 to 9 days were obtained (W.D. Taylor, unpublished). Freeport possessed a significantly longer mean particulate-P turnover time than Blair suggesting that sites with increasing effluent exposure possess longer dissolved TTs and shorter particulate TTs. It should be noted however that the same labeling issues that plagued the calculations of specific activity on the rock surface would affect the particulate TTs. The slow rates of PO_4^{3-}uptake cause uneven labeling resulting in particulate TTs that are overestimated. The increased dissolved PO_4^{3-} TTs suggest decreased PO_4^{3-} deficiency downstream of the point sources.

The elevated release rates obtained using the Hudson method could be due to the addition of high concentrations of competitive inhibitor (~ 5000 μg P L^{-1}) as discussed in Hudson & Taylor (1996). Higher amounts of regeneration were noted in lake water at the highest tested concentration of competitive inhibitor (> 5000 μg P L^{-1}), leading to greater amounts of ^{32}P displacement than under ambient PO_4^{3-} concentrations. The ideal concentration of competitive inhibitor that can be added to river water and prevent re-incorportation of ^{32}P without altering release rates should be assessed for the epilithon. Also an assessment of the incubation time required to evenly label the river epilithon with ^{32}P would allow for better results when using this method in future lotic studies.

Uptake lengths were longer at Blair than Freeport, but values for both sites (30 to 144 km) were considerably longer than those estimated for the upstream Winterbourne site (Barlow-Busch

et al., 2006; 162 m to 5.5 km). Uptake lengths, as a measure of PO_4^{3-} retention efficiency, have been estimated mainly in pristine rivers with fewer studies carried out to assess the capacity of effluent enriched streams or river reaches. These pristine environments often possess low SRP concentrations, rapid uptake, and short uptake lengths: 29- 455 m (Mulholland et al., 1990) and 109 – 2793 m (Butturini & Sabater, 1998). Longer uptake lengths have been observed among WWTP polluted rivers: 7.4 to 15.2 km (House & Denison 1997); 15 to 138 km (Pollock & Meyer 2001); 0.14 to 14 km (Marti et al ., 2004); 9 to 31 km (Haggard et al. 2005); 11 to 85 km, (Gibson & Meyer, 2007). Longer uptake lengths are indicative of decreased nutrient retention capabilities, illustrating that some rivers are saturated in their ability to assimilate nutrients. The Grand River uptake lengths are in the upper end of the previously published values, providing further evidence that the Grand River is impaired in its ability to assimilate the PO_4^{3-} added by the Waterloo and Kitchener WWTPs.

WWTP impacted streams have also been found to exhibit no correlation between river discharge and uptake length (Pollock & Meyer, 2001, Marti et al., 2004). Unaffected rivers on the other hand may demonstrate a strong positive relationship between the two (Butturini & Sabater, 1998). The lack of correlation between flow and uptake length observed in this study is similar to that of a study carried out in the Big Creek, a tributary of the Chattahoochee River affected by poultry litter inputs. In the Big Creek, no correlation was found between discharge and uptake length, and a positive correlation was found with effluent SRP (Pollock & Meyer, 2001). The failure to relate flow and uptake length in this study could also be due to the limited sampling dates, and relatively small range of flow values. The longer uptake lengths collected in the autumn and spring support the theory that greatest PO_4^{3-} retention can occur in the summer months.

3.5 Conclusions

There were several temporal and spatial trends in P kinetics within the Grand River. Firstly, among the five sampling dates the longest uptake lengths were observed in the spring and autumn.

Lower values were obtained in the summer months potentially indicating greater nutrient retention efficiency during these times. The spatial differences include: increased contribution to total uptake by the epilithon, increased epilithon biomass, decreased total uptake, increased rates of total PO_4^{3-} release from the seston and epilithon, decreased PO_4^{3-} turnover times, and increased PO_4^{3-} uptake lengths at Blair relative to Freeport. Although increased biomass does accompany the increased PO_4^{3-} loading brought on by the Kitchener WWTP, these increases do not appear large enough to compensate for the increased P loading, and decreased uptake velocities observed at Blair. The long PO_4^{3-} turnover times at both Freeport and Blair also indicate a significantly reduced P demand compared to the upstream Grand River.

Although both sites displayed lower rates of uptake than those observed at Winterbourne, it would appear that the site downstream of the Kitchener WWTP has much lower maximum rates of uptake, and is unable to assimilate the large P concentrations delivered by the plant. These significant P contributions have large-scale effects on the river's P-kinetics, limiting its ability to act as a net nutrient sink. The long uptake lengths observed in the Grand River provide evidence that the effluent's PO_4^{3-} additions are exceeding the river's assimilative capacity. These inputs appear to possess the ability to affect regional water quality, with the high PO_4^{3-} loads projected to be carried long distances to the downstream environment of L. Erie, with limited storage by the epilithon in the adjacent river reaches.

Chapter 4: Modelling the impacts of a nutrient point source: effect on phosphate concentration and $\delta^{18}O$-PO_4 values

4.1 Introduction

4.1.1 Processes affecting $\delta^{18}O$-PO_4 in lotic environments

Relating the rates of PO_4^{3-} uptake and release (chapter 3) to the expected $\delta^{18}O$ -PO_4 values (chapter 2) could result in a model capable of predicting the distance required to achieve a reset of the PO_4^{3-} pool to equilibrium, following a point source input. Such a model would provide results for determining when $\delta^{18}O$ -PO_4 is a valuable tool for studying P cycling in an effluent impacted river. Little work has gone into utilizing this tool in river environments and it is not clear if and when $\delta^{18}O$ -PO_4 analysis can divulge information on P cycling and sources in these systems.

In order to interpret $\delta^{18}O$ -PO_4 values in lotic environments, it is important to understand how $\delta^{18}O$-PO_4 signatures respond as the effluent PO_4^3 is assimilated, released, and carried downstream. It is also important to understand what is controlling the signatures above the point source, and how quickly this control will once again dominate downstream. Oxygen isotopes of PO_4^{3-} reflecting a WWTP effluent will occur for some distance downstream. The affected distance is dependent on the rate of PO_4^{3-} recycling, and the contribution of the effluent P to total river P. A conceptual model can be used to explain the major processes controlling the O isotopes of PO_4^{3-} downstream of a point source (Fig. 4.01). Their dominance is controlled by the size of the bio-available P pool. Equilibrium fractionation is dominant in a P-depleted environment, while source signatures are preserved longer when P is not present in biologically limiting concentrations. Values reflecting DOP remineralization are expected in extremely DIP-deprived environments. Relating this to the P regime observed in effluent-impacted rivers, one might expect upstream values to show either equilibrium or kinetic fractionation effects. The downstream environment should reflect effluent $\delta^{18}O$-PO_4 until biological recycling resets the P pool. Mixing of the plume with river water could mask the plume's isotopic signature, so dilution needs to be assessed to isolate

the fate of the effluent. Dilution effects will be dependent on the rate of plume dispersion, the ambient river SRP, the effluent SRP, as well as the deviation of the effluent $\delta^{18}O$ -PO_4 values from those upstream of the plant.

$\delta^{18}O$ -PO_4 analysis could also be a valuable tool for determining rates of PO_4^{3-} cycling without the use of PO_4^{3-} additions or radiolabelling. The difficulties associated with determining accurate rates of release can be observed in chapter 3 of this thesis, where three methods were tested and provided a range of values for each sampling date. Further difficulty exists in relating these "within-beaker" rates to whole-river P kinetics. Assumptions based on the cross-sectional geometry of a river site, as well as the roughness of the substrata, are required. These likely provide poor estimates of parameters that are highly variable in river ecosystems. Estimates of uptake by macrophytes and their associated epiphytes are also unknown. Using $\delta^{18}O$ -PO_4, all of these rates can be assessed based on the agreement between river DIP and equilibrium.

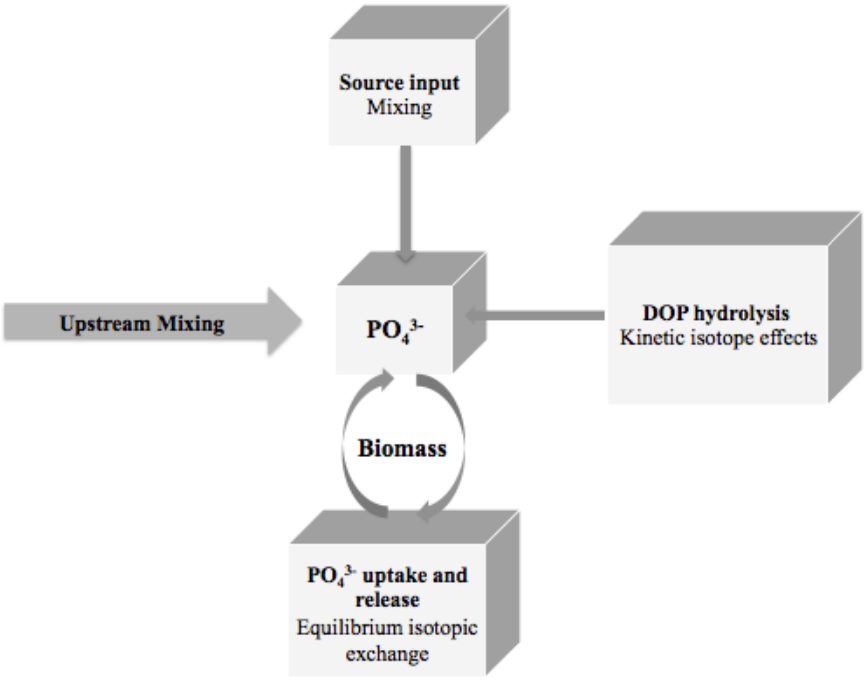

Figure 4.01: Conceptual model of the major processes affecting the $\delta^{18}O$ -PO_4 signatures in rivers.

4.1.2 Research objectives

Chapter 3 illustrated that inputs from two of the largest WWTPs in the Grand River watershed lead to sluggish PO_4^{3-} uptake rates, and long uptake lengths in the river. These experimental values for uptake and release allow for a model for PO_4^{3-} concentration following a point source input. This allows for predictions of PO_4^{3-} concentration in the downstream river reaches and observations based on the downstream "recovery curve" for SRP.

PO_4^{3-} kinetics and $\delta^{18}O$-PO_4 values calculated in the previous chapters of this thesis include: PO_4^{3-} uptake and regeneration rates by the seston and epilithon, steady-state PO_4^{3-} concentrations, and effluent $\delta^{18}O$ -PO_4 values. Use of theses rates will result in an underestimation of PO_4^{3-} uptake due to the absence of uptake by macrophytes and their associated epiphytes, and failure to account for the roughness of the substratum. This latter problem could significantly increase the effective surface area for PO_4^{3-} uptake. The extent of this underestimation will be assessed. There is also a failure to account for enzyme-driven DOP remineralization, based on the limited availability of the rates and conditions under which this occurs. WWTP "plume chases" were previously carried out in the Grand River, and involved measuring SRP at several sites downstream of the discharge points. These plume chases allow for an assessment of model fit.

Due to the limited use of $\delta^{18}O$ -PO_4 analysis in river systems, no model exists for predicting the response of $\delta^{18}O$ -PO_4 with distance from a point source. Based on the lengthy and burdensome nature of adapting this tool for freshwater samples, it is important to understand what river environments will lead to results that would illustrate important features of P cycling or source inputs. These estimates could also indicate what sites should be sampled. It is my contention that given the Grand River's seemingly typical uptake lengths amongst effluent-impacted rivers, this model could allow for an evaluation of the conditions that will permit $\delta^{18}O$ -PO_4 analysis to provide valuable insight on P cycling in riverine environments. This will involve determining when $\delta^{18}O$ -

PO_4 values reflecting source inputs can be isolated in the water column. These issues will be examined through the following questions:

1) What is the expected relationship between PO_4^{3-} concentration, $\delta^{18}O$ -PO_4, and distance downstream of a WWTP?
2) How well can the rates of uptake and release from the beaker incubation experiments estimate river P-kinetics?
3) How far downstream will effluent $\delta^{18}O$ -PO_4 signatures be retained under a range of end-member conditions?
4) Under what conditions would the use of $\delta^{18}O$ -PO_4 analysis be useful for assessing the contribution of effluent inputs on the downstream SRP pool? That is, what model parameters allow for source signatures to be observed in the downstream river reaches?

These questions will be answered using data collected from the Waterloo and Kitchener WWTPs, and their downstream river reaches as case studies.

4.2 Materials and Methods

4.2.1 Research sites

Two reaches along the Grand River, within the Region of Waterloo, were modeled for changing PO_4^{3-} and $\delta^{18}O$ -PO_4 with distance downstream. For a full watershed description refer to the Materials and Methods section in chapter 2. The first reach includes the river section immediately downstream of the Waterloo WWTP and the adjacent 6000 m stretch until the sampling site at Victoria Street. The second reach includes the 6000 m stretch starting at the confluence of the Kitchener WWTP, and ending at the sampling site in Blair (Fountain Street). These reaches were chosen to assess the length of the river impacted by two of the largest WWTPs in the watershed. Plume chases had previously been carried out for the Kitchener WWTP in July of 2010, 2011, and 2012 where SRP measurements were taken at discrete distances downstream of the plant's confluence, ending at Blair. Similarly, in August 2012, samples were collected below the

Waterloo WWTP at several sites downstream, ending at Victoria Street. Plume sampling was carried out by PhD candidate Eduardo Cejudo from the University of Waterloo. SRP samples were taken from the final effluent and from the river at several locations 2 to 5 times during the sampling dates. These data allowed the model fit to be determined. Cl^- concentration was also collected, allowing for the effect of dilution to be assessed. The gross and net uptake experiments described in chapter 3 of this report were carried out within these reaches, allowing for estimates of PO_4^{3-} uptake, PO_4^{3-}release, and steady-state PO_4^{3-} concentration.

4.2.2 Model description

In order to address the relationship between PO_4^{3-} concentration (measured as SRP) and distance downstream from a WWTP, the following equation was solved:

$$[{PO_4}^{3-}]\,(t) = [{PO_4}^{3-}{}_{Upstream}] + [{PO_4}^{3-}{}_{WWTP}] + [R_{Seston+Epilithon}] - [U_{Seston+Epilithon}] \qquad (4.1)$$

Where $PO_4^{3-}{}_{upstream}$ and $PO_4^{3-}{}_{WWTP}$ are measured in μg P L^{-1}, R is the amount of PO_4^{3-} being released and U is the amount of PO_4^{3-} being taken up by the seston and epilithon, measured in μg P L^{-1} min^{-1} at each time point (min) downstream. PO_4^{3-} (t) is calculated in units of μg P L^{-1} and represents the PO_4^{3-} concentration at each time point (min). The PO_4^{3-} concentration at each time point downstream is converted to the PO_4^{3-} concentration at each distance downstream using the river velocity (m min^{-1}). A value for $[PO_4^{3-}{}_{WWTP}]$ enters the model at time 0.

The relationship between $\delta^{18}O$ -PO_4 and distance downstream from a WWTP was predicted using weighted averages of the change to the PO_4^{3-} pool contributed by the different sources. This meant assuming mixing of the upstream and effluent $\delta^{18}O$ -PO_4, with inputs from the released PO_4^{3-} pool. The $\delta^{18}O$ -PO_4 in the mixture at any time point was calculated using the contribution (*f*) of each source to the total PO_4^{3-}:

$$\delta^{18}O - PO_4\,mix = (\delta^{18}O - PO_{4\,WWTP} \bullet fPO_{4\,WWTP}) + (\delta^{18}O - PO_{4\,Up} \bullet fPO_{4\,Up}) + (\delta^{18}O - PO_{4\,Equil} \bullet fPO_{4\,Release}) \qquad (4.2)$$

It was assumed that the upstream PO_4^{3-} was at the theoretical $\delta^{18}O$ -PO_4 equilibrium based on low SRP.

For simplicity in modeling it was also assumed that all PO_4^{3-} released has oxygen at isotopic equilibrium (Longinelli & Nuti, 1973, Eq. 1.2). Other processes are known to affect the signature of released PO_4^{3-}, particularly DOP hydrolysis. The impact of ignoring DOP hydrolysis on projected $\delta^{18}O$ -PO_4 signatures will be examined in the discussion portion of this chapter. The parameters describing projected PO_4^{3-} concentrations and $\delta^{18}O$ -PO_4 values will be described below

Uptake, Release and Steady-State PO_4^{3-}

Uptake was modeled using the Michaelis-Menten equation to describe the relationship between [PO_4^{3-}] and U (Eq. 3.7). Baseline model conditions were developed using the V_{max} and K_s values estimated for all seston and epilithon data separately over the summer of 2013. The Freeport data were used to estimate the uptake downstream of the Waterloo WWTP, and the values for Blair were used to estimate the uptake downstream of the Kitchener plant. Data from the two sites were not combined as higher effluent concentrations can lead to slower rates of uptake and longer uptake lengths, suggesting that reach-specific values for uptake and release should be used. However, I still had to assume that uptake kinetics are constant within the study reaches. This could lead to an overestimation of the uptake experienced immediately downstream of the plant, where the effects of the effluent's inputs are presumably highest.

Steady-state PO_4^{3-}concentrations were used to estimate the baseline upstream PO_4^{3-} prior to the WWTP inputs. This assumes that upstream of both plants PO_4^{3-} concentrations are low, such that uptake equals release. The SRP for Bridgeport (upstream of the Waterloo plant), and Victoria (upstream of the Kitchener plant) demonstrated low and relatively constant concentrations over the summer of 2012 (< 5 μg P L^{-1}; Section 2.3.1) suggesting the validity of this assumption. The mean steady state SRP for Freeport was used to model baseline upstream behavior for both river

reaches (SRP = 4.50 μg P L^{-1}). The rates of PO_4^{3-} release were calculated using the site-specific mean release rate from the summer of 2013 measured using the gross minus net approach for both Freeport and Blair. This relied on assuming a constant release rate for the entire stretch of river. Although release values were also calculated using the steady-state approach and the Hudson method, the gross minus net values were intermediate between the other two methods. The Hudson values probably overestimated PO_4^{3-} release as discussed in chapter 3. The steady-state values relied on several key assumptions including the fact that the river achieved a steady state, and that this could be captured in the laboratory. The gross minus net values rely on assuming that SRP is a suitable proxy for PO_4^{3-} concentration. Since both the estimates of gross uptake velocity and net uptake velocity rely on SRP values for their calculation, this could lead to an overestimate of total release.

Depth

A mean depth estimate was required for each reach to convert epilithon uptake and release rates to units of μg P L^{-1} h^{-1}. Depth was estimated using the daily average flow obtained from the GRCA monitoring stations for the downstream site at Doon (close to Blair) and the upstream site at Bridgeport during the summer of 2012. Discharge was translated to depth using the discharge-hydraulic radius relationship established for the sites at Bridgeport and Blair (Jamieson, 2010) as described in section 3.2.6. An average of the depth calculated using equations 3.8 and 3.9 was used to estimate the modeled reach depths. The assumption is that both modeled reaches will exhibit hydrologic characteristics (flow and depth) that are an average of the upstream site at Bridgeport and the downstream site at Blair.

Travel Time

Travel time was calculated using river discharge data (Q) from the GRCA monitoring station at Brantford accessed via Environment Canada's hydrometric database. Travel times were

previously estimated for several Grand River reaches, under different flow regimes, by the GRCA. Travel times were found through hydraulic modeling calibrated with dye tracer studies (Mark Anderson, personal communication). The relationship between travel time and river discharge was found, and converted to river velocity using the distance between two sites. The sites chosen to calculate travel time for the Waterloo reach were from the Waterloo WWTP to the GRCA monitoring site at Brantford. The sites chosen for the Kitchener reach were from the Kitchener WWTP to Brantford. Estimates of travel time were required in order to convert time-dependent uptake and release rates to values representing distance downstream from the two WWTPs. Baseline model velocity was calculated using the mean river flow at Brantford over the summer of 2012.

Table 4.01: Baseline PO_4^{3-} model conditions for the Waterloo and Kitchener reaches. MM parameters are calculated from all gross uptake experimental data from chapter 3 (Fig. 3.20). Release rates are average values from chapter 3 using the gross minus net approach (Table 3.03). Depth and velocity were calculated using the mean river flow over the summer of 2012. Upstream $[PO_4^{3-}]$ is the average steady state SRP measured at Freeport (Table 3.04). Effluent $[PO_4^{3-}]$ is the average SRP measured in the Waterloo and Kitchener WWTP effluent from the plume chases carried out in 2010, 2011 and 2012.

	Seston		Epilithon						
	V_{max} ($\mu g\ P\ L^{-1}\ h^{-1}$)	K_s ($\mu g\ P\ L^{-1}$)	V_{max} ($\mu g\ P\ cm^{-1}\ h^{-1}$)	K_s ($\mu g\ P\ L^{-1}$)	Release ($\mu g\ P\ cm^{-1}\ h^{-1}$)	Depth (cm)	Velocity ($cm\ s^{-1}$)	Upstream $[PO_4^{3-}]$ ($\mu g\ P\ L^{-1}$)	Effluent $[PO_4^{3-}]$ ($\mu g\ P\ L^{-1}$)
Waterloo	0.2	47	0.5	351	0.02	61	36	4.5	52
Kitchener	0.1	30	0.5	481	0.03	61	37	4.5	178

$\delta^{18}O$ -PO_4 Sources

The $\delta^{18}O$ -PO_4 values chosen to represent base conditions for equilibrium and the WWTP inputs were taken as the mean values observed in chapter 2. That is, the theoretical equilibrium was calculated from mean temperature and $\delta^{18}O$ –H_2O from the summer of 2012 (12.1 ‰). The mean WWTP isotopic compositions were also used for the Waterloo and Kitchener plants, with values of 11.4, and 18.3‰ respectively.

4.2.3 Model fit

The fit of the model for change in PO_4^{3-} concentration following the Kitchener and Waterloo WWTP inputs was determined through calculations of the coefficient of determination (R^2), and visual comparison of field data to the model-generated curves. SRP data for plume chases that took place on three consecutive summers (July 8th 2010, July 13th 2011, and July 18th 2012) for the Kitchener WWTP, and one summer for the Waterloo WWTP (August 22nd 2012) were used to validate the model. This allowed for R^2 values to be calculated that compared modeled PO_4^{3-} with field-collected SRP. This was only done to assess model fit for the river reach greater than 1 m downstream. That is, the effluent discharge point (time = 0) was excluded from this calculation because the model used the effluent SRP to predict downstream PO_4^{3-}. The model's baseline conditions were altered to match the river flow, accessed via the GRCA hydrometric database. This would alter the depth and travel time estimates used. Several plume chases were carried out on each of the four dates, ranging from 2 to 5 separate sampling events per date. However, only 1 to 2 plume chases per date had corresponding effluent SRP and Cl^- samples collected. Plume chases that had effluent data were used to assess model fit.

4.2.4 Modeling dilution

The effect of dilution was modelled for each plume chase event using the corresponding Cl^- data. Cl^- is often used as a tracer for WWTP effluent because effluent is significantly elevated in Cl^- concentration relative to upstream concentrations. Also Cl^- is conservative in nature, meaning the concentration of Cl^- is not significantly impacted by biological uptake or adsorption (Jarvie et al., 2012).

Dilution factors (DF) were calculated for each site sampled using the equation:

$$DF = \frac{(C_e - C_b)}{(C_p - C_b)} \tag{4.4}$$

where C represented the measured Cl^- concentration of the effluent (e), background (b), and sampling point (p). The background Cl^- level was that measured at the upstream site at Bridgeport.

4.2.5 Statistical analysis

The relationship between dilution factor and distance downstream was modeled using non-linear least squares regression. The line that best fit the relationship was determined, and the corresponding equation parameters that minimized the sum of squared errors (SSE) were estimated. Lines were fit for each plume chase event, as well as for all combined data for the Kitchener WWTP where sampling occurred on more than one day. This allowed for a DF to be calculated for each modelled distance downstream. Effluent PO_4^{3-} was corrected for dilution by dividing them by their distance-specific DF.

Similarly, where modeled PO_4^{3-} values did not fit measured plume chase values, iterative determination of the ideal model parameters that reduced the SSE was carried out (as discussed in the results section below). All statistical analysis was carried out in GraphPad Prism 6, and through visual examination of the parameter values that optimized the goodness of fit between modeled and measured data. The model was generated in both Stella v. 10.01 and Microsoft Excel.

4.3 Results

4.3.1 Model fit for dilution and PO_4^{3-} concentration: Waterloo Reach

Chloride downstream of the Waterloo WWTP declined in the sampled 6000 m reach (Fig. 4.02). Dilution was modeled assuming exponential rise (Fig 4.03) and PO_4^{3-} concentration declined to below 10 µg P L^{-1} (Fig. 4.04). Dilution-alone accounted for most of the decline in PO_4^{3-}, with the contribution of dilution increasing with distance as plume dispersion increased and rates of PO_4^{3-} uptake fell. The plume SRP samples however exhibited lower concentrations than the model projections. The SRP:Cl^- ratios of Fig 4.05 illustrate that SRP is decreasing relative to Cl^- concentration on both sampling events from August 22nd 2012. The relationship between SRP:Cl^- and distance downstream was fit to a line for exponential decline, with R^2 values for the two plume chases at 0.80 and 0.81. There appeared to be an initial rapid decline, followed by a rising trend greater than 3000 m downstream. The baseline values for uptake appeared to underestimate the

extent of the decline in SRP, and model fit was poor for both sampling events on this date (Fig. 4.06).

One possible reason for the underestimation of uptake was the underestimation of substrate roughness. Iterative determination of the epilithon V_{max} value that optimized model fit was carried out. Increasing the rate of release was also necessary to improve agreement between modeled and field-collected values. This suggests that both release and uptake are underestimated downstream of the Waterloo WWTP. One plume chase on August 22nd was carried out at night (2:50 am) while the other was during the day at a similar time of day that the ^{32}P uptake and release experiments were carried out (11:10 am). PO_4^{3-} uptake is not expected to be light dependent in most cases, but Barlow-Busch (1997) found changes in uptake velocity over the diel that were not consistent or predictable (as discussed in section 3.4.1). Thus, optimal model parameters were fit to the mean daytime and mean nighttime sampling points separately. The combined model parameters that resulted in the best fit for the daytime and nighttime samples (Table 4.02) produced R^2 values of 0.74 and 0.78 respectively (Fig. 4.07). The best-fit V_{max} values were 20 and 52 times larger than the rates I estimated in the lab for the daytime and nighttime sampling respectively. The rates of release were 13 and 23 times larger respectively.

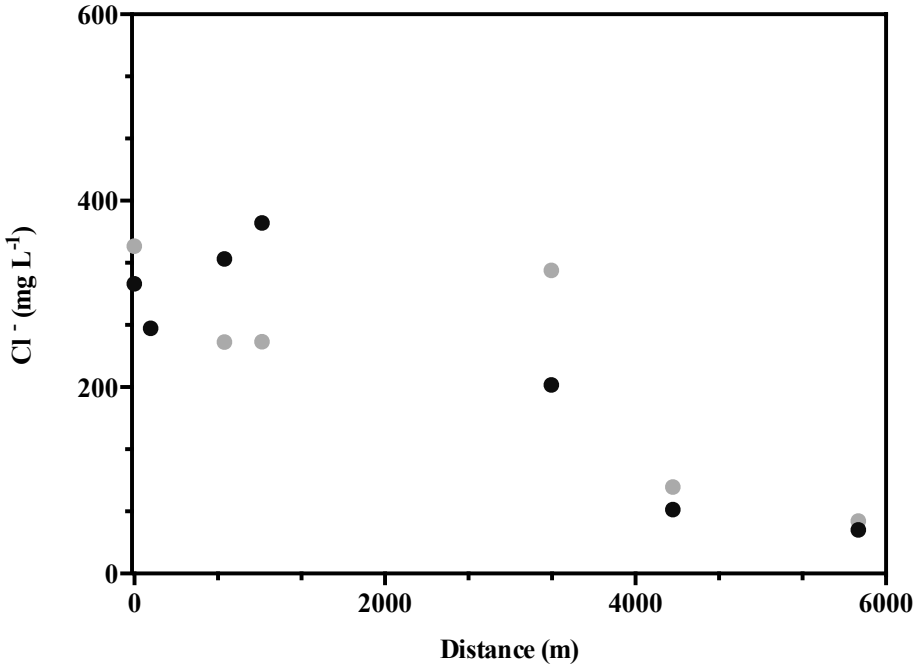

Figure 4.02: Plot of Cl^- concentration with distance downstream of the Waterloo WWTP (distance: 0 m) for plume chases carried out on August 22nd 2012. Different colour data points represent different plume chases.

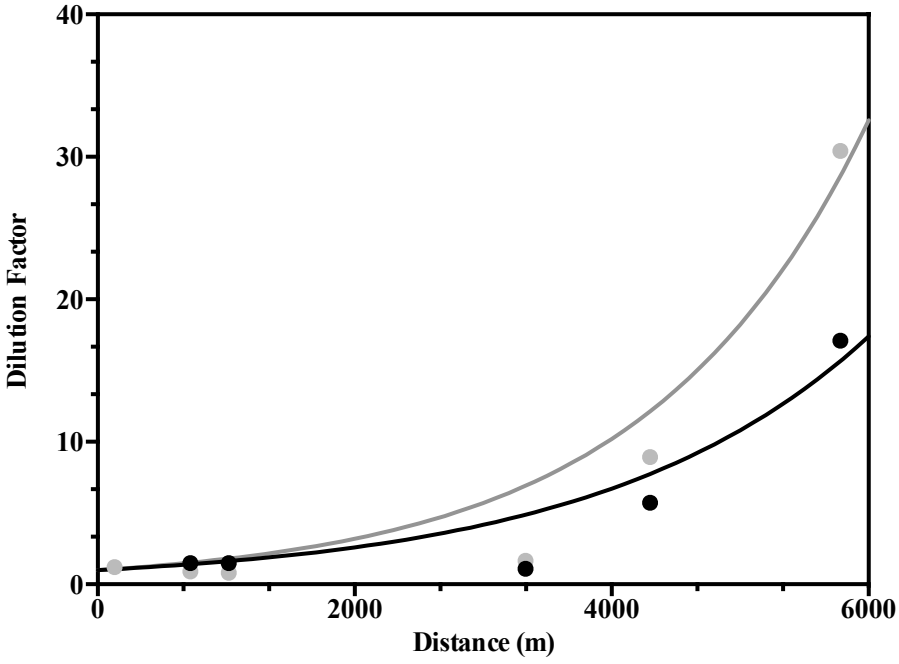

Figure 4.03: Plots of dilution factor with distance downstream of the Waterloo WWTP (distance: 0 m) for plume chases carried out on August 22nd 2012. Different colours represent different plume chases. Lines were fit using non-linear least squares regression, assuming exponential rise.

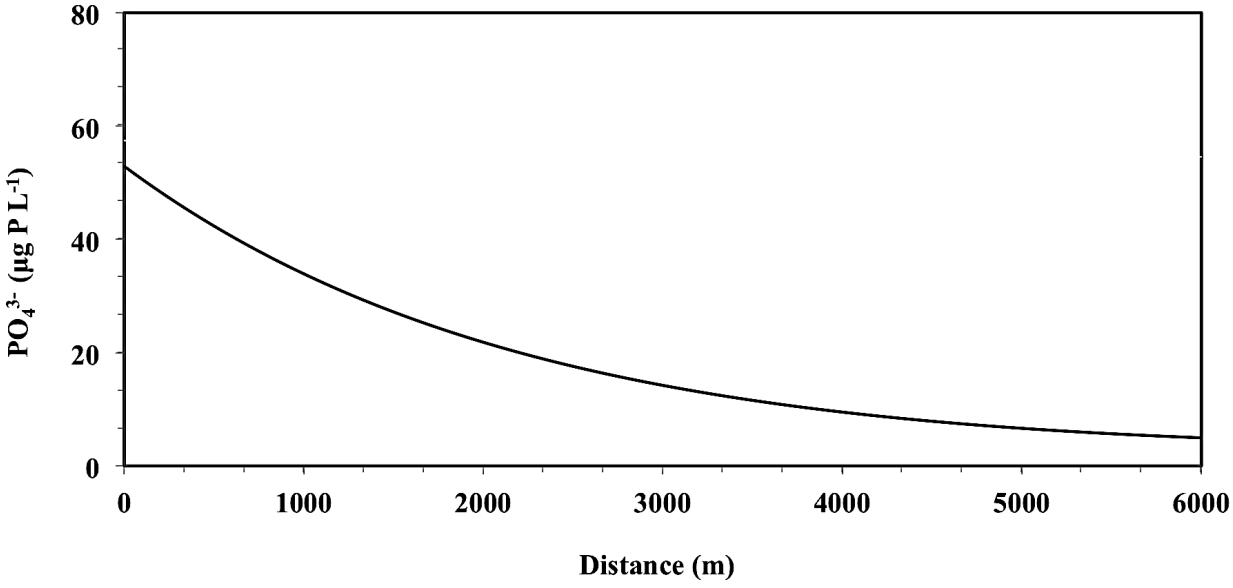

Figure 4.04: Modeled decline in PO_4^{3-} concentration with distance downstream of the Waterloo WWTP (distance: 0 m) due to dilution and biological uptake/release. Baseline model conditions are used as described in Table 4.01.

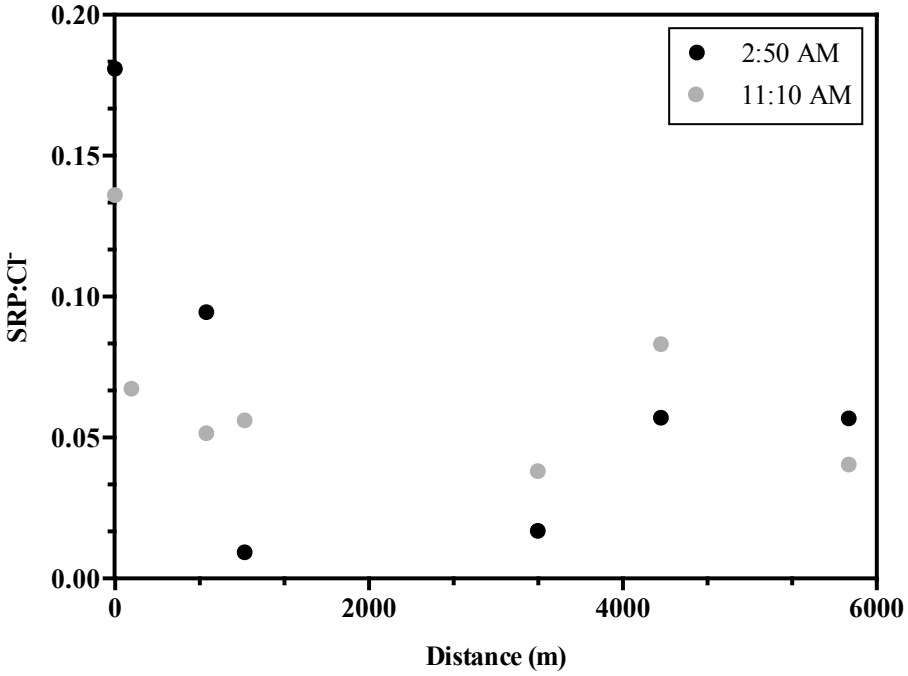

Figure 4.05: SRP:Cl^- downstream of the Waterloo WWTP (distance: 0 m) for plume chases carried out on August 22nd 2012. Two plume chases were carried out, with the time of the day that the effluent samples were collected included.

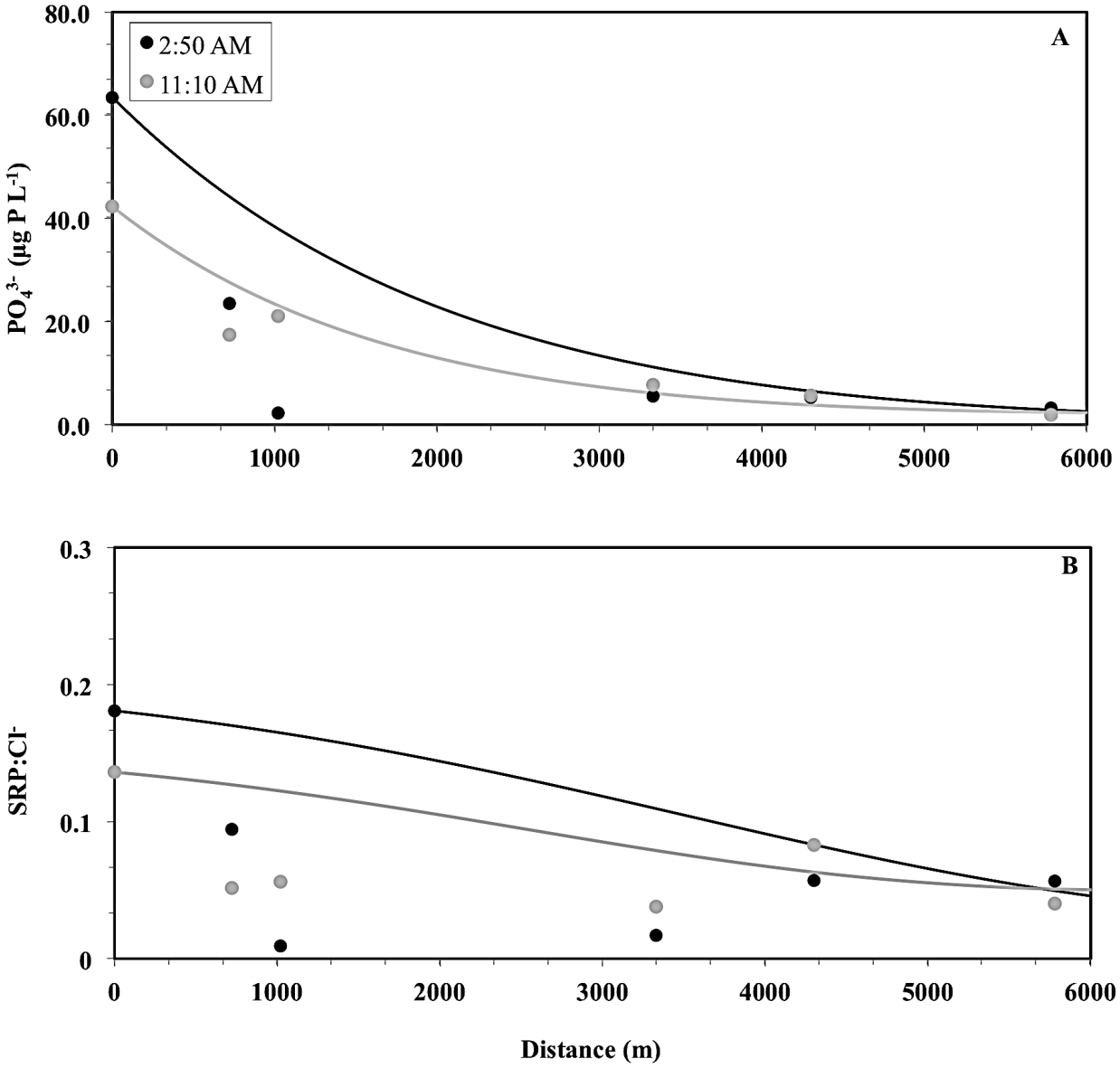

Figure 4.06: Model projected change in a) PO_4^{3-} concentration, and b) Cl^- corrected PO_4^{3-} downstream of the Waterloo WWTP (distance: 0 m) due to dilution and biological uptake/release for plume chases carried out on August 22nd 2012. The model curve was generated using baseline model conditions (Table 4.01). Also included are the SRP and SRP:Cl^- concentrations from the two plume chases that occurred on this date.

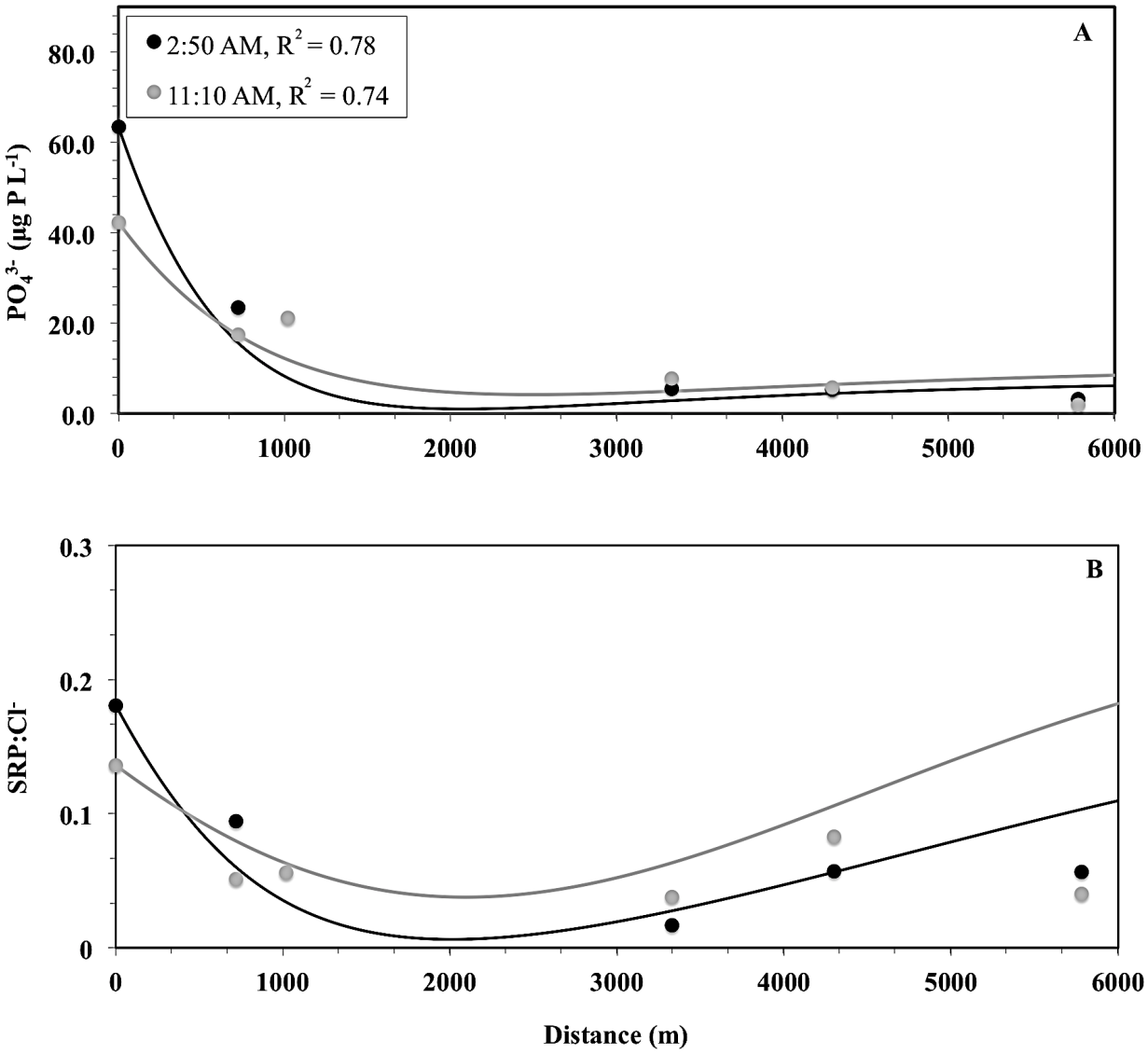

Figure 4.07: Model projected change in a) PO_4^{3-} concentration, and b) Cl- corrected PO_4^{3-} downstream of the Waterloo WWTP (distance: 0 m) due to dilution and biological uptake/release for plume chases carried out on August 22nd 2012. The model curves were generated using best-fit uptake and release rates (Table 4.03) and the plume chases from 2:50 AM and 11:10 AM. Best-fit rates were estimated using the daytime and nighttime SRP values separately, in order to minimize the SSE.

4.3.2 Model fit for dilution and PO_4^{3-} concentration: Kitchener Reach

The Kitchener plume demonstrated rapid Cl^- reduction within the first few hundred meters, which became constant in the remaining sampled reach on all three sampling dates (Fig 4.08). Lines were fit for each date assuming hyperbolic increase to the estimated maximum dilution factor (Fig 4.09). A slow decrease in concentration was projected with most of the decline occurring in the initial 500 m stretch (Fig. 4.10). Dilution alone could account for most of the decline in PO_4^{3-} concentration. The same systematic underestimation of PO_4^{3-} uptake rates was not observed below the Kitchener WWTP as the Waterloo plant. Lack of fit occurred in the downstream portion of the curves, where modeled PO_4^{3-} concentrations were lower than the field collected values. This lead to noticeable discrepancies between modeled and sampled values that were particularly evident on July 18th 2012 (Fig. 4.11). Effluent samples were not collected for the nighttime plume chases in the Kitchener reach therefore model fit could only be assessed for the daytime sampling events.

The SRP:Cl^- plots showed little to no decline over the sampled distance (Fig. 4.12). ANCOVA was used to test whether the change in SRP:Cl^- was significantly different than zero at 95% confidence. For July 8th 2010, this resulted in 2 out of the 5 chases possessing positive slopes that were significantly different from zero, but not from each other. The remaining chases from this date did not possess slopes that were significantly different from 0. Likewise, all 4 plume chases carried out on July 13th 2011 possessed slopes that were not significantly different than 0. Only 1 chase out of the 3 carried out on July 18th 2012 was non-zero, and it too was positive. Lack of decline in these ratios infers that the change in SRP is of the same magnitude as the change in Cl^-. An interesting trend observed downstream of both plants was a rise in SRP:Cl^- with distance, often resulting in ratios that surpassed that of the effluent. This trend was observed on all 5 of the Kitchener plume chases carried out on July 8th, 3 out of the 5 plume chases carried out on July 13th, and all 3 of the chases carried out on July 18th. It was also observed during both plume chases at the Waterloo WWTP on August 22nd. This was remedied downstream of the Waterloo plant through calculation of the best- fit release rate already discussed.

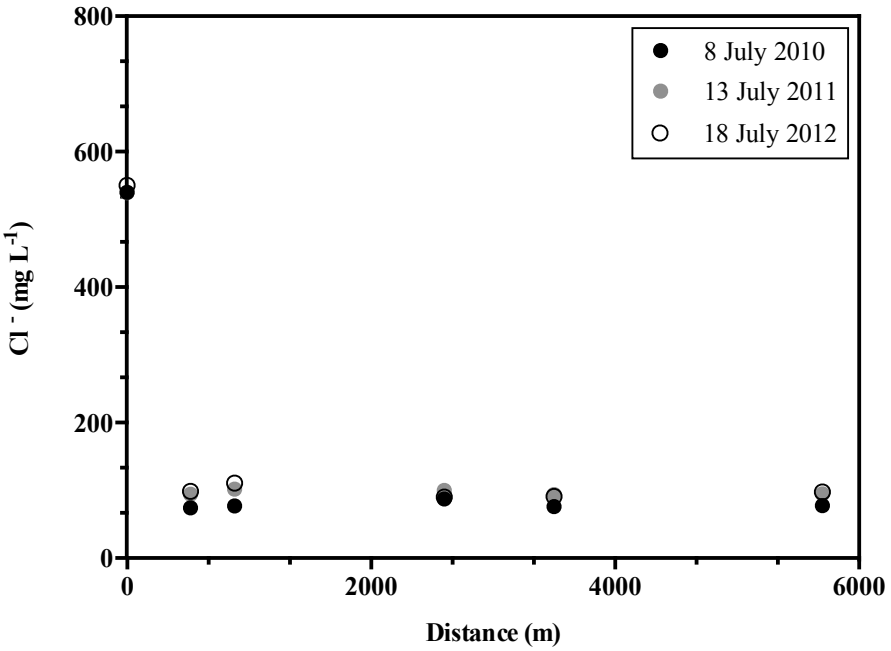

Figure 4.08: Plot of Cl^- concentration with distance downstream of the Kitchener WWTP (distance: 0 m) for plume chases carried out on three dates. Each date includes the mean Cl^- concentration at each distance for the multiple plume chases carried out over the same day.

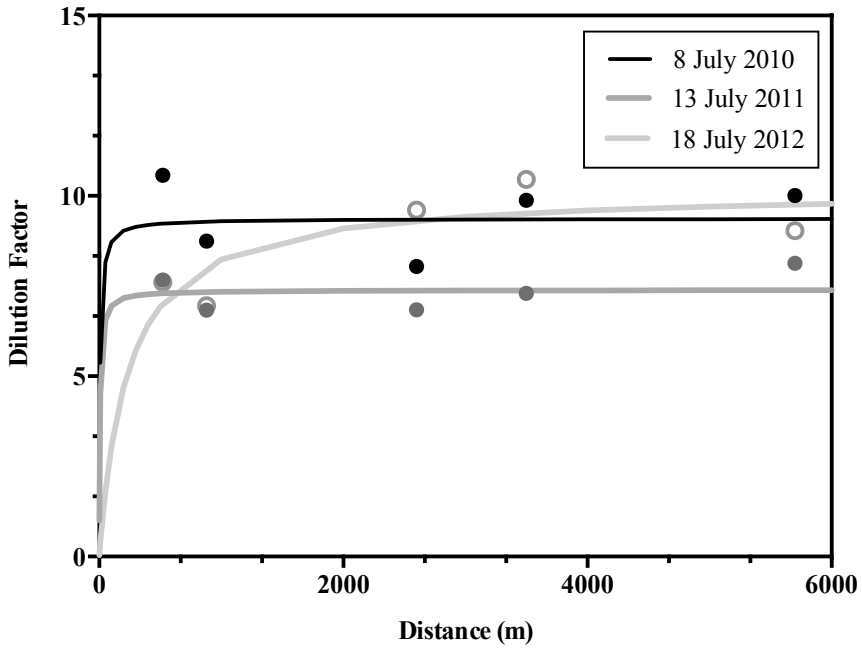

Figure 4.09: Plots of dilution factor with distance downstream of the Kitchener WWTP (distance: 0 m) for plume chases carried out on three dates. Each date includes the mean from the multiple plume chases from the sampled date. Lines were fit using non-linear least squares regression, assuming hyperbolic increase.

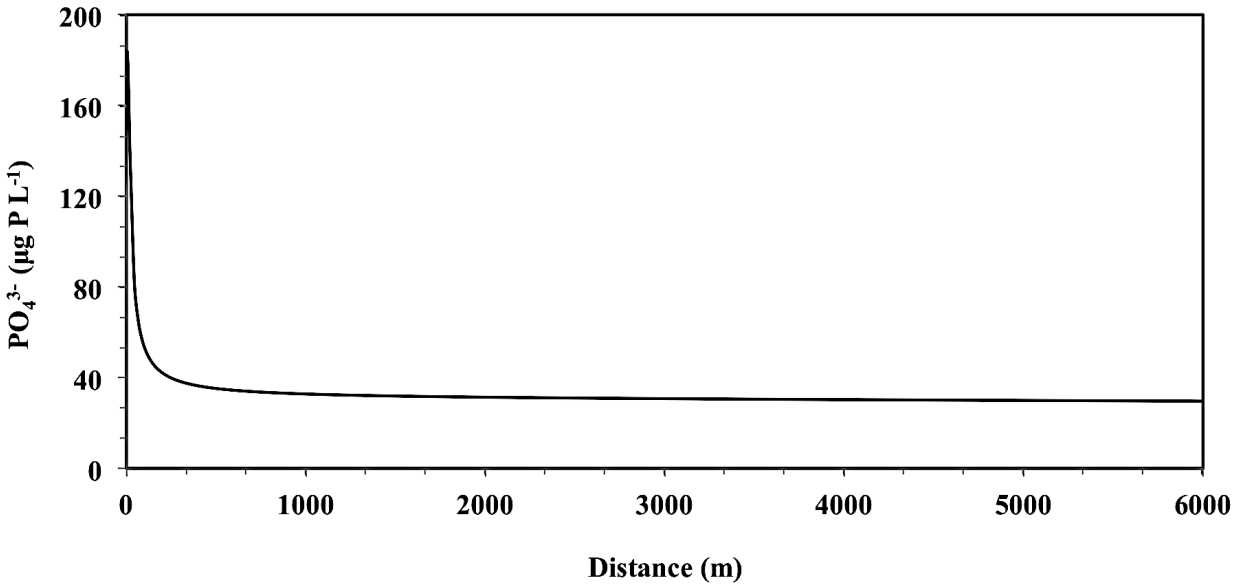

Figure 4.10: Modeled decline in PO_4^{3-} concentration with distance downstream of the Kitchener WWTP (distance: 0 m) due to dilution and biological uptake/ release. The model curve was generated using baseline model conditions (Table 4.01).

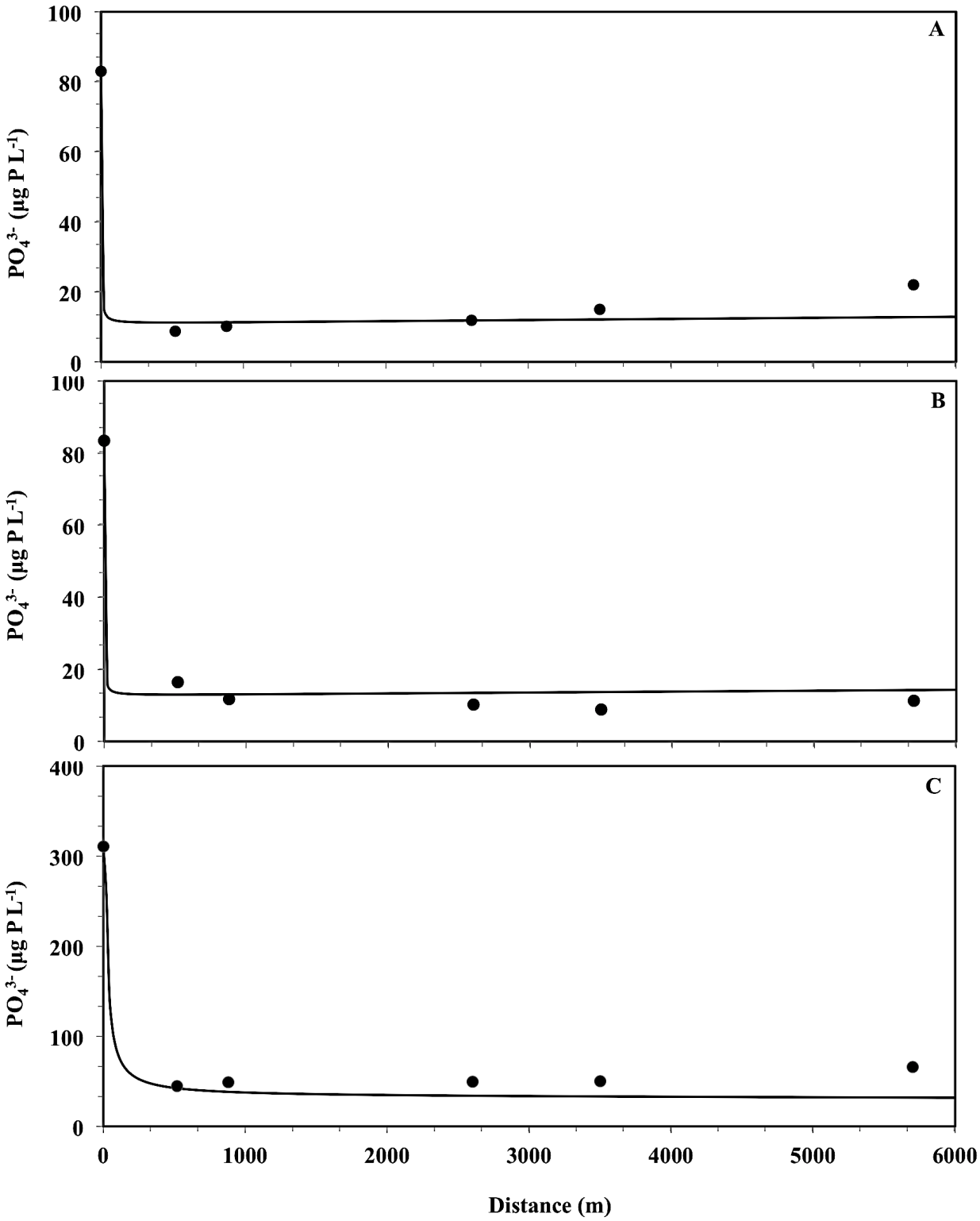

Figure 4.11: Model projected change in PO_4^{3-} concentration downstream of the Kitchener WWTP (distance: 0 m) due to dilution and biological uptake/release for plume chases carried out on a) July 8th 2010, b) July 13th 2011, and c) July 18th 2012. The model curves were generated using baseline model conditions (Table 4.01). Also included are the SRP values from the plume chase samples collected during the daytime, which consists of a single sampling event on July 8th and July 18th, and the average of two events on July 13th.

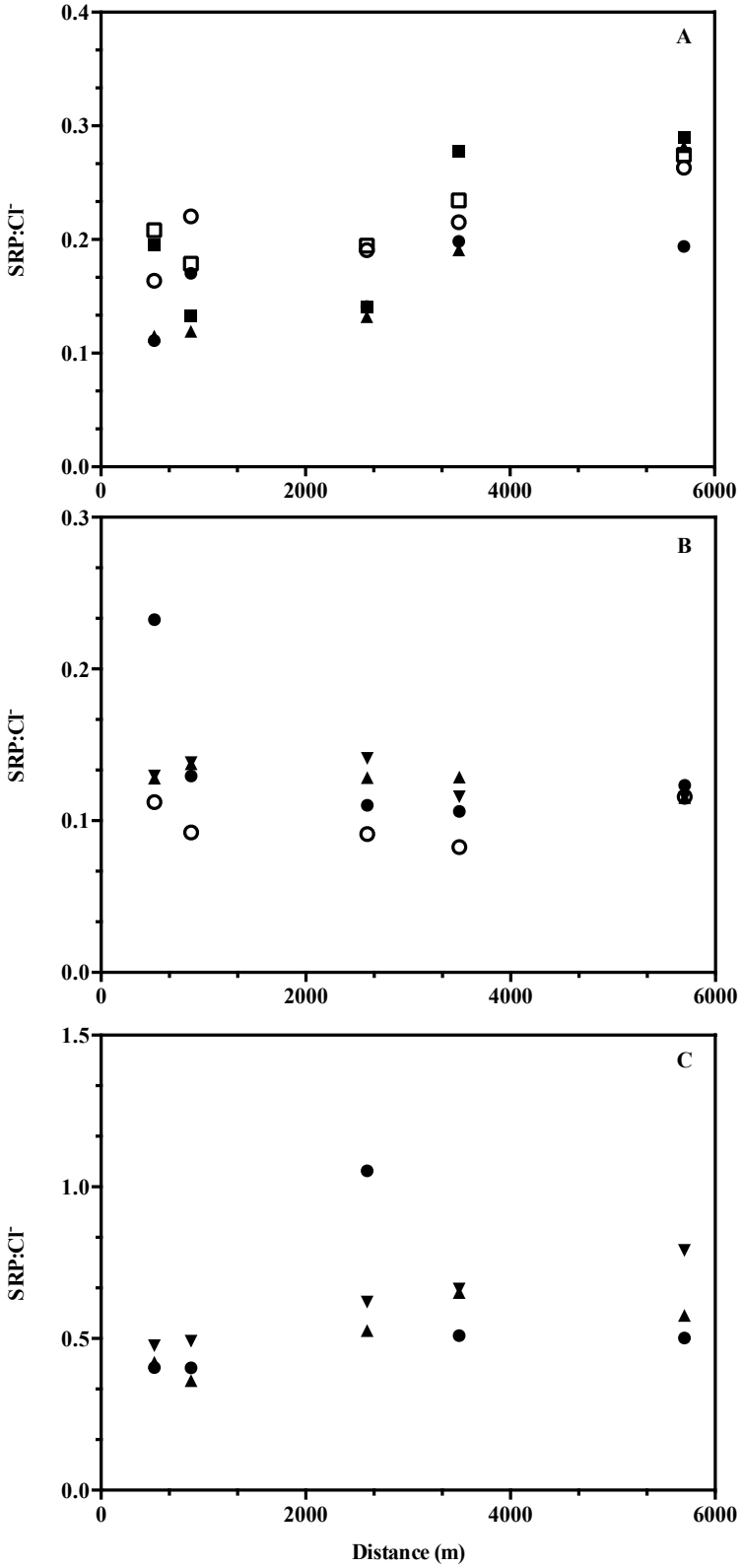

Figure 4.12: SRP:Cl⁻ downstream of the Kitchener WWTP (distance: 0 m) for plume chases carried out downstream of the Kitchener plant on a) July 8th 2010, b) July 13th 2011, and c) July 18th 2012. Different symbols represent different plume chases carried out over the same date.

TP samples were collected for the Kitchener plume chases, allowing the SRP:Cl^- slopes to be compared to the change in TP:Cl^- with distance from the WWTPs (Table 4.02, Fig. 4.13). One plume chase on July 8th had a TP:Cl^- slope that was significantly different from its corresponding SRP:Cl^- slope. The slope of the relationship for TP:Cl^- was not significantly different from zero, while the SRP:Cl^- possessed a significantly positive slope. On July 13th, two plume chases possessed negative TP:Cl^- slopes that were significantly different from their corresponding SRP:Cl^- slopes ($p < 0.001$). They were not significantly different from each other, and the SRP:Cl^- possessed non-significant slopes on this date. July 18th possessed no TP:Cl^- slopes that were significantly non-zero, or significantly different from their corresponding SRP:Cl^- slopes.

Table 4.02: ANCOVA results for the slopes of Cl^- corrected SRP and TP with distance downstream of the Kitchener WWTP, for the plume chases carried out on three dates. The plume chases have been numbered to represent different sampling events carried out on the same date. The P-values assess the null hypothesis, H_0: slope = 0. Bolded values represent plume chases that had SRP:Cl^- slopes that were significantly different from their corresponding TP:Cl^- slopes at 95% confidence.

		SRP:Cl^-			TP:Cl^-		
Date	**Plume Chase**	**Slope**	**R^2**	**P-Value**	**Slope**	**R^2**	**P-Value**
July 8th 2010	1	1.2×10^{-5}	0.5	0.17	-2.6×10^{-5}	0.2	0.39
	2	1.3×10^{-5}	0.6	0.10	-2.1×10^{-5}	0.7	0.07
	3	**1.5×10^{-5}**	**0.7**	**< 0.05**	**-2.2×10^{-5}**	**0.7**	**0.06**
	4	2.6×10^{-5}	0.5	0.13	-1.2×10^{-5}	0.1	0.64
	5	2.5×10^{-5}	0.7	< 0.05	-6.8×10^{-5}	0.5	0.08
July 13th 2011	1	-1.4×10^{-5}	0.3	0.30	-2.5×10^{-5}	0.6	0.08
	2	-2.7×10^{-7}	0.0	0.93	-5.1×10^{-5}	0.5	0.07
	3	**-3.1×10^{-6}**	**0.6**	**0.08**	**-5.2×10^{-5}**	**0.9**	**< 0.05**
	4	**-4.3×10^{-6}**	**0.4**	**0.19**	**-5.6×10^{-5}**	**0.9**	**< 0.05**
July 18th 2012	1	2.0×10^{-5}	0.0	0.79	n/m	n/m	n/m
	2	4.3×10^{-5}	0.6	0.11	7.0×10^{-6}	0.0	0.88
	3	4.8×10^{-5}	0.8	< 0.05	1.9×10^{-5}	0.1	0.51

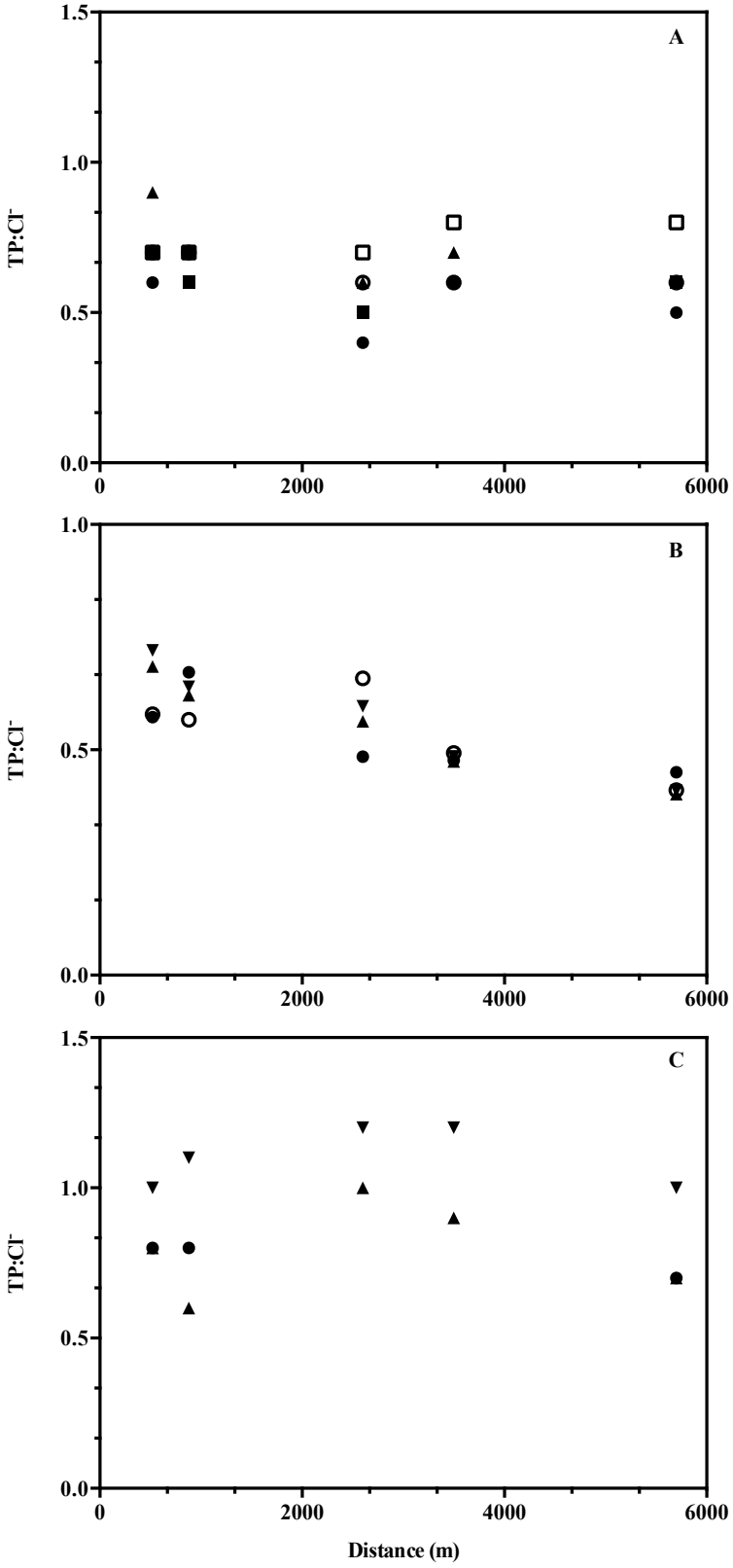

Figure 4.13: TP:Cl$^-$ with distance from a WWTP confluence (Dist.: 0) for plume chases carried out downstream of the Kitchener plant on a) July 8th 2010, b) July 13th 2011, and c) July 18th 2012. Different symbols represent different plume chases carried out over the same date.

One possible reason for increasing SRP:Cl^- is increased release with distance from the plants. In order to improve model fit in the Kitchener reach, best-fit release rates were estimated (Table 4.03). Best-fit rates of release were 3 and 10 times higher than baseline values for July 8th and July 18th, respectively. For the plume chases from July 13th, it was found necessary to increase the epilithon V_{max} value to improve model fit, with no change to the baseline release. This V_{max} was 5 times larger than the baseline value. Inclusion of these best-fit rates resulted in superior model fit for every sampling date (Fig. 4.14).

Table 4.03: Epilithon best-fit uptake parameters. Seston uptake parameters were kept constant as the underestimation in uptake was thought to be caused by decreased surface area estimates for the epilithon. Values with an asterisk are the unchanged, baseline values. Best-fit values were found for the daytime and nighttime samples separately in the Waterloo reach, where effluent samples were available for the day and night.

	Epilithon		
Date	**V_{max} (μg P cm^{-2} h^{-1})**	**K_s (μg P L^{-1})**	**Release (μg P cm^{-2} h^{-1})**
Waterloo			
Daytime:			
August 22nd 2012	16.1	351*	0.47
Nighttime:			
August 22nd 2012	28.9	351*	0.62
Kitchener			
July 8th 2010	0.5*	481*	0.11
July 13th 2011	2.7	481*	0.03*
July 18th 2012	0.5*	481*	0.36

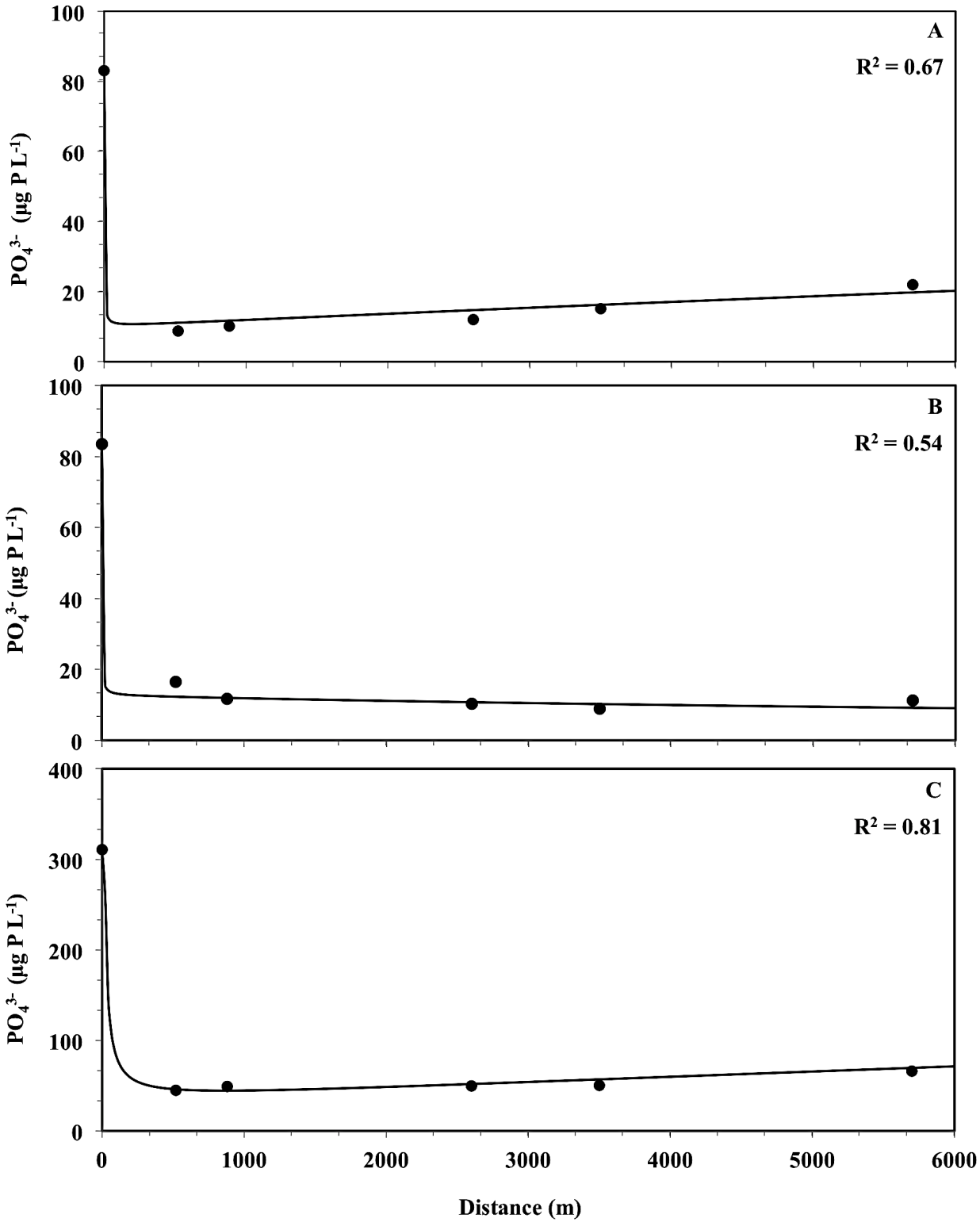

Figure 4.14: Model projected change in PO_4^{3-} concentration downstream of the Kitchener WWTP (distance: 0 m) due to dilution and biological uptake/release for plume chases carried out on a) July 8th 2010, b) July 13th 2011, and c) July 18th 2012. The model curve was generated using best-fit uptake and release rates (Table 4.03). Also included are the SRP values from the plume chase samples collected during the daytime, which consists of a single sampling event on July 8th and July 18th, and the average of two events on July 13th. Best-fit rates were estimated using the mean SRP values shown, in order to minimize the SSE.

4.3.3 Change in $\delta^{18}O\text{-}PO_4$ with distance downstream

Since Waterloo effluent $\delta^{18}O\text{-}PO_4$ was not significantly different than the mean equilibrium (chapter 2), little change in river $\delta^{18}O\text{-}PO_4$ is projected below the Waterloo WWTP (Fig. 4.15). The mean effluent signature however, was based on only two samples and the $\delta^{18}O\text{-}PO_4$ of effluent can be variable even within a single WWTP. Effluent $\delta^{18}O\text{-}PO_4$ signatures were taken from other published reports, including the range observed by Gruau et al. (2005; 16.6 to 18.4‰), Young et al. (2009; 8.4 to 13.6‰), and the single sample collected in Breaker (2009; 25.2‰). This allowed me to predict the distance required for the river to return to equilibrium under a range of effluent $\delta^{18}O\text{-}PO_4$ values (Fig. 4.16). The difference between river $\delta^{18}O\text{-}PO_4$ and equilibrium must be greater than the analytical error associated with the method. The average standard deviation associated with the method derived in McLaughlin et al. (2004) was 0.3‰ therefore any values within this range of the equilibrium are considered reset to equilibrium. The mean equilibrium value chosen for the model (12.1‰) appears to be fairly indicative of the equilibrium expected among freshwater rivers, with 12.2‰ being the average equilibrium for all rivers and streams presented in Young et al. (2009).

The distance required to return the observed $\delta^{18}O\text{-}PO_4$ signature to equilibrium will also depend on the concentration of PO_4^{3-} expelled by the plant, relative to background concentrations. Fig 4.17 shows the effect of altering the effluent PO_4^{3-} concentration for both the Waterloo and Kitchener plants, under best-fit model conditions. The chosen effluent concentrations include the range observed for both the Waterloo (33.5 to 63.5 μg P L^{-1}) and Kitchener (61.6 to 650.1 μg P L^{-1}) WWTPs from the plume chases, as well as the effluent samples I collected over the summer of 2012 (chapter 2). Best-fit conditions for the Kitchener reach were taken from July 18th 2012 when the best model fit was achieved. This date also possessed the highest rate of PO_4^{3-} release, allowing for a prediction of the distance required to achieve equilibrium when PO_4^{3-} recycling rates are high. Comparing the two river reaches can result in an assessment of the effect of dilution. As mentioned, the Kitchener reach undergoes rapid plume dispersion, while the Waterloo plant displays much slower rates of dispersion. The river distance required to achieve a reset to equilibrium is noted on

each graph, with distances ranging from 1.3 to 3.2 km for the Waterloo plant, and consistently longer than 10 km for the Kitchener reach. In the Waterloo reach these effective lengths for $\delta^{18}O$-PO_4 analysis are consistent with the river distance where pre-effluent SRP is re-achieved downstream of the plant (1 to 3 km).

The two highest effluent SRP values resulted in similar downstream $\delta^{18}O$-PO_4 signatures in the Kitchener reach. This is because these two effluent concentrations were far greater than the background SRP, resulting in $\delta^{18}O$-PO_4 values that were highly reflective of the source signature. The lowest effluent SRP resulted in $\delta^{18}O$-PO_4 values that were more reflective of mixing between upstream and downstream values, but a long return to near-equilibrium was still predicted. The Waterloo plant possessed significantly lower effluent SRP values than the Kitchener plant. This meant a smaller effluent range was tested, and altering this concentration had less of an impact on downstream $\delta^{18}O$-PO_4 signatures. The model was also sensitive to the $\delta^{18}O$-PO_4 signature of the effluent, which can cause marked variations in the initial $\delta^{18}O$-PO_4 (time 0). Under all tested end-member values, the Kitchener reach exhibits a slow return to equilibrium, even when release rates are at their highest. The best-fit Waterloo model showed a much faster return to equilibrium due to the increased rates of PO_4^{3-} recycling and lower effluent concentrations. This still allowed for source signature isolation in plume samples taken 2 to 3 km downstream of the plant.

Rates of uptake and release were also altered to observe their effect on downstream $\delta^{18}O$-PO_4 (Fig. 4.18, 4.19). Three different epilithon V_{max} and release values were tested using the July 18th 2012 model downstream of the Kitchener plant, including the best-fit release and V_{max}, ten times the best-fit values, and the smallest release and V_{max} values that would allow equilibrium to be achieved in the sampled 6000 m river reach. It was found necessary to increase V_{max} by a factor of 25 to observe a return to equilibrium 5.9 km below the Kitchener plant, when all other parameters were kept constant. Multiplying the best-fit release by 10 allowed a return to equilibrium within 6.0 km of the plant. This release is two orders of magnitude larger than the

largest release rate measured at Blair using the gross minus net approach (June 6th 2013: chapter 3). Similarly, three different epilithon V_{max} and release values were tested using the August 22nd 2012 model downstream of the Waterloo reach. The fastest reset to equilibrium was achieved when the best-fit V_{max} was increased by a factor of 5, resulting in equilibrium 700 m below the Waterloo plant's confluence.

Figure 4.20 shows the effect of altering the a) effluent concentration, b) effluent $\delta^{18}O\text{-}PO_4$, and c) uptake/release on river $\delta^{18}O\text{-}PO_4$ downstream of the Kitchener WWTP, beyond the sampled reach (> 6 km downstream) assuming there are no tributaries or other WWTPs. This creates a model for a typical WWTP and illustrates the "effective length" for $\delta^{18}O\text{-}PO_4$ sampling in effluent impacted rivers. The combination of epilithon V_{max} and release rates included in fig. 4.20 are outlined in Table 4.04 and include: the best-fit values for July 8th 2010 (V_{max}: 0.5 μg P cm^{-2} h^{-1}, release: 0.1 μg P cm^{-2} h^{-1}), the best-fit values for July 13th 2011 (V_{max}: 2.7 μg P cm^{-2} h^{-1}, release: 0.03 μg P cm^{-2} h^{-1}), and the best-fit values for July 18th 2012 (V_{max}: 0.5 μg P cm^{-2} h^{-1}, release: 0.4 μg P cm^{-2} h^{-1}) downstream of the Kitchener WWTP.

Table 4.04: Model conditions and parameter ranges for fig. 4.20 for modeling PO_4^{3-} concentration and $\delta^{18}O\text{-}PO_4$ values below a typical WWTP. The range of effluent SRP are taken from the Kitchener WWTP from the plume chase data in this chapter and the range observed in chapter 2 of this thesis. The range of effluent $\delta^{18}O\text{-}PO_4$ values is taken from previously published final effluent samples. The range of uptake and release values are taken from the best-fit parameters outlined in table 4.03.

$\delta^{18}O\text{-}PO_4$ Equilibrium: 12.1‰, K_s: 481 μg P L^{-1}, Velocity: 37 cm s^{-1}, Depth: 61 cm				
Effluent Parameter Values:		**Best-fit Parameter Values:**		
Effluent SRP (μg P L^{-1})	**Effluent $\delta^{18}O\text{-}PO_4$ (‰)**	**Date**	**Epilithon V_{max} (μg P cm^{-2} h^{-1})**	**Release (μg P cm^{-2} h^{-1})**
61.6	8.4	July 8, 2010	0.5	0.1
355.8	16.8	July 13, 2011	2.7	0.03
650.1	25.2	July 18, 2012	0.5	0.4

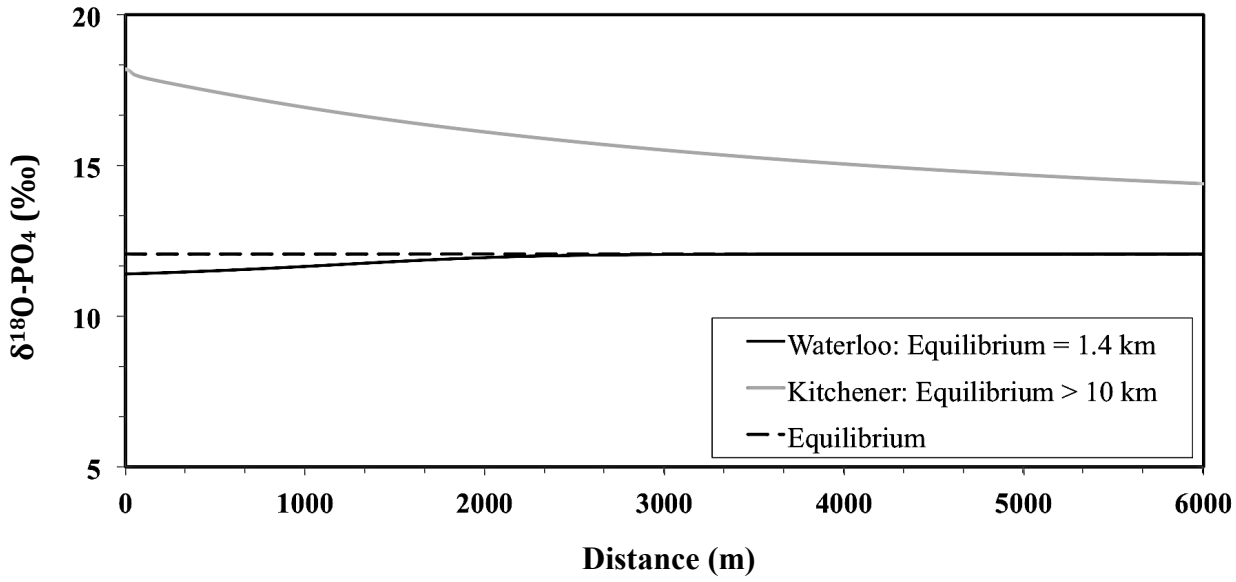

Figure 4.15: Model projected change in $\delta^{18}O\text{-}PO_4$ with distance downstream from two WWTPs. Modeled curves were generated using the best-fit rates of uptake and release (Table 4.03), and baseline effluent and equilibrium $\delta^{18}O\text{-}PO_4$ (Waterloo: 11.4‰, Kitchener: 18.3‰, equilibrium: 12.1‰). The best-fit rates of P kinetics are taken from the daytime for August 22nd 2012, and July 18th 2012 for the Waterloo and Kitchener reach respectively. A mean effluent concentration for each reach is used (Waterloo: 52 μg P L^{-1}, Kitchener: 178 μg P L^{-1}). Also included are the distances required to return the isotopic compositions to equilibrium ± 0.3‰.

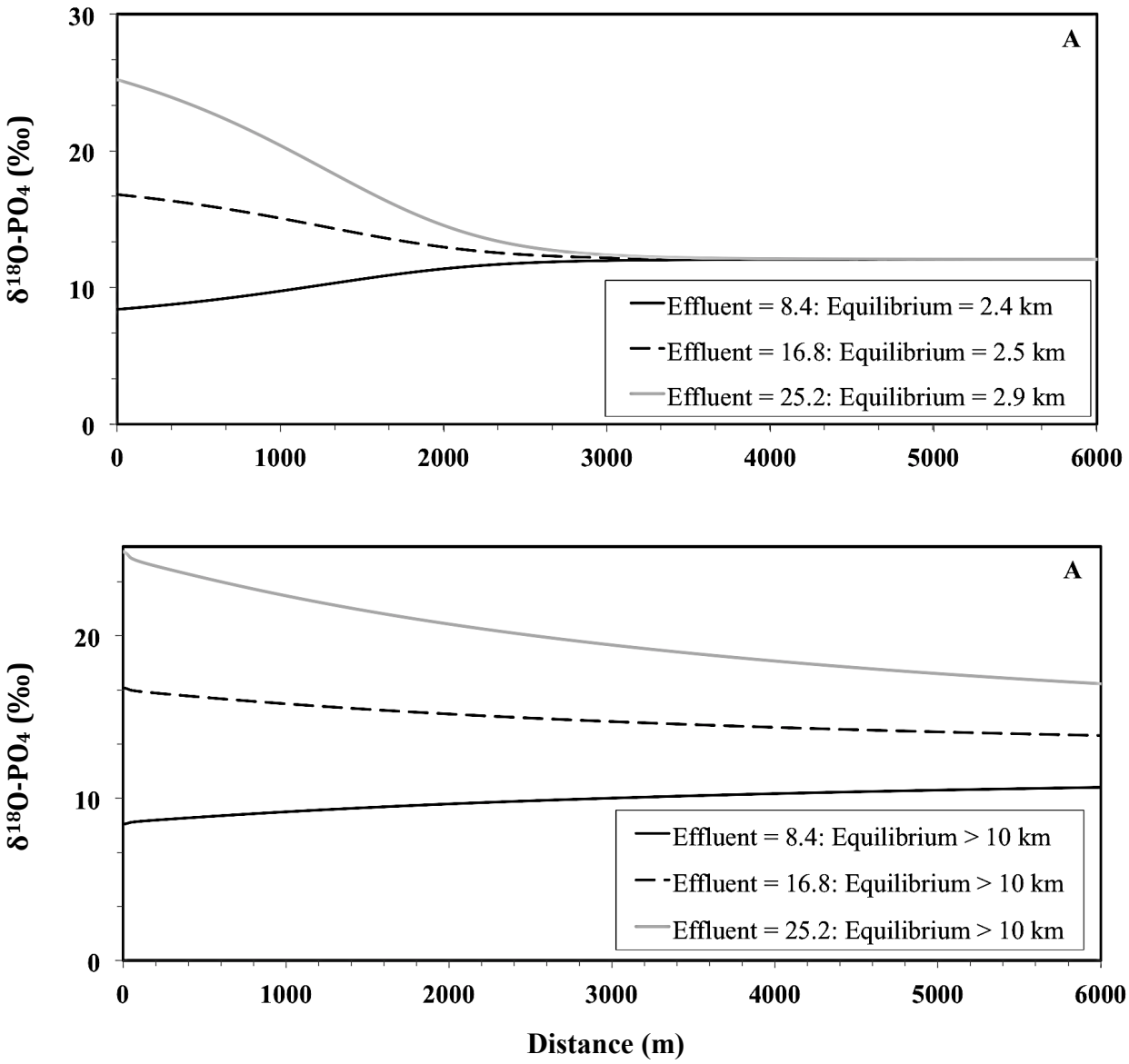

Figure 4.16: Model projected change in $\delta^{18}O\text{-}PO_4$ with distance downstream from the a) Waterloo, and b) Kitchener WWTP, using the range of effluent $\delta^{18}O\text{-}PO_4$ values available in published reports (8.4 to 25.2‰). Modeled curves are generated using best-fit model rates (Table 4.03), and a mean effluent concentration for each reach (Waterloo: 52 µg P L^{-1}, Kitchener: 178 µg P L^{-1}). The best-fit rates of P kinetics are taken from the daytime August 22nd 2012 sampling at the Waterloo reach, and the best-fit rates for July 18th 2012 for the Kitchener reach. Also included are the distances required to return the isotopic compositions to equilibrium ± 0.3‰

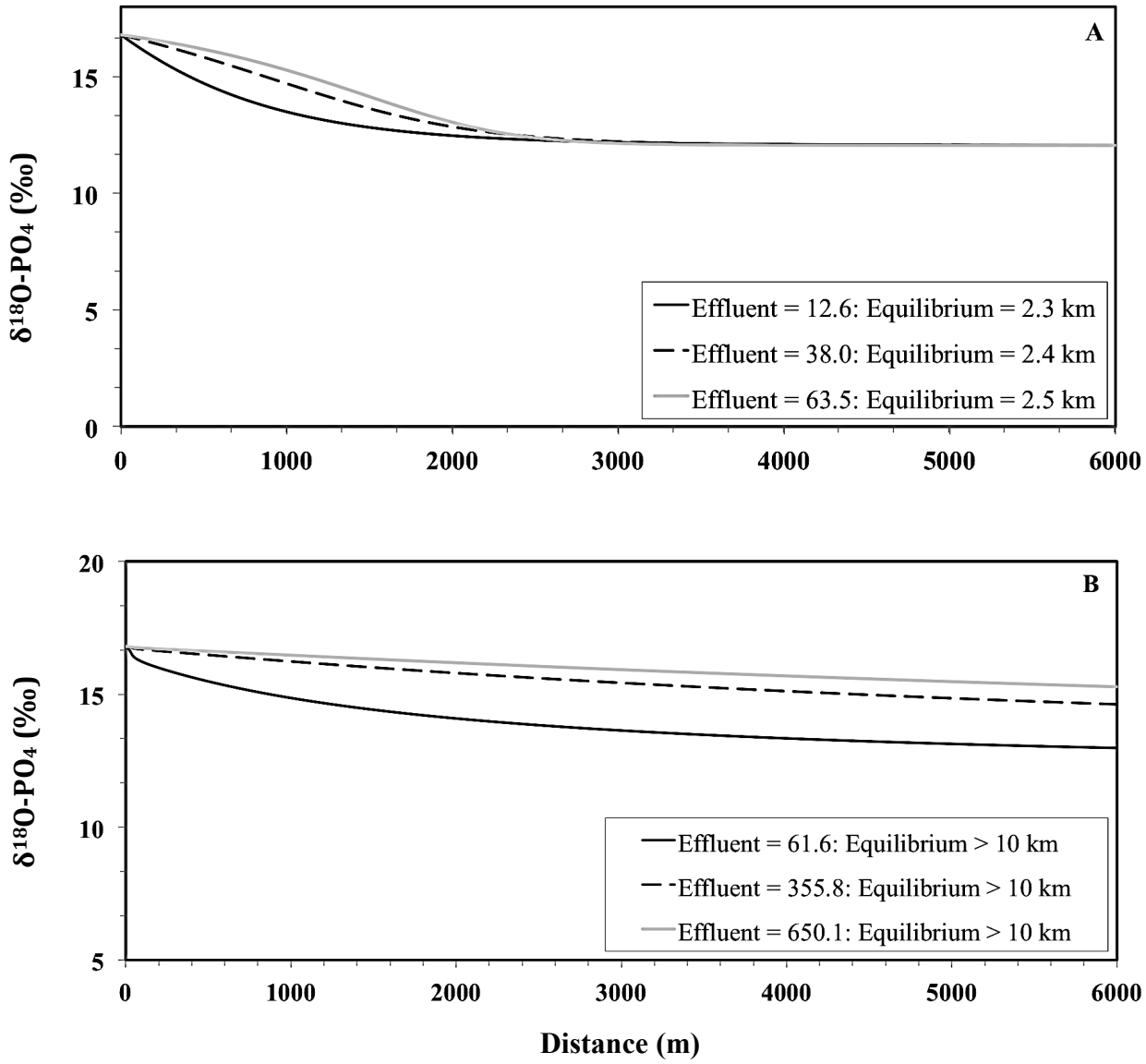

Figure 4.17: Model projected change in $\delta^{18}O\text{-}PO_4$ with distance downstream from the a) Waterloo, and b) Kitchener WWTP using the range of effluent SRP (Waterloo: 12 to 64 μg P L^{-1}, Kitchener: 61 to 650 μg P L^{-1}). Modeled curves are generated using best-fit model conditions (Table 4.03), and an average $\delta^{18}O\text{-}PO_4$ value for the effluent of 16.8‰. The best-fit rates of P kinetics are taken from the daytime August 22nd 2012 sampling at the Waterloo reach, and the best-fit rates for July 18th 2012 for the Kitchener reach. Also included are the distances required to return the isotopic compositions to equilibrium ± 0.3‰.

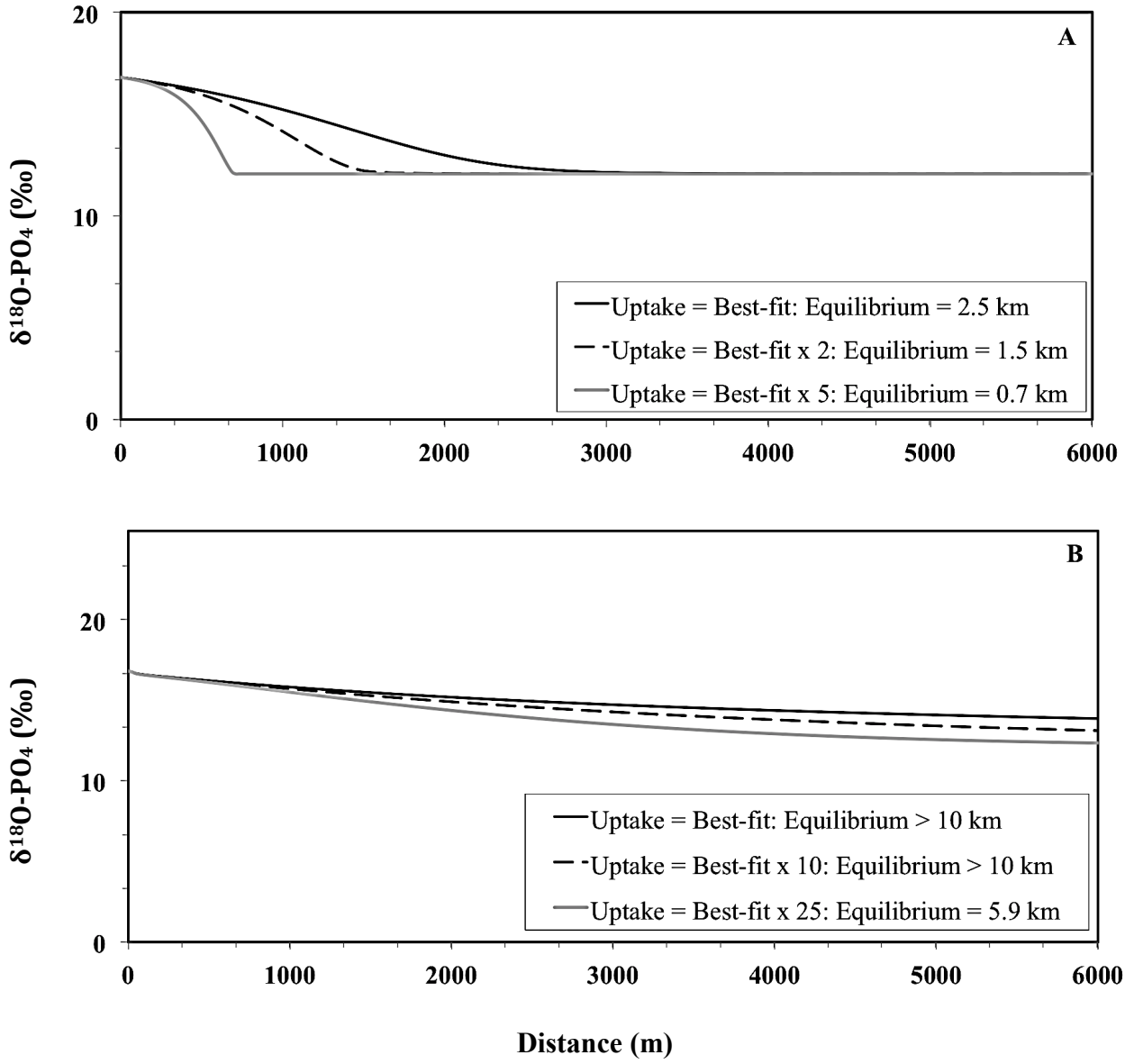

Figure 4.18: Model projected change in $\delta^{18}O\text{-}PO_4$ with distance downstream from the a) Waterloo, and b) Kitchener WWTP using a range of epilithon V_{max} values (Waterloo: 16.1, 32.2, 80.6 μg P cm^{-2} h^{-1}, Kitchener: 0.5, 5.4, 13.0 μg P cm^{-2} h^{-1}). Modeled curves are generated using best-fit model conditions, an average $\delta^{18}O\text{-}PO_4$ value for the effluent of 16.8‰ and a mean effluent concentration (Waterloo: 52 μg P L^{-1}, Kitchener: 178 μg P L^{-1}). Also included are the distances required to return the isotopic compositions to equilibrium ± 0.3‰.

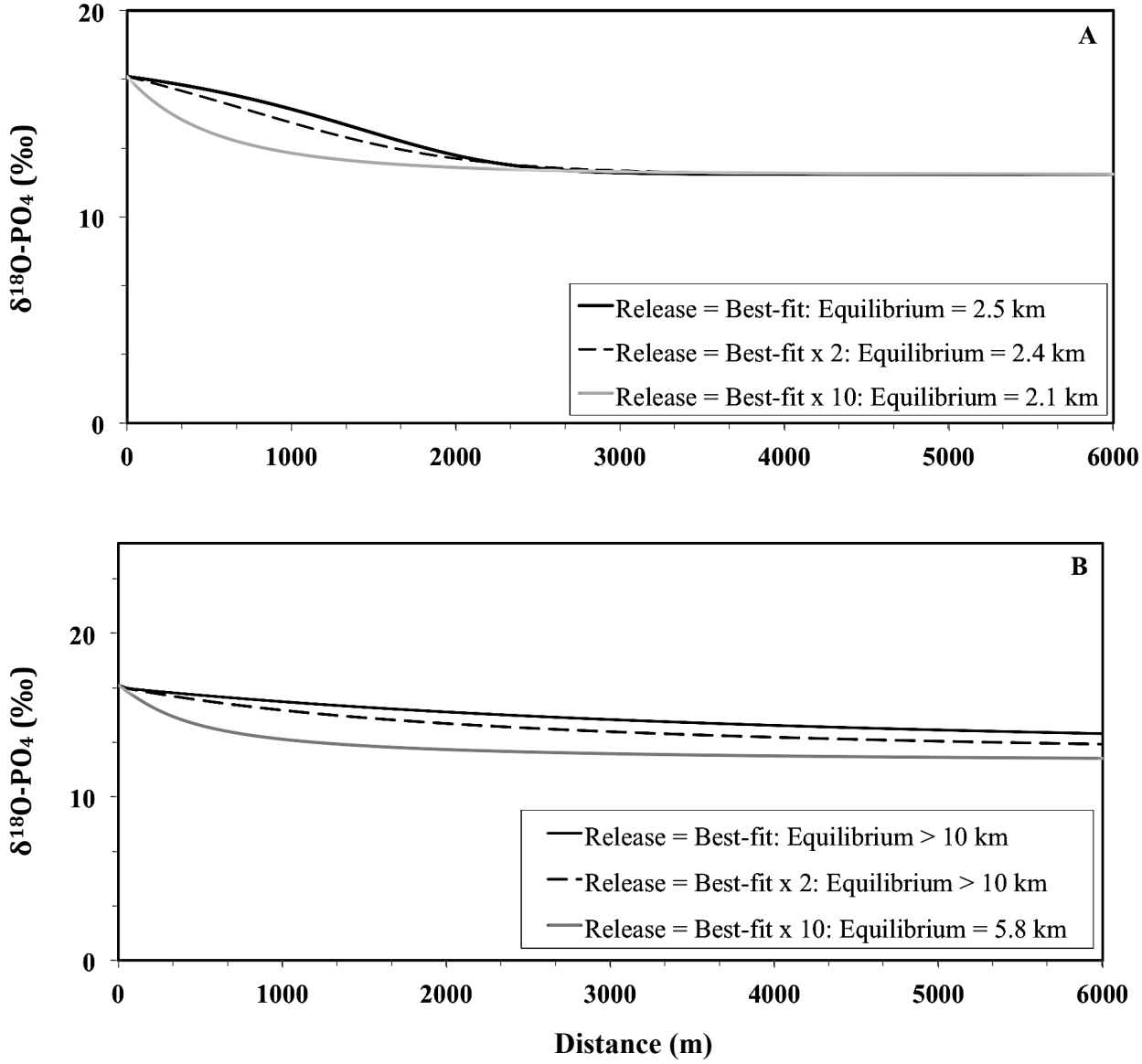

Figure 4.19: Model projected change in $\delta^{18}O\text{-}PO_4$ with distance downstream from the a) Waterloo, and b) Kitchener WWTP using a range of release values (Waterloo: 0.5, 0.9, 4.7 μg P cm^{-2} h^{-1}, Kitchener: 0.4, 0.7, 4.3 μg P cm^{-2} h^{-1}). Modeled curves are generated using best-fit model conditions, an average $\delta^{18}O\text{-}PO_4$ value for the effluent of 16.8‰ and a mean effluent concentration (Waterloo: 52 μg P L^{-1}, Kitchener: 178 μg P L^{-1}). Also included are the distances required to return the isotopic compositions to equilibrium ± 0.3‰.

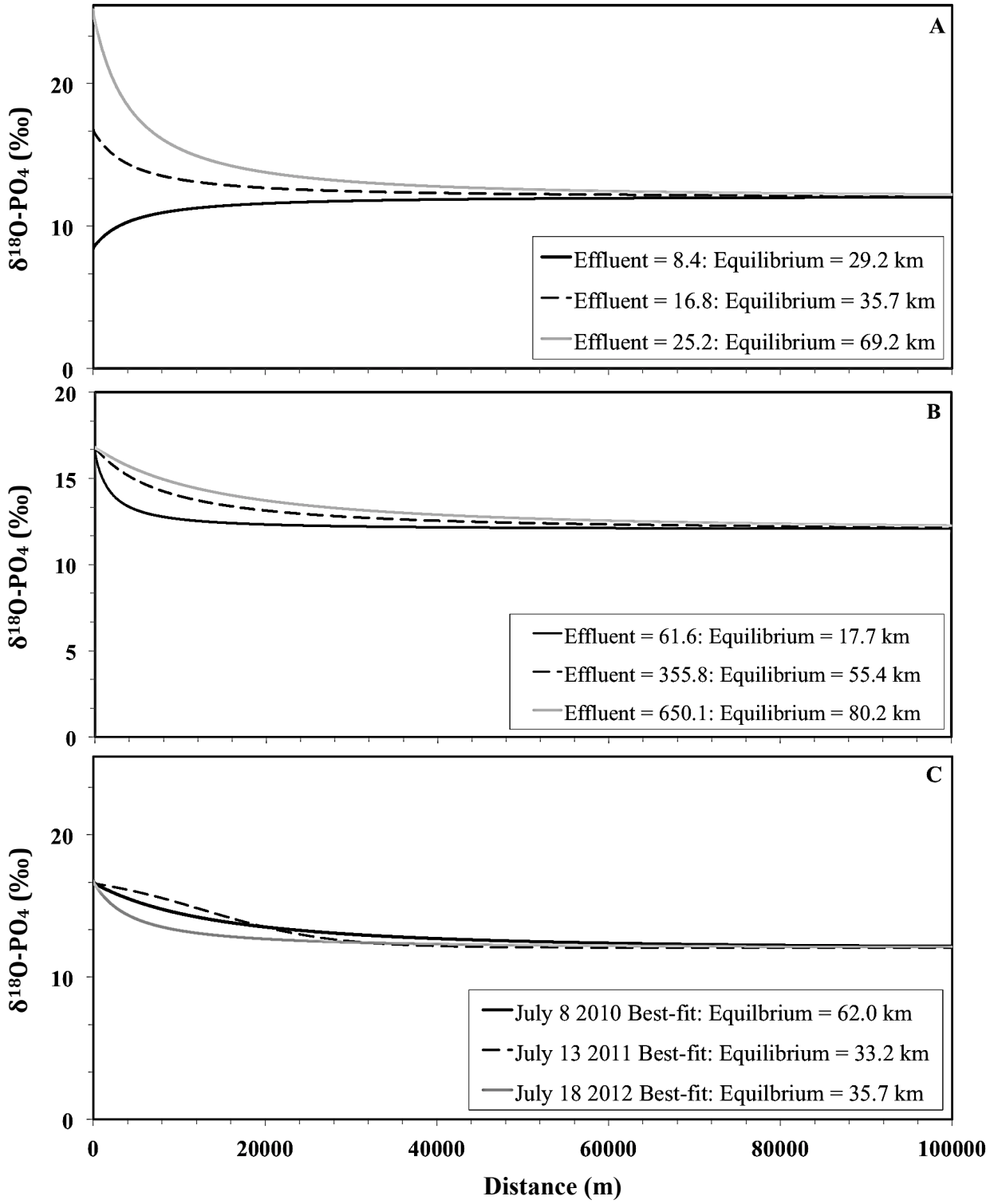

Figure 4.20: Model projected change in $\delta^{18}O\text{-}PO_4$ with distance downstream of a WWTP for a typical river reach under a range of a) effluent $\delta^{18}O\text{-}PO_4$, b) effluent SRP, and c) epilithon V_{max} and release values (table 4.04). Modeled curves are generated using best-fit model conditions (Table 4.03), an average $\delta^{18}O\text{-}PO_4$ value for the effluent of 16.8‰ and an average effluent SRP of 178 μg P L^{-1}. The best-fit rates of P kinetics are taken from July 18th 2012 for the Kitchener reach. Also included are the distances required to return the isotopic compositions to equilibrium ± 0.3‰.

4.4 Discussion

The Waterloo WWTP possessed lower effluent SRP and higher uptake rates than the Kitchener WWTP, thus the 6 km river reach downstream of the Waterloo plant exhibited a faster return to pre-effluent PO_4^{3-} concentrations. Using the best-fit estimates for uptake and release resulted in a significant portion of this decline attributable to biological cycling. This was not observed in the Kitchener reach, where most of the decline could be explained by dilution alone. It appears the "within-channel" processes have little impact on reducing PO_4^{3-} concentrations, even under the summer low flow conditions where they are thought to contribute most intensely (Jarvie et al., 2012). Other effluent-enriched rivers have exhibited similarly low rates of PO_4^{3-} retention, with the majority of the decline in concentration caused by dilution. For example, in the River Kennet physical dilution was found to be a primary regulator of downstream PO_4^{3-} concentration following WWTP inputs (Neal et al., 2000). Similarly, within Big Creek, a tributary of the Chattahoochee River, the decline in SRP following a poultry processing plant's input was largely attributable to dilution (Pollock & Meyer, 2001).

It appears to be difficult to estimate suitable uptake and release rates using the ^{32}P tracer experiments outlined in chapter 3. The rapid decline in SRP:Cl^- in the Waterloo reach indicates SRP retention within the biota. There is significant discrepancy between the rates collected in beakers and best-fit model values. This could be caused by the use of beaker experiments to measure uptake and release. These experiments cause significant alterations to the enclosed communities, potentially altering P kinetics. Factors such as stream current and temperature have been shown to affect the rates of PO_4^{3-} uptake, and would be altered upon removal of these communities from the river (Barlow-Busch et al., 2006). Alternatively, the unaccounted for P uptake may be due to underestimated substrata roughness that would alter the effective surface area of the epilithon.

Uptake by macrophytes, and their large surface area covered with epiphytes, is also not accounted for. The fitted V_{max} was many times larger than the value observed in the lab, which could

reflect that macrophytes can play a significant role in P remediation in the Grand River. The role of macrophytes in P retention through P uptake is thought to be small (Withers & Jarvie, 2008) and a larger portion of their P demands may be provided by the sediments (Carignan and Kalff, 1980, Chambers et al., 1989). Epiphytes may represent a much larger source of P uptake from the water column (Sand-Jensen & Borum, 1991). Pelton et al. (1998) however noted significant P uptake by macrophytes in the LaPlatte River. Macrophytes were found to contribute to P uptake from the water column, with uptake rates that were less than but still similar to those of the epiphytes. In the Grand River these plants are hypothesized to actively assimilate PO_4^{3-} prior to their peak in biomass, when they experience nutrient limitation (Hood, 2012). Following this peak, release rates are higher than uptake creating conditions of net PO_4^{3-} release. Greater amounts of PO_4^{3-} release could occur prior to this peak, if the macrophytes possess significant polyphosphate reserves, or other P storage forms (Chapin, 1990) or if they obtain most of their P from the sediments. The uptake by macrophytes from the water column versus the sediments has not been determined. The reappearance of macrophytes also coincides with increased biomass of grazing invertebrates, which would further increase P release through egestion (Wetzel, 2001). This could mean that the contribution of macrophytes to P kinetics is important for accurate predictions of release rates, which were underestimated in both river reaches.

The uptake underestimation may be less important downstream of the Kitchener plant for several reasons. One possible explanation is outlined in Hood (2012) where reach-specific macrophyte surveys were carried out downstream of the Waterloo and Kitchener WWTPs. Macrophyte biomass was found to be reduced immediately downstream of both WWTPs, potentially due to the toxicity of the effluent and high turbidity leading to growth inhibition. This was particularly evident downstream of the Kitchener plant where a survey from 2007 found no macrophyte biomass for 2 km downstream of the confluence (Hood, 2012). Macrophyte communities recover quicker within the Waterloo reach, where effluent concentrations are lower.

The Waterloo plant possessed a "dead-zone" of only 0.5 km or less (Hood, 2012). The biomass of other biological communities (i.e., epilithon, benthic invertebrates) may also be reduced within the "dead zone". Rehabilitation of these communities is expected closer to the Waterloo WWTP, potentially explaining the higher uptake and release estimates required close to this plant's confluence.

The lack of decline in the SRP:Cl^- ratios downstream of the Kitchener WWTP illustrates that the in-stream processes had little impact on reducing SRP at the time of sampling. Not all variation in SRP, however, could be explained by dilution-alone. Rising SRP:Cl^- appeared in most of the plume chases. Possible explanations for this trend include:

1) Increased rates of dilution caused by groundwater inputs. This could decrease Cl^- concentrations more rapidly than river plume dispersion alone. The Cl^- concentrations do not however show a more rapid decline with distance, which would be expected following an influx of low Cl^- water. This would also increase dilution corrected TP concentrations, which was not observed.
2) Additional sources (i.e. urban inputs) delivering P and contributing to the downstream SRP pool. These could also include subsurface inputs along the river reach. This would also be expected to increase dilution corrected TP, which was not observed.
3) Increasing importance of release processes with distance downstream. Higher rates of release could be due to: biological release, abiotic desorption, or DOP remineralization. Some of these processes may increase downstream from the WWTP. This appears to be the most likely explanation for this phenomenon based on the available data.

Rising SRP:Cl^- from July 8th 2010 and July 18th 2012 could be due to the increased biomass of macrophytes and their associated communities with distance from the plant, as discussed above. If this was the case an increase in the TP:Cl^- ratios would be expected as well. That is, an increase to the SRP pool originating from the benthic communities would be accompanied by an increase in

total water column P. Increases to the DIP pool originating from the seston would cause constant TP:Cl^- values, i.e. DOP to SRP, or PP to SRP. Either a significantly negative slope or no slope was found for all dilution-corrected TP data downstream of the Kitchener WWTP. Either a positive slope or no slope was found for all dilution-corrected SRP data. This could provide evidence that DIP desorption from the suspended sediments or DOP remineralization are significant P release processes downstream of the Kitchener plant.

Both the rates of desorption and DOP remineralization are expected to increase as SRP falls. Adsorption-desorption processes were found to be highly significant for controlling nutrient dynamics in systems with high suspended solid concentrations (James et al., 1999). The EPC is the estimated equilibrium P concentration where no net sorption takes place. SRP values exceeding this point experience higher rates of sorption than desorption (Froelich, 1988). Exposing sediments to high concentrations of PO_4^{3-} have been shown to increase the EPC (James et al., 1999, Haggard et al., 2004). This means when ambient SRP is driven below the EPC due to dilution, greater rates of desorption are expected. The EPC of sediments from two P-rich rivers in southern Ontario was between 10 and 25 $\mu g\ P\ L^{-1}$ (Hill, 1982). Rates of adsorption-desorption are expected to be dependent on other factors as well, including pH, particle size, and iron, aluminum, and organic content (Klotz, 1985).

Rates of DOP remineralization also increase with decreasing SRP. The enzymes responsible are induced under low PO_4^{3-} conditions. DOP cycling may be controlled by alkaline phosphatase (APase) activity, and APase is used as an indicator of P limitation (Klotz, 1985). APase activity has been measured in the Grand River immediately upstream of the Waterloo WWTP (Jiahua Li & WD Taylor, unpublished undergraduate research project, 2012). They observed an increase in SRP and loss of DOP in laboratory-incubated filtrates at a rate of 2.1 $\mu g\ P\ L^{-1}\ h^{-1}$. The rate at which methyl fluorescein phosphate degrades to methyl fluorescein was measured. It was shown to be similar, at 1.4 $\mu g\ P\ L^{-1}\ h^{-1}$. Higher rates (2.62 $\mu g\ P\ L^{-1}\ h^{-1}$) were found in unfiltered water, when the particulate phase was included. This is likely due to the association of APase with bacteria and algal cells. Using

the river depths estimated for July 8th 2010 and July 18th 2010 (described in section 4.2.2) allows this value to be converted to areal units, and compared to the best-fit release estimates. DOP remineralization represents 2.3 and 0.9% of total release for these dates respectively. Higher APase activity would be required downstream of the two WWTPs to explain the model discrepancies. However, lower enzyme activity would be expected at theses sites due to higher SRP concentrations.

This may indicate the adsorption-desorption mechanism is the main contributor to the measured net release. Both suspended and benthic sediments have been shown to act as P sources in WWTP impacted rivers (Withers & Jarvie, 2008). When P concentrations fall below the estimated EPC, the sediments can perpetuate high P conditions in the downstream reaches. This can cause persistently high nutrient concentrations; even when effluent concentrations are reduced (Haggard et al., 2005).

The slow decline in P concentration predicted by the model is similar to the results observed amongst WWTP polluted streams studied in Marti et al. (2004). In this study, 15 rivers were sampled for changes in nutrient concentration, including PO_4^{3-}. After correcting for dilution, approximately half of these rivers showed a decline in net nutrient concentration, while the remaining rivers showed no significant nutrient retention. The rivers that displayed positive net nutrient uptake rates possessed uptake lengths of several kilometers. They also noted that several streams possessed an increase in dilution corrected nutrient concentrations with distance, such as those found in this study. The increasing release rates noted in this study are similar to those from other effluent impacted streams (Marti et al., 2004, Haggard et al., 2005, Gibson & Meyer, 2007).

Due to the low rates of PO_4^{3-} turnover, effluent-dominated $\delta^{18}O\text{-}PO_4$ signatures are predicted many kilometers from the Kitchener WWTP. This is true under a range of effluent SRP values. The Kitchener plant was also shown to possess unique effluent $\delta^{18}O\text{-}PO_4$ values. Therefore, sampling undertaken for the purpose of isolating effluent $\delta^{18}O\text{-}PO_4$ could occur at a variety of

locations downstream. Although the Waterloo reach reduces the incoming P loads much quicker than the Kitchener reach, it is still possible to isolate effluent affected $\delta^{18}O\text{-}PO_4$ samples. The return to equilibrium is projected to occur several kilometers downstream. This suggests the applicability of this method in both stream reaches. Seasonally, the highest rates of PO_4^{3-} uptake may be expected in the summer growing season when low flows, warmer temperatures and increased light availability allow greater biomass accrual, as discussed in chapter 3. A reduced effective length for $\delta^{18}O\text{-}PO_4$ analysis would accompany increased rates of PO_4^{3-} uptake, as observed in fig. 4.20 where the July 13th 2011 best-fit rates were tested. This date possessed elevated uptake and baseline release rates and resulted in one of the shortest effective lengths (approximately 30 km). The highest rates of release may be expected after the summer growing season, when the biomass are no longer actively assimilating PO_4^{3-} to meet their growth requirements. The highest rates of release were estimated for July 18th 2012 and still resulted in a return to equilibrium greater than 35 km downstream (fig. 4.20). Increasing the modeled rates of uptake and release beyond those observed in the plume chases or beaker experiments (fig. 4.19) showed that best-fit values had to be increased an order of magnitude or more to create equilibrium conditions within the 6 km sample reach.

Kinetic fractionation associated with enzymes carrying out DOP hydrolysis is not considered in the model projections. Extracellular DOP remineralization has been found to result in a heavy residual PO_4^{3-} pool, with enzymes such as alkaline phosphatase and 5'-nucleotidase leaving a -30 and -10‰ fractionation effect respectively upon the newly incorporated O atoms (Liang & Blake, 2006). This could be used as an explanation for future results that are depleted relative to those projected by the model. The SRP:Cl^- showed patterns suggesting the importance of PO_4^{3-} release processes with distance downstream. If this trend was caused by DOP remineralization, there would be a significant impact on modeled $\delta^{18}O\text{-}PO_4$ values. Wherever these processes begin to dominate, the $\delta^{18}O\text{-}PO_4$ values would be expected to decline. The associated fractionation effects

are dependent on the rate of conversion of DOP to DIP, and the enzymes responsible. As stated, APase activity is not expected to be high enough in these SRP enriched stream reaches. Remineralization carried out by 5'-nucleotidase has been observed in marine waters regardless of high PO_4^{3-} concentrations (Ammerman & Azam, 1991) and would have a depleting effect on the measured $\delta^{18}O$ -PO_4.

The other hypothesis for the rising SRP:Cl^- involves increasing rates of PO_4^{3-} desorption. As the incoming DIP pool becomes diluted, desorption processes could become more prevalent, causing increasing rates of PO_4^{3-} release from mineral surfaces. The associated fractionation is expected to be small. A fractionation factor of only 1‰ was found in Liang & Blake (2007) where lighter isotopes were associated with the released PO_4^{3-}. This may be expected to have little impact on the modeled projections.

4.5 Conclusions

The explanations presented above to explain the discrepancies between P kinetics measured in the beaker experiments versus the stream modeling exercise are not the sole explanations, nor are they mutually exclusive. It seems likely that the uptake rates collected in beakers would be underestimates when applying them to whole river reaches. This is based on the unknowns including substratum roughness and the contribution of the macrophytes and their associated epiphytes. This could be further complicated by the seasonal-dependence of when the macrophyte communities carry out net uptake versus release, and the proportion of PO_4^{3-} they obtain from the sediments. The reemergence of macrophytes and other benthic community species with distance from the plant would further challenge the use of a constant release rate, V_{max} and K_s. Processes like desorption and DOP remineralization would also increase with distance from the WWTP as nutrient concentrations fall. Estimating the rates of these processes below the WWTPs would offer valuable insight, and aid model projections. Even under the best-fit model conditions however the

river is projected to carry the incoming PO_4^{3-} loads long distances. Little retention of the effluent PO_4^{3-} is projected, and the increasing rates of release perpetuate these high P concentrations.

This exercise illustrates the difficulties associated with applying rates of P kinetics collected through beaker experiments to an ecosystem level. This is especially important in stream environments where significant spatial and temporal variation is expected. Demonstrations such as this show the potential value of a method such as $\delta^{18}O\text{-}PO_4$ analysis. This method would allow verification of these rates of uptake and release without any assumptions about community structure, or river morphology. It would also allow for discernment of processes such as DOP remineralization versus DIP desorption, and distinguishing between source inputs. These processes can be difficult to separate using concentration data alone. The low rates of biological cycling and the unique effluent $\delta^{18}O\text{-}PO_4$ values allow for source inputs to be isolated in the water column under a range of end-member values. This presents evidence of the potential value of this tool for eliciting information on P cycling in effluent-impacted, river ecosystems.

Chapter 5: Summary

The effect of point source inputs on P cycling and $\delta^{18}O$- PO_4 signatures was examined in this thesis in order to determine the usefulness of the stable isotope approach for studying P dynamics in effluent-impacted rivers. The ability of the Grand River to assimilate the PO_4^{3-} added by two WWTPs, and the in-stream processes responsible for P retention, were also examined. I looked at the $\delta^{18}O$- PO_4 signatures from several river sites and observed $\delta^{18}O$- PO_4 values that were elevated above equilibrium. Above the WWTPs this could be caused by inputs from the Conestogo River, a tributary of the Grand River, where a single sample was analyzed and showed elevated $\delta^{18}O$- PO_4. The second WWTP was also shown to possess $\delta^{18}O$- PO_4 signatures that were elevated compared to equilibrium and could be the cause of the elevated river values below the plant. The difficulties I experienced when trying to isolate pure Ag_3PO_4 for mass spectrometric analysis illustrate that further work is required to develop a more effective method for $\delta^{18}O$- PO_4 analysis, in samples possessing low SRP and high DOC typical for temperate rivers. This would allow $\delta^{18}O$- PO_4 analysis to become a plausible method for P dynamics in river environments. The fact that the river is not at equilibrium at any of the sites yields important information on river P kinetics, indicating slow cycling above and below the WWTPs.

Rates of PO_4^{3-} uptake and release were determined in beakers using ^{32}P-PO_4 analysis. These rates were collected from sites below two of the largest WWTPs in the Grand River watershed, which are approximately 20 km apart, and used to model P dynamics within their associated river reaches. Rates of uptake were much lower than those observed in beaker experiments upstream of both plant's inputs (Barlow-Busch et al., 2006). The ability to relate these rates to whole river P-kinetics however was shown to be limited, with SRP measured at several sites downstream of the two WWTPs allowing for an assessment of model fit. Best-fit estimates for modeling *in-situ* SRP were up to 50 times

greater than those of the beaker experiments. Much higher rates of uptake were required downstream of the first WWTP than the second, more effluent-impacted river reach. Underestimated release processes were a major source of discrepancy between whole river P-kinetics and beaker incubations downstream of the second WWTP, where increasing dilution corrected SRP with distance was observed on every sampled date.

The discrepancies between modeled baseline PO_4^{3-} concentrations and field-collected SRP values were hypothesized to be caused by several unaccounted for P processes in the Grand River. These include: uptake and release by macrophytes and their associated epiphytes, desorption/adsorption with distance from the WWTPs, and enzymatic DOP remineralization. Several of these processes could be determined in the river at the ecosystem scale using $\delta^{18}O\text{-}PO_4$ analysis, including whether desorption was responsible for the rising SRP:Cl^- with distance downstream of the Kitchener WWTP. Also the activity of 5' nucleotidase or other enzymes carrying out DOP hydrolysis could be determined using this method, based on the effect of these enzymes on the observed $\delta^{18}O\text{-}PO_4$ signatures (McLaughlin et al. 2013). The enzymes presence could then be confirmed using beaker experiments (e.g. Ammerman & Azam, 1991), with beaker experiments potentially being better suited to verify the presence or absence of these processes, as opposed to estimating the rates of these processes in a whole river system. The current $\delta^{18}O\text{-}PO_4$ signatures for the downstream sites were all elevated, suggesting significant DOP remineralization was not occurring below the second WWTP, but further work is required to validate these values.

Although the rates of uptake and release collected in the beaker experiments were not directly relatable to modeling PO_4^{3-}-kinetics in the river reaches, there is still potential value in these rates for comparing uptake kinetics between the biological compartments (e.g. seston vs. epilithon) and the sestonic size-fractions. These rates can also be used to compare sites and systems where similar beaker experiments were used, with beaker or

chamber experiments receiving widespread use in a variety of stream environments. It is worth noting, that the problems plaguing the rates of PO_4^{3-} uptake and release collected in the beaker experiments in chapter 3 should not affect the major conclusions drawn where rates were compared between the WWTP-impacted sites and those collected in the previous study above the WWTPs (Barlow-Busch et al., 2006). Another use for carrying out beaker experiments in future Grand River studies would be to validate the high rates of release estimated in the best-fit model, by determining if specific processes (e.g. DOP remineralization, DIP desorption) are occurring at measurable rates.

Even with the best-fit estimates of uptake and release described above, the P kinetics below the second WWTP were very sluggish, causing the plant's impacts to persist for long distances downstream. This is relevant to the potential of using $\delta^{18}O\text{-}PO_4$ in these river reaches, where effluent signatures are projected to be observable for many kilometers. Results based on this method eliminate the effect of scaling, assumptions about community structure, or the requirement for estimates of river morphology that can make conclusions based on chamber or beaker incubations difficult to apply to a whole river. Overall, the stable isotope approach could be a valuable tool for assessing the dominant P retention processes, and rates of these processes, in effluent-impacted river ecosystems at the whole ecosystem scale.

Bibliography

Ammerman, J.W., Azam, F. 1991. Bacterial 5'-nucleotidase activity in estuarine and coastal marine waters: Characterization of enzyme activity. *Limnology and Oceanography* **36**: 1427 – 1436.

Anderson, M. 2012. Assessment of future water quality conditions in the Grand and Speed Rivers. Water Management Plant Assimilative Capacity Working Group Report, Grand River Conservation Authority, Cambridge, ON.

Angert, A., Weiner, T., Mazeh, S., Sternberg, M. 2012. Soil phosphate stable oxygen isotopes across rainfall and bedrock gradients. *Environmental Science and Technology* **46**: 2156-2162.

Aukes, P. 2012. Use of Liquid Chromatography – Organic Carbon Detection to Characterize Dissolved Organic Matter from a Variety of Environments, *MSc. Thesis: University of Waterloo.*

Barlow-Busch, L. 1997. Phosphate uptake by seston and epilithon in the Grand River. *M.Sc. thesis: University of Waterloo.*

Barlow-Busch, L., Baulch, H.M., Taylor, W.D. 2006. Phosphate uptake by seston and epilithon in the Grand River, southern Ontario*, Aquatic Sciences* **68**: 181-192.

Basu, B.K., Pick, F.R. 1996. Regulating Phytoplankton and Zooplankton Biomass in Temperate Rivers. *Limnology and Oceanography* **41**: 1572-1577.

Basu, B.K., Pick, F.R. 1994. Longitudinal and seasonal development of planktonic chlorophyll a in the Rideau River, Ontario. *Canadian Journal of Fisheries and Aquatic Sciences* **52**: 804 – 815.

Benitez-Nelson, C.R., Buesseler, K.O. 1998. Measurement of comogenic ^{32}P and ^{33}P activities in rainwater and seawater. *Analytica Chimica Acta* **70**: 64-72.

Blake, R.E., O'Neil, J.R., Garcia, G.A. 1997. Oxygen isotope systematics of biologically mediated reactions of phosphate: I microbial degradation of organophosphorus compounds. *Geochimica Et Cosmochimica* **20**: 4411-4422.

Blake, R.E., O'Neil, J.R., Garcia, G.A. 1998. Effects of microbial activity on the $\delta^{18}O$ of dissolved inorganic phosphate and textural features of synthetic apatites. *American Mineralogist* **83**: 1516-1531.

Blake, R.E., O'Neil, J.R., Surkov, A.V. 2005. Biogeochemical cycling of phosphorus: Insights from oxygen isotope effects of phosphoenzymes. *American Journal of Science* **305**: 596-620.

Bothwell, M.L. 1985. Phosphorus limitation of lotic periphyton growth rates: An intersite comparison using continuous-flow troughs (Thompson River system, British Columbia). *Limnology and Oceanography* **30**: 527-542.

Breaker, B.K. 2009. Phosphate-oxygen isotope ratios as a tracer for sources and cycling of phosphorus in the Illinois River watershed. *MSc Thesis: University of Arkansas.*

Butturini, A., and Sabater, F. 1998. Ammonium and phosphate retention in a Mediterranean stream. Hydrological versus temperature control. *Canadian Journal of Fisheries and*

Aquatic Sciences **55**: 1938–1945.

Carignan, R., Kalff, J. 1980. Phosphorus Sources for Aquatic Weeds: Water or Sediments? *Science* **207**: 987-989.

Carpenter, S.R., Caraco, N.F., Correll, D.L., Howarth, R.W., Sharpley, A.N., Smith, V.H. 1998. Nonpoint pollution of surface waters with phosphorus and nitrogen. *Ecological Society of America* **8**: 559-568.

Chambers, P.A., Prepas, E.E., Bothwell, M.L., Hamilton, H.R. 1989. Roots versus shoots in nutrient uptake by aquatic macrophytes in flowing waters. *Canadian Journal of Fisheries and Aquatic Sciences* **46**: 435-439.

Chapin, F.S., Schulze, E.D., Mooney, H.A. 1990. The ecology and economics of storage in plants. *Annual Review of Ecology, Evolution and Systematics* **21**: 423 -447.

Colman, A.S., Blake, R.E., Karl, D.M., Fogel, M.L., Turekian, K.K. 2005. Marine phosphate oxygen isotopes and organic matter remineralisation in the oceans. *Proceedings of the National Academy of Sciences* **102**: 13023-13028.

Cooke, S.E. 2006. *Water quality in the Grand River: A summary of current conditions (2000-2004) and long term trends*. Cambridge, Grand River Conservation Authority.

Corning, K.E., Duthie, H.C., Paul, B.J. 1989. Phosphorus and glucose uptake by seston and epilithon in boreal forest streams*. Journal of the North American Benthological* Society **8**: 123–133.

Dodds, W., 2006. Eutrophication and trophic state in rivers and streams, *Limnology and Oceanogr*aphy **51**: 671-680.

Dodds, W.K. 1993. What controls levels of dissolved phosphate and ammonium in surface waters? *Aquatic Sciences* **55**: 132-142.

Elsbury, K.E., Paytan, A., Ostrom, N., Kendall, C., Young, M.B., McLaughlin, K., Rollog, M.E., Watson, S. 2009. Using oxygen isotopes of phosphate to trace phosphorus sources and cycling in Lake Erie. *Environmental Science and Technology* **43**: 3108- 3114.

Ensign, S.H., Doyle, M.W. 2006, Nutrient spiraling in streams and river networks. *Journal of Geophysical Research* **111**: G04009.

Froelich, P.N. 1988. Kinetic control of dissolved phosphate in natural rivers and estuaries: A primer on the phosphate buffer mechanism. *Limnology and Oceanography* **33**: 649 – 668.

Gibson, C.A. and Meyer, J.L. 2007. Nutrient Uptake in a Large Urban River. *Journal of the American Water Resources Association* **43**: 576–587.

Goldhammer, T., Max, T., Brunner, B., Einsiedl, F., Zabel, M. 2011. Marine sediment pore-water profiles of phosphate d18o using a refined micro-extraction. *Limnology and Oceanography* **9**: 110-120.

Grand River Conservation Authority. 2011. About the Grand River. *GrandRiver.ca*. From http://www.grandriver.ca/index/document.cfm?sec=74&sub1=0&sub2=0.

Grand River Conservation Authority. 2013. Grand River Watershed GIS Viewer. *GrandRiver.ca.* From http://grims.grandriver.ca/imf/imf.jsp?site=grca_viewer& ddsid=22623d.

Gruau, G., Legeas, M., Riou, C., Gallacier, E., Martineau, F., Henin, O. 2005. The oxygen isotope

composition of dissolved anthropogenic phosphates: A new tool for eutrophication research? *Water Research* **39**: 232-238.

Gruau, G., Legeas, M., Riou, C., Gallacier, E., Martineau, F., Henin, O. 2005. The oxygen isotope composition of dissolved anthropogenic phosphates: A new tool for eutrophication research? *Water Research* **39**: 232-238.

Haggard, B.E., Ekka, S.A., Matlock, M.D., Chaubey, I. 2004. Phosphate Equilibrium between stream sediments and water: potential effect of chemical amendments. *American Society Of Agricultural and Biological Engineers* **47**: 187-194.

Haggard, B.E., Storm D.E., Stanley, E.H. 2001. Effects of a point source input on stream nutrient retention. *Journal of the American Water Resources Assoc*iation **37**: 1291–1299.

Haggard, B.E., Sharpley, A.N. 2007. Phosphorus transport in streams: processes and modeling consideration, p 105-130 *in*: Radcliffe, D.E., & Cabrera, M.L. (Eds.). Modeling phosphorus in the environment. CRC Press Taylor and Francis Group, Boca Raton, FL.

Healey, F.P. 1980. Slope of the Monod Equation as an Indicator of Advantage in Nutrient Competition. *Microbial Ecology* **5**: 281-286.

Hill, A.R. 1982. Phosphorus and major cation mass balances for two rivers during low summer flows. *Freshwater Biology* **12**: 293 – 304.

Hillebrand, H., Kahlert, M. 2001. Effect of grazing and nutrient supply on periphyton biomass and nutrient stoichiometry in habitats of different productivity. *Limnology and Oceanography* **46**: 1881 – 1898.

Horner R.R., Weleh E.B., Veeiistra R.B. 1983. Development of nuisance periphytic algae in laboratory streams in relation to enrichment and velocity, p. 121-134 *in*: Wetzel, R.G. (Eds.). Periphyton of Freshwater Ecosystems. Springer, Netherlands.

Hood, J.L. 2012. The role of submersed macrophytes in river eutrophication and biogeochemical nutrient cycling, *PhD Thesis: University of Waterloo.*

Horner, R.R., Welch, E.B., Seeley, M.R., Jacoby, J.M. 1990. Responses of periphyton to changes in current velocity, suspended sediment and phosphorus concentration*. Freshwater Biology* **24**: 215–232.

House, W.A., and F.H. Denison. 1997. Nutrient dynamics in a lowland stream impacted by sewage effluent: Great Ouse. England. *Science of the Total Environment* **205**: 25–49.

Hudson, J.J., Taylor, W.D. 1996. Measuring regeneration of dissolved phosphorus in planktonic communities, *Limnology and Oceanogr*aphy **41**: 1560-1565.

Huo, S., Zan, F., Xi, B., Li, Q., Zhang, J. 2011. Phosphorus fractionation in different trophic sediments of lakes from different regions, China. *Journal of Environmental Monitoring* **4**: 1088-1095.

Hwang, S., Havens, K.E., Steinman, A.D. 1998. Phosphorus kinetics of planktonic and benthic assemblages in a shallow subtropical lake, *Freshwater Biology* **40**: 729-745.

Jaisi, D.P., Kukkadapu, R.K., Stout, L.M., Varga, T., Blake, R.E. 2011. Biotic and Abiotic Pathways of Phosphorus Cycling in Minerals and Sediments: Insights from Oxygen Isotope Ratios in Phosphate, *Environmental Science and Technology* **45**: 6254-6261.

James, W.F., Barko, J.W., Eakin, H.L. 1999. Sorption characteristics of sediments in the Upper Mississippi River System above Lake Pepin, *Water Quality Technical Notes Collection* (WQTN PD-04), U.S. Army Engineer Research and Development Center, Vicksburg, MS. www.wes.army.mil/el/elpubs/wqtncont.html

Jamieson, T.S. 2010. Quantification of Oxygen Dynamics in the Grand River Using a Stable Isotope Approach, *PhD Thesis: University of Waterloo.*

Jarvie H.P., Neal C., Withers P.J.A. 2006. Sewage-effluent phosphorus: a greater risk to river eutrophication than agricultural phosphorus? *Science of the Total Environment* **360**: 246–53.

Jarvie, H.P., Sharpley, A.N., Scott, J.T., Haggard, B.E., Bowes, M.J., Massey, L.B. 2012. Within-River Phosphorus Retention: Accounting for a Missing Piece in the Watershed Phosphorus Puzzle. *Environmental Science and Technology* **46**: 13284-13292.

Karl, D., Tien, G. 1992. MAGIC: A sensitive and precise method for measuring dissolved phosphorus in aquatic environments. *Limnology and Oceanography* **37**: 105-116.

Klotz, R.L. 1985. Factors controlling phosphorus limitation in stream sediments. *Limnology and Oceanography* **30**: 543-553.

Knud-Hansen, C. 1994. Historical perspective of the phosphate detergent conflict. *Natural Resources and Environmental Policy Seminar.*

Krishnaswami, S., Lal, D., Somayajulu, B.L.K., Dixon, F.S., Stonecipher, S.A., Craig, H. 1972 Silicon, radium, thorium, and lead in seawater: in-situ extraction by synthetic fibre. *Earth and Planetary Science Letters* **16**: 84-90.

Lal, D., Chung, Y., Platt, T., Lee, T. 1988. Twin cosmogenic radiotracer studies of phosphorus recycling and chemical fluxes in the upper ocean. *Limnology and Oceanography* **33**: 1559- 1567.

Lal, D., Lee, T. 1988. Cosmogenic ^{32}P and ^{33}P used as tracers to study phosphorus recycling in the upper ocean. *Nature* **333:** 752-754.

Li, X. 2009. Tracing the flow of phosphorus, carbon and nitrogen in aquatic ecosystems, *Doctoral Dissertation: Florida State University*.

Liang, Y., Blake, R.E. 2006. Oxygen isotope composition of phosphate inorganic compounds: Isotope effects of extraction methods, *Organic Geochemistry* **37**: 1263-1277.

Liang, Y., Blake, R.E. 2009. Compound- and enzyme-specific phosphodiester hydrolysis mechanisms revealed by **d**18O of dissolved inorganic phosphate: Implications for marine P cycling, *Geomicha et Cosmochimica Acta* **73**: 3782-3794.

Longinelli, A., Bartelloni, M., Cortecci, G. 1976. The isotopic cycle of oceanic phosphate. *Earth and Planetary Science Letters* **32**: 389-392.

Longinelli, A., Nuti, S. 1973. Revised phosphate-water isotopic temperature scale. *Earth and Planetary Science Letters* **19**: 373-376.

Mainstone, C.P., Parr, W. 2002. Phosphorus in rivers- ecology and management. *Science of the Total Environment* **282**: 25-47.

Markel, D., Kolodny, Y., Luz, B., Nishri, A. 1994. Phosphorus cycling and phosphorus sources in L. Kinneret: Tracing by oxygen isotopes in phosphate, *Israel Journal of Earth Sciences* **43**: 165-178.

Markel, D., Kolodny, Y., Luz, Boaz, Nishri, A. 1994. Phosphorus cycling and phosphorus sources in Lake Kinneret: Tracing by oxygen isotopes in phosphate. *Israel Journal of Earth Sciences* **43**: 165-178.

Marti, E., Grimm, N.B., Fisher, S.G. 1997, Pre- and Post-Flood Retention Efficiency of Nitrogen in a Sonoran Desert Stream. *Journal of the North American Benthological Society* **16**: 805-819.

Martic, E., Aumatell, J., Gode, L., Poch, M., Sabater, F. 2004. Nutrient Retention Efficiency in Streams Receiving Inputs from Wastewater Treatment Plants. *Journal of Environmental Qual*ity **33**: 285 -293.

McLaughlin K., Sohm J., Cutter, G., Lomas, M., Paytan, A. 2013. Phosphorus cycling in the Sargasso Sea: Investigation using the oxygen isotopic composition of phosphate, enzyme labeled fluorescence, and turnover times, *Global Biogeochemical Cycles* **27**: 1-13.

McLaughlin, K., Cade-Menun, B., Paytan, A. 2006 a. The oxygen isotopic composition of phosphate in Elkhorn Slough, California: A tracer for phosphate sources. *Estuarine Coastal and Shelf Science* **70**: 499-506.

McLaughlin, K., Chavez, F., Pennington, J., Paytan, A. 2006 b. A time series investigation of the oxygen isotopic composition of dissolved inorganic phosphate in Monterey Bay, California. *Limnology and Oceanography* **51**: 2370-2379.

McLaughlin, K., Kendall, C., Silva, S., Young, M., Paytan, A. 2006 c. Phosphate oxygen isotope ratios as a tracer for sources and cycling of phosphate in north San Francisco Bay, California. *Journal of Geophysical Research* **111**: G03003.

McLaughlin, K., Silva, S., Kendall, C., Stuart-Williams, H., Paytan, A. 2004. A precise method for the analysis of $\delta^{18}O$ of dissolved inorganic phosphate in seawater. *Limnology and Oceanography: Methods* **2**: 202- 212.

Meybeck, M. 1982. Carbon, nitrogen, and phosphorus transport by world rivers. *American Journal of Science* **282**: 401-450.

Meyers, J.L., Likens, G.E. 1979. Transport and Transformation of Phosphorus in a Forest Stream Ecosystem. *Ecology* **60**: 1255-1269.

Mulholland, P.J., Steinman, A.D., Elwood, J.W. 1990, Measurement of phosphorus uptake length in streams: Comparison of radiotracer and stable PO4 releases, *Canadian Journal of Fisheries and Aquatic Sci*ences **47**: 2351– 2357.

Murphy, J., Riley, J.P.1962. A modified single solution method for the determination of phosphate in natural waters. *Analytica Chimica Acta* **27:** 31-36.

Newbold, J.D., Elwood, J.W., O'Neill, R.V., Sheldon, A.L. 1983. Phosphorus Dynamics in a Woodland Stream Ecosystem: A Study of Nutrient Spiraling. *Ecology* **64**: 1249-1265.

Newbold, JD. 1992. Cycles and spirals of nutrients. p. 379 – 408, *In*: Calow, P., and Petts, G. (Eds.) Rivers Handbook, Blackwell Scientific Publications, London.

Paytan, A., McLaughlin, K. 2011. Tracing the sources and biogeochemical cycling of phosphorus in aquatic systems using isotopes of oxygen in phosphate. p. 419-437, *In:* M. Baskaran (Ed.), Handbook of environmental isotope geochemistry, Springer, Berlin.

Pelton D.K., Levine, S.N., Braner, M. 1998. Measurements of phosphorus uptake by macrophytes and epiphytes from the La Platte River (VT) using 32P in streams microcosms. *Freshwater Biology* **39**: 285–299.

Pollock, J.B., Meyer, J.L. 2001. Phosphorus Assimilation Below a Point Source in Big Creek. Proceedings of the 2001 Georgia Water Resources Conference, April 26 and 27, 2001, Athens, Georgia.

Puceat, E. Joachimski, MM. Bouilloux, A. Monna, F. Bonin, A. Motreuil, S. Morinière, P. Hénard, S. Mourin, J. Dera, G. Quesne, D. 2010. Revised phosphate–water fractionation equation reassessing paleotemperatures derived from biogenic apatite. *Earth and Planetary Science Letters* **298**: 135-142.

Reddy, K.R., Kadlec, R.H., Flaig, E., Gale, P.M. 2010. Phosphorus Retention in Streams and Wetlands: A Review. *Critical Reviews in Environmental Science and Technology* **29**: 83-146.

Region of Waterloo. (2012). Kitchener Wastewater Treatment Plant Upgrades. Newsletter Issue 1: March.

Rigler, F.H. 1966. Radiobiological analysis of inorganic phosphorus in lake water. *Verhandlungen der Internationalen Vereinigung fur Theoretische und Angewandte Limnologie* **16**: 465–470.

Rosamond, M.S. 2013. Nitrous oxide and nitrate in the Grand River, Ontario: sources, production, pathways and predictability. *PhD thesis: University of Waterloo.*

Rosemond, A.D., Brawley, S.H, Mulholland, P.J. 2000. Seasonally shifting limitation of stream periphyton: response of algal populations and assemblage biomass and productivity to variation in light, nutrients, and herbivores. *Canadian Journal of Fisheries and Aquatic Sciences* **57:** 66 – 75.

Ruttenberg, K.C. 2003. The global phosphorus cycle. *Treatise on Geochemistry* **8**: 585-643.

Sabater, S., Guasch, H., Romani, A. Munoz, I. 2002. The effect of biological factors on the efficiency of river biofilms in improving water quality. *Hydrobiologia* **469**: 149-156.

Sand-Jensen, K., Borum, J. 1991. Interactions among phytoplankton, periphyton, and macrophytes in temperate freshwaters and estuaries. *Aquatic Botany* **41**: 137-175.

Taft, J.L., Taylor, W.R., McCarthy, J.J. 1975. Uptake and release of phosphorus by phytoplankton in the Chesapeake Bay estuary. *Marine Biology* **33**: 21-32.

Tamburini, F., Bernasconi, S.M., Angert, A., Weiner, T., Frossard, E. 2010. A method for the analysis of the δ18-O of inorganic phosphate extracted from soils with HCl. *European Journal of Soil Science* **61**: 1025-1032.

Tarapchak, S.J., Rubitschun, C. 1981, Comparisons of soluble reactive phosphorus and orthophosphorus concentrations at an offshore station in southern Lake Michigan, *Journal of Great Lakes Res*earch **7**: 290–298.

Weiner, T., Mazeh, S., Tamburini, F., Frossard, E., Bernasconi, S.M., Chiti, T., Angert, A. 2011. A method for analyzing the d18O of resin-extractable soil inorganic phosphate. *Rapid Communications in Mass Spectrometry* **25**: 624-628.

Webster, J.R., Benfield, E.F., Golladay, S.W., Hill, B.H., Hornick, L.E., Kazmierczak, R.F., Perry, W.B. 1987. Experimental studies of physical factors affecting seston transport in streams. *Limnology and Oceanogr*aphy **32**: 848-863.

Wetzel, R. G. 2001. Limnology: Lake and River Ecosystems. p. 242-250, Academic Press, San Diego.

Winterbourn, M.J., Fegley, A. 1989. Effects of nutrient enrichment and grazing on periphyton assemblages in some spring-fed, south island streams. New Zealand Natural Sciences **16**: 57 – 65.

Withers, P.J.A., Jarvie, H.P. 2008. Delivery and cycling of phosphorus in rivers: A review. *Science of the Total Environment* **400**: 379-395.

Withers, P.J.A., Jarvie, H.P., Hodgkinson, R.A., Palmer-Felgate, E.J., Bates, A., Neal, M., Howells, R., Withers, C.M., Wickam, H.D. 2009. Characterization of phosphorus sources in rural watersheds. *Journal of Environmental Quality* **38**: 1998-2001.

Young, M., McLaughlin, K., Kendall, C., Strongfellow, W., Rollog, M., Elsbury, K., Donald, E., Paytan, A. 2009. Characterizing the oxygen isotopic composition of phosphate sources to aquatic ecosystems. *Environmental Science and Technology* **43**: 5190-5197.

Zohar, I., Shaviv, A., Klass, T., Roberts, K., Paytan, A. 2010. Method for the Analysis of Oxygen Isotopic Composition of Soil Phosphate Fractions. *Environmental Science and Technology* **44**: 7583 – 7588.

Appendix A:

$\delta^{18}O$-PO_4 values for all river sites and effluent samples over the summer of 2012. This includes the data presented in chapter 2, as well as the eliminated data points.

Site	Date	SRP (µg P L^{-1})	% O Yield	δ18O (‰ VSMOW)	Temperature (°C)	Conductivity (µS cm^{-1})	Offset from Equilibrium (‰ VSMOW)
Bridgeport	May 23rd	1.4	10	22.2	19.4	458	11
Bridgeport	June 6th	1.5	5.9	17.8	16.4	526	6
*Bridgeport	June 20th	4	4.8 ± 0.5	15.5 ± 0.4	24.9	451	5
Bridgeport	July 3rd	3	12.4 ± 2.8	21.7 ± 2.9	23.8	448	11
*Bridgeport	July 17th	1.7	2	12	25.3	427	1
*Bridgeport	August 2nd	11.5	1.3 ± 0.1	7.8 ± 1.0	23.7	409	-4
Bridgeport	August 21st	11.2	7.5 ± 0.1	12.7 ± 0.3	19.1	401	0
Victoria	May 23rd	1.9	19.2	24.3	19.8	626	13
*Victoria	June 6th	2.1	35.8 ± 0.9	26.0 ± 0.4	17.3	652	14
Victoria	June 20th	2.7	16.1 ± 1.1	23.5 ± 0.3	25	621	13
Victoria	July 17th	7.5	9.3 ± 2.0	18.0 ± 0.2	25.4	582	7
*Blair #1	May 23rd	5.3	35.7 ± 2.8	26.0 ± 0.2	21	660	15
Blair #2	May 23rd	5.3	13.0 ± 1.4	28.4 ± 0.6	21	660	17
*Blair #1	June 6th	16.7	29.8 ± 0.2	22.1 ± 1.9	18.1	728	10
Blair #2	June 6th	16.7	13.3 ± 0.8	35.2 ± 0.7	18.1	728	23
Blair #1	June 20th	57.8	4.9	30.6	25.8	751	21
Blair #2	June 20th	57.8	8.1	17	25.8	751	7
Blair #1	July 3rd	70	14.2 ± 0.2	22.6 ± 0.4	24.6	638	12
Blair #2	July 3rd	70	13.8	23.5	24.6	638	12
*Blair	July 17th	70.4	0.6 ± 0.1	12.2 ± 0.6	26.1	737	1.6
*Blair	August 21st	46	0.8 ± 0.2	10.4 ± 1.2	20	673	-2
Conestogo R.	June 20th	5.9	13.0 ± 0.4	26.6 ± 0.1	26.8	444	17

* Possess low or high O yields and were eliminated from Table 2.05